2008

Characterization of Yeast 18S rRNA Dimethyl Transferase, Dim1p

Nagesh Pulicherla
Virginia Commonwealth University

CHARACTERIZATION OF YEAST 18S rRNA DIMETHYL TRANSFERASE, DIM1P

A Dissertation submitted in partial fulfillment of the requirements for the degree of Doctor of Philosophy at Virginia Commonwealth University.

by

NAGESH PULICHERLA
Bachelor of Pharmacy, Rajiv Gandhi University of Health Sciences, India, 2002

Director: JASON P. RIFE, Ph.D.
ASSOCIATE PROFESSOR, DEPARTMENT OF MEDICINAL CHEMISTRY

Virginia Commonwealth University
Richmond, Virginia
May 2008

Acknowledgement

I would like to express my gratitude to Dr. Jason Rife for his invaluable guidance, support and patience throughout the project. I greatly appreciate the help of Dr. Heather O'Farrell and Dr. Gloria Culver at all stages of the project. I would like to thank Leah Pogorzala, Zhili Xu, Dr. Elaine Sia for their help in the yeast experiments and Dr. Scott Henderson in microscopy.

I would like to thank my committee members, Dr. Glen Kellogg, Dr. Richard Westkaemper, Dr. Michael Holmes, Dr. Neel Scarsdale and also Dr. Tonie Wright and Dr. Darrell Peterson for their helpful suggestions. I would also like to thank the members of the Institute for Structural Biology and Drug Discovery for their help in various ways.

I would like to thank the Department of Medicinal Chemistry, for giving me admission into their Ph.D. program and teaching assistantship. We are also thankful to the funding agencies, NIH, A. D. Williams, and Jeffress Memorial trust for the financial support.

Finally, I would like to thank my family and friends, especially my parents, Naga Malleswari and Satyanarayana Reddy Pulicherla; my brother, Ganesh; my wife, Suparna; and my grand mother for their motivation and support. I dedicate this dissertation to my family.

Table of Contents

Page

List of Tables

Page

List of Figures

Page

List of Abbreviations

4-CN	4-chloro-1-naphthol
DTT	Dithiothreitol
HEPES	4-(2-hydroxyethyl)-1-piperazineethanesulfonic acid
LSU	large subunit
β-ME / 2-ME	2-mercaptoethanol
MIC	minimal inhibitory concentration
MgOAc	magnesium acetate
NLS	nuclear localization signal
SAM	S-adenosyl-L-methionine
SSU	small subunit
TCA	trichloroacetic acid
TRIS	tris(hydroxymethyl)aminomethane

Abstract

Characterization of Yeast 18S rRNA Dimethyl transferase, Dim1p

By Nagesh Pulicherla, Ph.D.

A Dissertation submitted in partial fulfillment of the requirements for the degree of Doctor of Philosophy at Virginia Commonwealth University.

Virginia Commonwealth University, 2008

Major Director: Dr. Jason P. Rife
Associate Professor, Department of Medicinal Chemistry

Eukaryotic ribosome biogenesis, a dynamic and coordinated multistep process which requires more than 150 trans-acting factors, has been intensely studied in the yeast *Saccharomyces cerevisiae*. This evolutionarily conserved process involves numerous cleavages of pre-rRNA, modification of nucleotides, and concomitant assembly of the ribosomal proteins onto the rRNA. Considerable information is available about the importance of conserved pre-rRNA cleavage events in ribosome biogenesis; however, very little is known about the exact role of modified nucleotides, which cluster within the functionally important regions of the ribosome. One conserved group of modifications is

the dimethylation of two adjacent adenosines at the 3′ end of the small subunit rRNA which is ubiquitously carried out by the Dim1/KsgA methyltransferase family. Although dimethylation and KsgA are dispensable for survival in bacteria, the eukaryotic enzyme Dim1 is essential because of its requirement in the early pre-rRNA processing events. Similarly, few other members of the family have also evolved to carryout a second unrelated function in the cell. Almost all of the information about Dim1 was obtained from *in vivo* experiments in yeast, and has been determined that it is an indispensable part of a RNA-protein complex carrying out the pre-rRNA processing. Sequence analysis clearly shows that eukaryotic and archaeal enzymes have an extra insert in their C-terminal domain which is absent in bacterial enzymes and a better understanding of Dim1's function is only possible by its structural characterization which is the aim of this study.

After several attempts, the yeast Dim1p was expressed under mild conditions in *E. coli* and purified in soluble form. Dim1p was able to methylate bacterial 30S subunits both *in vivo* and *in vitro*, indicating its ability to recognize bacterial substrate. Supporting our hypothesis, neither the bacterial nor archaeal orthologs were able to complement the processing function of Dim1p in yeast, tested using the plasmid shuffling technique. Our results suggest that the C-terminal insert of Dim1p, along with some structural features of the N-terminal domain, is important for its function in pre-rRNA processing. Further studies are required to understand the complex interactions between proteins and RNA involved in the ribosome biogenesis.

CHAPTER 1: Introduction

Ribosome Biogenesis in Eukaryotes

The ribosome is the enzyme essential for protein synthesis and is among the most fundamental molecular machines in all cells. Bacterial ribosomes have also been exploited therapeutically for more than 60 years in the pharmaceutical industry and continue to be a validated target for anti-infective agents. Hence, there has been a constant enthusiasm to study its structural, functional and biogenetic aspects in detail.

Ribosomes consist of two unequal subunits; large subunit (50S/60S) and small subunit (30S/40S) in prokaryotes/eukaryotes, respectively. Their synthesis involves transcription of rRNA, pre-rRNA processing, modification and simultaneous assembly of ribosomal proteins. Although prokaryotic and eukaryotic ribosomes have similar architecture and carryout the same function, there are significant differences in their biogenesis with the pathway being more complicated in eukaryotes than prokaryotes. This work is focused on the biogenesis of small subunit, specifically a conserved dimethylation of two adjacent adenosines observed in the small subunit rRNA and the conserved enzyme family carrying out the process.

Eukaryotic ribosome biogenesis, a dynamic and coordinated multistep process which requires more than 150 trans-acting factors, has been intensely studied in the yeast *Saccharomyces cerevisiae* and extensively reviewed[1-7]. It is also a costly demand for the

cell, considering the amount of cellular metabolites and energy that it utilizes[8]. Eukaryotic ribosomes contain a copy of each of the four ribosomal RNAs; 5S, 5.8S, 18S, and 25/28S (yeast/ higher eukaryotes) rRNA and about 75 different ribosomal proteins. All three transcription machineries (RNA polymerases I, II and III), are utilized to ensure the high efficiency and accuracy of ribosome production. Pol I transcribes 25S/28S, 5.8 and 18S rRNA, Pol III synthesizes 5S rRNA, whereas Pol II transcribes the mRNAs for the ribosomal proteins.

In eukaryotes, ribosome synthesis starts in the nucleolus, the specialized nuclear compartment which is also the site of rRNA transcription and most maturation steps. The basic organization of the eukaryotic rRNA operon is similar in all species and the yeast rDNA unit is shown in Figure 1. The yeast rDNA unit is 9.1 kb long and present in 100 to 200 head-to-tail copies on chromosome XII. It consists of the 35S pre-rRNA operon and two nontranscribed spacers, NTS1 and NTS2, interrupted by the 5S rRNA gene. The 35S pre-rRNA operon contains the sequences for the mature 18S, 5.8S, and 25S rRNAs separated by the two internal transcribed spacers, ITS1 and ITS2, and flanked at either end by two external transcribed spacers, the 5′-ETS and 3′-ETS. RNA polymerase I transcribes the entire 35S pre-rRNA whereas 5S rRNA gene is transcribed in the opposite direction by RNA polymerase III.

As soon as the transcription of 35S rRNA is completed, the transcript is processed to remove the spacers by endo- and exoribonucleases and extensively modified, mainly by pseudouridylation (ψ) and 2′-O-ribose methylation (CH_3) which are guided by small ribonucleoprotein particles (snoRNPs). More than 150 of such non-ribosomal trans-acting

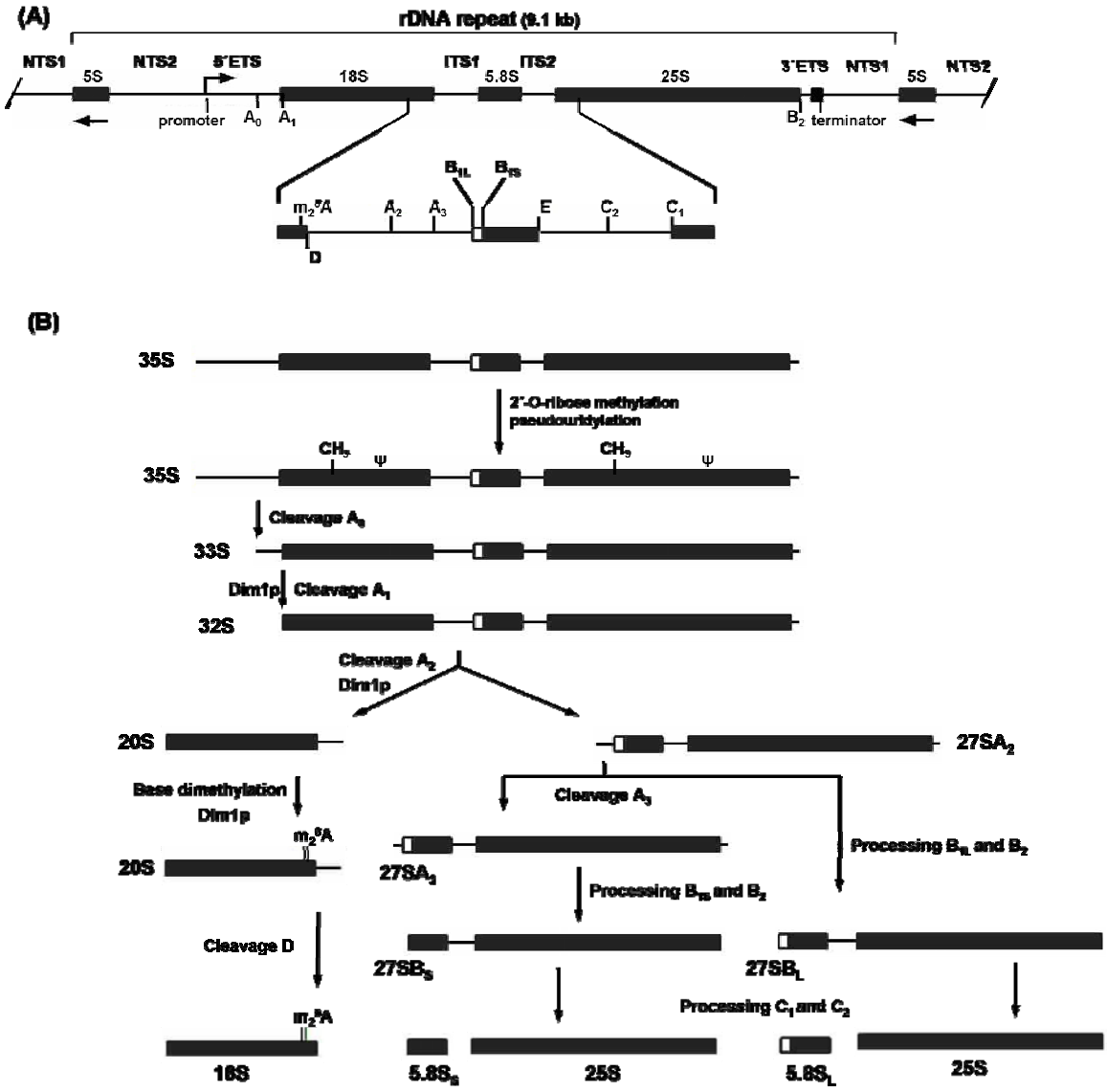

Figure 1: Structure and processing of pre-rRNA in *Saccharomyces cerevisiae*. (A) shows the yeast rDNA unit, 35S pre-rRNA operon and specified processing sites. (B) Processing of the 35S precursor to the mature rRNA species.

factors[5,9] are involved in these processing and modification events which are probably preceded and accompanied by the assembly of r-proteins[10], forming large RNP particles. Many components involved in the complex steps of ribosome formation have been identified and characterized in the yeast *Saccharomyces cerevisiae*, owing to its excellent genetic and biochemical suitability. Therefore, budding yeast has become an attractive 'model organism' to study many aspects of eukaryotic ribosome biogenesis.

The pathway by which the primary 35S precursor is processed into the mature 18S, 5.8S, and 25S rRNA is depicted in Figure 1. The earliest processing site is at A_0 in the 5'-ETS, 90 nucleotides upstream of the 5' end of mature 18S rRNA. Processing at A_0 yields the 33S pre-rRNA, which is rapidly cleaved at site A_1, producing the 32S pre-rRNA. Cleavage at A_2 in ITS1 then splits the 32S pre-rRNA into the 20S and $27SA_2$ pre-rRNAs, which are destined to form the mature species of the small and large ribosomal subunit, respectively. The 5' part of the molecule, 20S pre-rRNA, is exported to the cytoplasm where it is cleaved at site D leading to the mature 18S rRNA. Processing of the $27SA_2$ pre-rRNA, occurs by two alternative pathways yielding mature 5.8S and 25S rRNAs.

90S Pre-ribosome and SSU processome

As the 35S rRNA is transcribed, several factors including snoRNAs, ribosomal and non-ribosomal proteins associate with it, co- and post-transcriptionally, to form a 90S particle in the nucleolus. It is the first and largest pre-ribosomal particle identified by its sedimentation characteristics. After initial processing events at sites A_0, A_1, A_2, it is cleaved into 66S and 43S particles, the precursors to the 60S and 40S subunits (Figure 2).

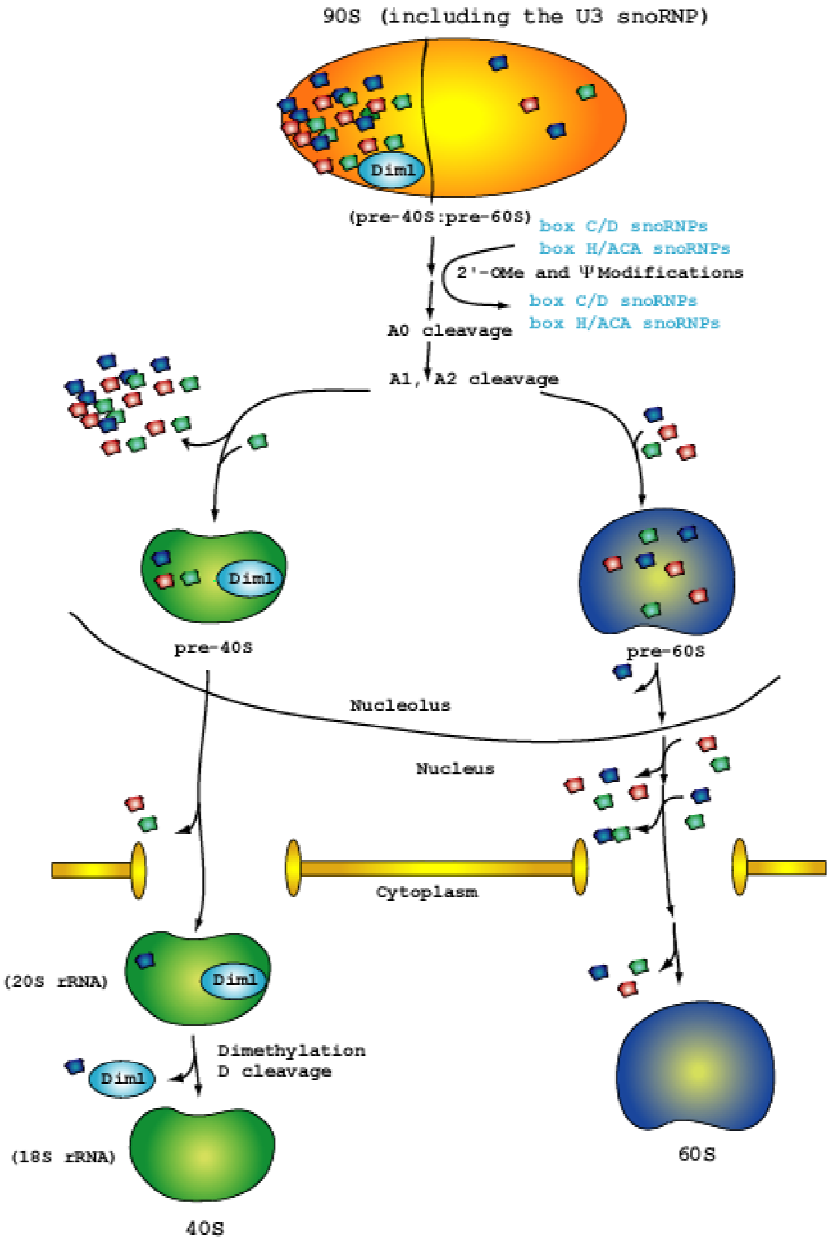

Figure 2: Ribosome biogenesis in *Saccharomyces cerevisiae*. Dim1 binds to the 90S pre-ribosome very early, in the nucleolus and remains associated until the late cytoplasmic stage. Base dimethylation is the penultimate step in 40S subunit biogenesis.

Accordingly, it was initially thought to contain the synthetic machinery of both 40S and 60S subunits, however, it was recently found that 90S pre-ribosome predominantly includes 40S subunit processing factors[11]. Along with the 35S rRNA, 90S precursor contains U3 snoRNA, proteins associated with U3, and factors required for 18S rRNA synthesis, but only a few 60S processing factors. This discovery and further analysis of pre-ribosomal particles were made possible by the development of efficient purification protocols, especially the 'tandem affinity-purification' (TAP) method[12], combined with sensitive methods such as mass spectroscopy to identify the associated proteins.

Another breakthrough in the study of ribosome biogenetic pathway was obtained from the analysis of pre-rRNA transcripts by Miller chromatin spreads[13,14]. The technique helped in the observation of growing pre-rRNA transcripts by electron microscopy. Observations made in the 1970s suggested that the pre-rRNA processing machinery assembles co-transcriptionally onto the nascent transcripts and forms the 'terminal knobs' at the 5′ end of each 35S pre-rRNA molecule which were considered as the growing 90S pre-ribosomes. It was thought that the 90S pre-ribosome splits in to 66S and 43S particles only after the transcription of 35S pre-rRNA is completed[15-17]. The appearance of the 35S primary rRNA transcript when the pre-rRNAs are analyzed by both northern blot and pulse-chase analysis also indicated that the cleavage in ITS1 occured after completion of transcription of the entire gene. Contrary to this long-held view, the Beyer, Baserga and Dragon groups have recently shown that the processing of the yeast pre-rRNA does often occur before the completion of transcription[18]. The yeast chromatin spreads (Miller spreads) revealed that in cells growing exponentially under optimal growth conditions, the

co-transcriptional cleavage of pre-rRNA in ITS1 was observed in 55% of the transcripts, thereby separating the pre-rRNAs destined for the small and large subunits. However, neither co-transcriptional nor post-transcriptional cleavage in ITS1 is obligatory for further events.

Summarizing the above information, a predominantly 40S processing machinery assembles co-transcriptionally beginning at the 5′ end and forms the 'knobs' at the growing end of 35S pre-rRNA. The components of these initial 'terminal knobs' are essential for cleavages at sites A_0-A_2 and hence designated as the small subunit (SSU) processome[1,3,18,19]. In a slight majority of the transcripts co-transcriptional cleavage occurs in ITS1 separating the 18S rRNA as a 43S particle from the growing strand. Few 60S processing factors would then start associating with the remaining strand containing 5.8S and 25S rRNA and form small particles at the new 5′ end, termed as large subunit (LSU) knobs[18,20] (Figure 3). In transcripts where the co-transcriptional cleavage does not occur, the mature 90S precursors formed at the end of transcription undergo cleavage in ITS1 to release 43S particle and pre-60S particle.

After the cleavage in ITS1, many of the factors including U3 snoRNA and its associated proteins are released from the 43S particles rapidly leaving behind a relatively elementary pre-40S particle with only a few non-ribosomal components[21]. These core factors characterized in yeast (Enp1p, Dim1p, Dim2p, Hrr25p and Rrp12p) are detected even in the earliest SSU processome/ 90S pre-ribosomes. Other factors (Nob1p, Rio2p and Tsr1p) appear to bind later to more advanced pre-40S particles, possibly after A_0–A_2 cleavages but before nuclear exit. The pre-40S subunits are then transported through the

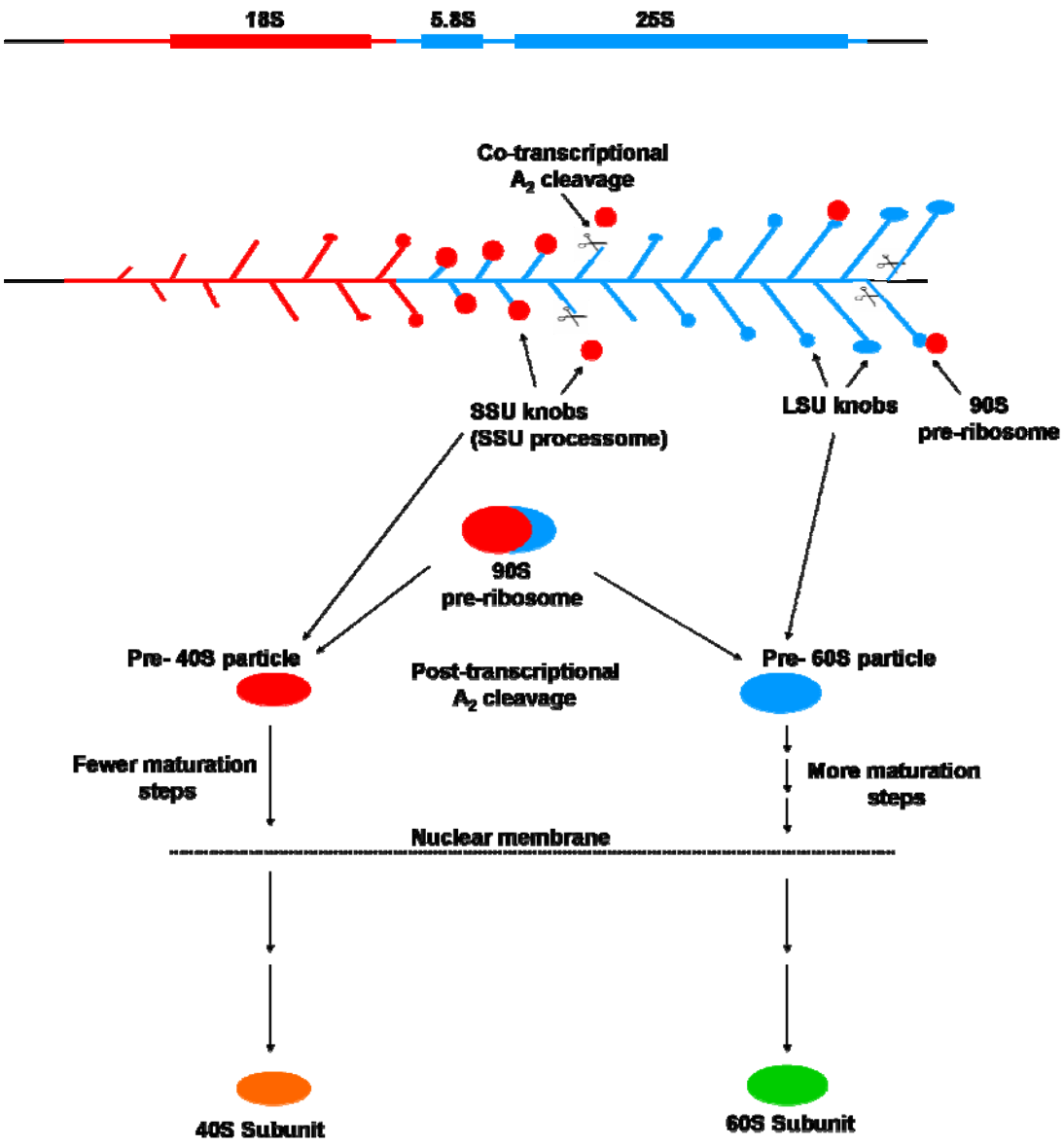

Figure 3: Co-transcriptional processing of *S. cerevisiae* rRNA transcripts. Schematic of rRNA gene is shown at the top. The region before A_2 site is colored red and the region after A_2 is in blue. Co-transcriptional A_2 cleavage is observed in slight majority of the transcripts (55 %) which releases the 'SSU knob', shown as red circles. Alternatively, the 90S pre-ribosome are cleaved post-transcriptionally to give the 43S and 66S particles.

nucleoplasm and the nuclear pore complex to the cytoplasm, where final maturation events occur including a pre-rRNA processing event to produce 18S rRNA from 20S pre-rRNA[22]. The few factors that remain associated with the late 40S pre-ribosomes are involved in the final maturation of 40S subunits and are released gradually during these final stages.

The pre-60S maturation, in contrast to pre-40S maturation, is more complicated and includes several well characterized nucleoplasmic and cytoplasmic intermediates[1,22]. The pre-60S particles released after the end of transcription as the LSU knobs or following the cleavage of 90S particle have fewer non-ribosomal factors. Immediately after their release, more than 50 non-ribosomal proteins associate with these earliest nucleolar pre-60S ribosomes, which then undergo enormous reengineering on their path from the nucleolus to the cytoplasm[23]. During the movement from the nucleolus towards the nuclear pore, many of the factors disassemble from the pre-60S precursors in sequential steps, whereas a few proteins associate transiently at later stages (Figure 2). After export to the cytoplasm, only few factors are left on the pre-60S subunits which are released after the final maturation steps.

Ribosome biogenesis in higher eukaryotes is very similar to that of yeast. Many of the non-ribosomal factors have homologs in vertebrates and have been found in mammalian pre-ribosomes[24,25].

Ribosome biogenesis in Prokaryotes

Prokaryotic ribosome biogenesis is relatively simpler in contrast to the eukaryotic process. The mature rRNAs (23S, 5S and 16S) in prokaryotic ribosomal subunits are

synthesized as a single transcript with additional intervening and flanking regions of RNA (including tRNA). The pre-rRNA transcript is then processed to obtain the mature rRNAs and this process involves several non-ribosomal factors and RNases[26]. Several of these factors have good sequence homology with that of eukaryotes. Similar to eukaryotes, the processing, modification of nucleotides and the association of ribosomal proteins occur co-transcriptionally on the pre-16S rRNA. However, the order of pre-16S processing and 30S subunit assembly events is still largely unknown. Much of the current understanding about 30S subunit assembly resulted from *in vitro* studies that demonstrated that functional 30S subunits could be reconstituted *in vitro* from a mixture of 30S subunit proteins and purified 16S from *E. coli*[27]. During the *in vitro* reconstitution, a 21S particle was obtained at low temperatures (0 to 15˚C) and it was designated as Reconstitution Intermediate (RI)[28-30]. A corresponding analog of the RI was also observed in the *in vivo* assembly pathway[31,32], supporting the *in vitro* reconstitution experiments. The RI undergoes a rate-limiting conformational rearrangement in the folding of 16S rRNA, yielding a more compact 26S particle, designated as RI*. *In vitro*, this high activation energy barrier is overcome by heating RI to 42˚C, while *in vivo*, this step likely requires chaperones[33]. In both cases, once this barrier is crossed the remaining ribosomal proteins readily assemble, even at low temperature. Assembly maps have also been similarly constructed for the 50S subunit[34,35].

Nucleotide Modification

The pre-rRNA processing and subunit assembly events are accompanied by modification of nucleotides, another important process observed in all forms of life. The

nucleotide modifications are of three main types; conversion of uridine to pseudouridine (ψ), 2'-O-ribose methylation, and alterations to bases, most of which undergo methylation at different positions. The number of modified sites increases with the complexity of the organism, with *Escherichia coli* having 11 pseudouridines, 4 ribose methylations, and 19 base methylations; *Saccharomyces cerevisiae* have 44 pseudouridines, 55 ribose methylations and 10 base methylations; *Homo sapiens* have 91 pseudouridines, 105 ribose methylations and 10 base methylations[36,37]. The modification patterns show some evolutionary conservation with a distinct clustering in regions implicated in ribosomal function[38-40], and most sites modified in the yeast rRNA are also modified in vertebrates. Current values for the archaea range substantially depending on the temperature at which they are grown, with some having considerably more pseudouridines and ribose methylations than bacteria[41].

Modifications in *E. coli* are mediated by site-specific protein enzymes such as ribose methylases or pseudouridine synthases, without the involvement of a RNA guide component[42,43]. By contrast, the pseudouridylations and ribose methylations in eukaryotes are carried out by two families of site-specific, small nucleolar RNA–protein complexes (snoRNPs). Members of one family, box H+ACA snoRNPs, are responsible for pseudouridylations and the other, box C+D snoRNPs, are responsible for 2′-O-ribose methylations. In both processes, the sites for modification are selected by the RNA component (different guide snoRNAs belonging to box C+D and box H+ACA classes) through base pairing with a conserved sequence, and catalysis is mediated by a type-specific protein component[7,44]. The archaea use a similar C+D snoRNP for ribose

methylation[45] and proteins related to those in the H+ACA snoRNPs have also been identified[46].

In contrast to the 2'-O-ribose methylation and pseudouridine formation, base methylation is mediated by specific protein enzymes without any involvement of guide snoRNAs. The most well characterized among these is the dimethylation of two adjacent adenosines localized in the loop of the 3´-terminal helix (helix 45 in *Escherichia coli*) of small subunit rRNA (Figure 4). This region is one of the most highly conserved sequences in the small subunit rRNA[47,48]. Interestingly, this dimethylation is also highly conserved in all organisms from prokaryotes to vertebrates, including organelles such as mitochondria and chloroplasts with respect to the number of methyl groups added and their position on the small subunit rRNA[49]. Even the enzymes carrying out this dimethylation are also universally conserved, belonging to the Dim1/KsgA family of methyltransferases (referred as Dim1p in Yeast).

The dimethylation of two adjacent adenosines is a late event in the biogenetic pathway. In eukaryotes, it occurs on the cytoplasmic pre-40S particles[50] and in prokaryotes, the modification occurs on a late intermediate, most probably a 26S particle[51]. In contrast, most of the sno-RNA directed pseudouridylations and ribose methylations occur very early. In eukaryotes, some of them occur co-transcriptionally during the formation of SSU processome, on the 35S pre-rRNA transcript[18,37,52,53] and the remaining occur soon after the cleavage at site A_2.

The effect of nucleotide modification on rRNA is one of the oldest questions in RNA science and information is still limited. Their effects include altered steric properties

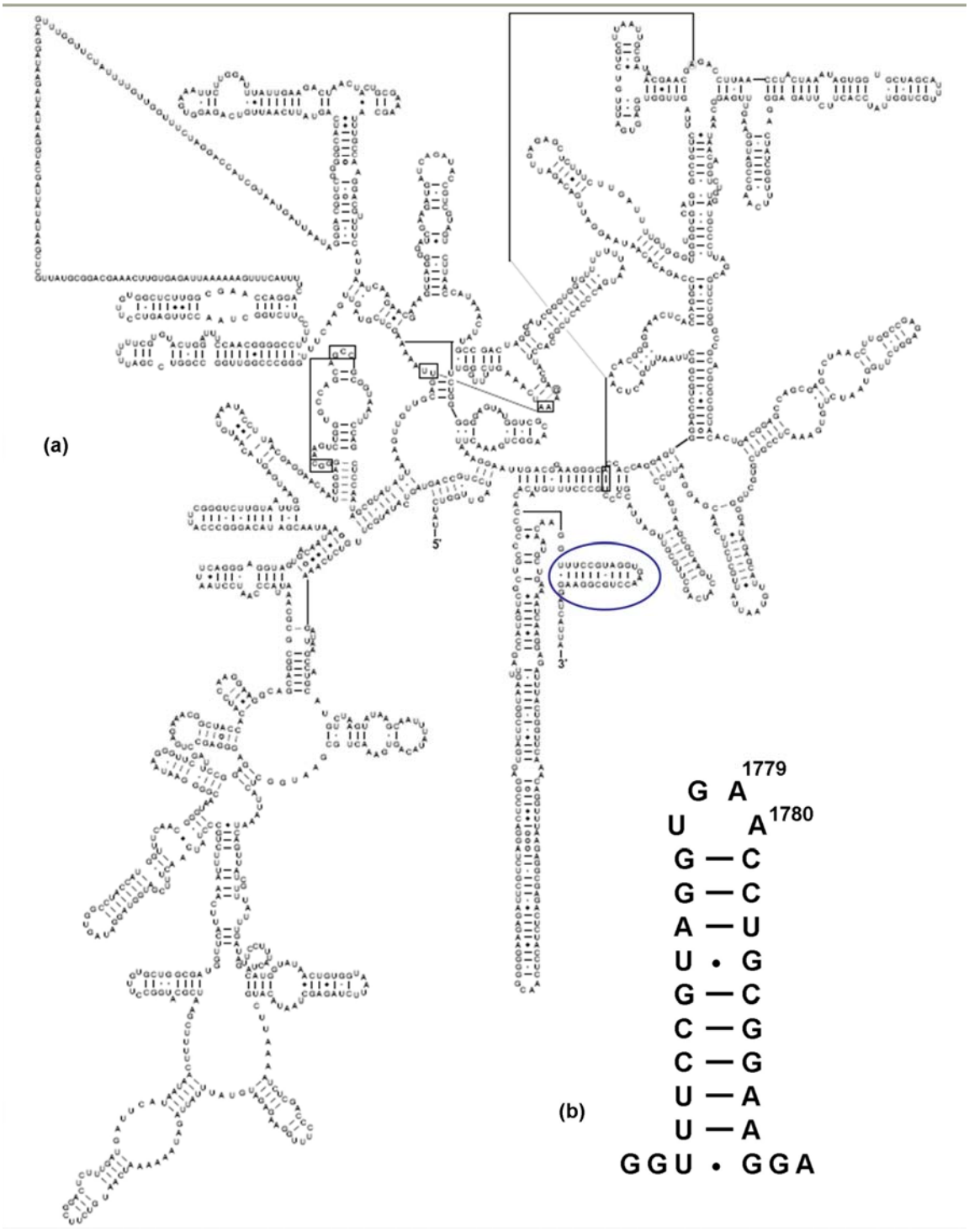

Figure 4: (a) Secondary structure of *S. cerevisiae* 18S rRNA. The universally conserved 3´ terminal helix is circled in blue. (b) conserved adenosines (1779 and 1780) in the helix.

in all cases, different hydrogen-bonding potential, enhancement of local base stacking (pseudouridylation) and increased structural rigidity for both single- and double-stranded regions (pseudouridylation and 2'-O-methylation)[54,55]. Methylation of 2′-OH favours the 3′ endo configuration and prevents hydrolysis of internucleotide bonds[56]. Although most of the modified nucleotides cluster within the functionally important regions of the ribosome[38], so far, no single rRNA modification has been found to be essential for ribosome function[57-60]. However, when the pseudouridylations and 2'-O-methylations were blocked on a global level, strong negative effects were observed on the yeast growth[61,62]. Similarly, eubacterial subunits reconstituted with unmodified RNA are active in peptide-bond synthesis but have much less activity than subunits reconstituted with natural rRNA[59,60,63]. Thus, it seems probable that most individual modifications contribute a small, non-essential benefit and that, in aggregate, a large benefit is provided by the full ensemble of modifications. Interestingly, modifications are essentially absent from areas dominated by ribosomal proteins: the external surfaces and periphery of the interface regions[38]. So the rRNA modifications might act as a molecular mortar to stabilize the required RNA conformations[64] and fine-tune the translation process[65-67] or they might play a role in 'building' the vital domains of the subunits properly, rather than a direct involvement in the chemistry or structural changes associated with the translation process.

Similarly, though the dimethyladenosines in the 3′-terminal helix of small subunit rRNA have been universally conserved, a distinct cellular function could not be ascribed yet. However, in eukaryotes the conserved modifying enzyme is essential for survival because of its role in another process.

Dim1

The Dim1/KsgA family belongs to a well-characterized group of S-adenosyl-L-methionine (SAM) dependent methyltransferases (also known as AdoMet dependent MTases) which includes DNA, RNA, protein and small molecule methyltransferases[68]. All the enzymes in this group have a characteristic Rossman-like fold in their SAM binding domain, which consists of a central β-sheet surrounded by a variable number of α-helices, and they share several conserved motifs[69,70]. Many of these AdoMet dependent methyltransferases have been well characterized structurally and biochemically, and their mechanisms have been explored. While most of the methyltransferases transfer a single methyl group onto their target, the members of Dim1/KsgA family, with a very few exceptions, transfer two methyl groups onto the exocyclic nitrogen of each of the two adjacent adenosines (A_{1779}, A_{1780} in *Saccharomyces cerevisiae* and A_{1518}, A_{1519} in *Escherichia coli*). This reaction consumes four molecules of the co-factor (SAM) which is then converted to S-adenosyl-homocysteine (Figure 5). This process also requires the target adenosine bases facing the inner side of the loop to 'flip out', in order to be methylated by the enzyme. This process has been extensively studied in DNA methyltransferases, whose target bases reside within the double helix[71, 72].

In eukaryotes, Dim1 is not important for its methyltransferase function, but for an indispensable role in pre-rRNA processing in the early steps of ribosome biogenesis. The putative yeast 18S rRNA dimethylase gene, *DIM1*, was originally identified by its ability to dimethylate the *E. coli* 16S rRNA in vivo and restore the kasugamycin sensitivity of the *ksgA* mutant of *E. coli*[73]. Further functional characterization of the *DIM1* gene has been

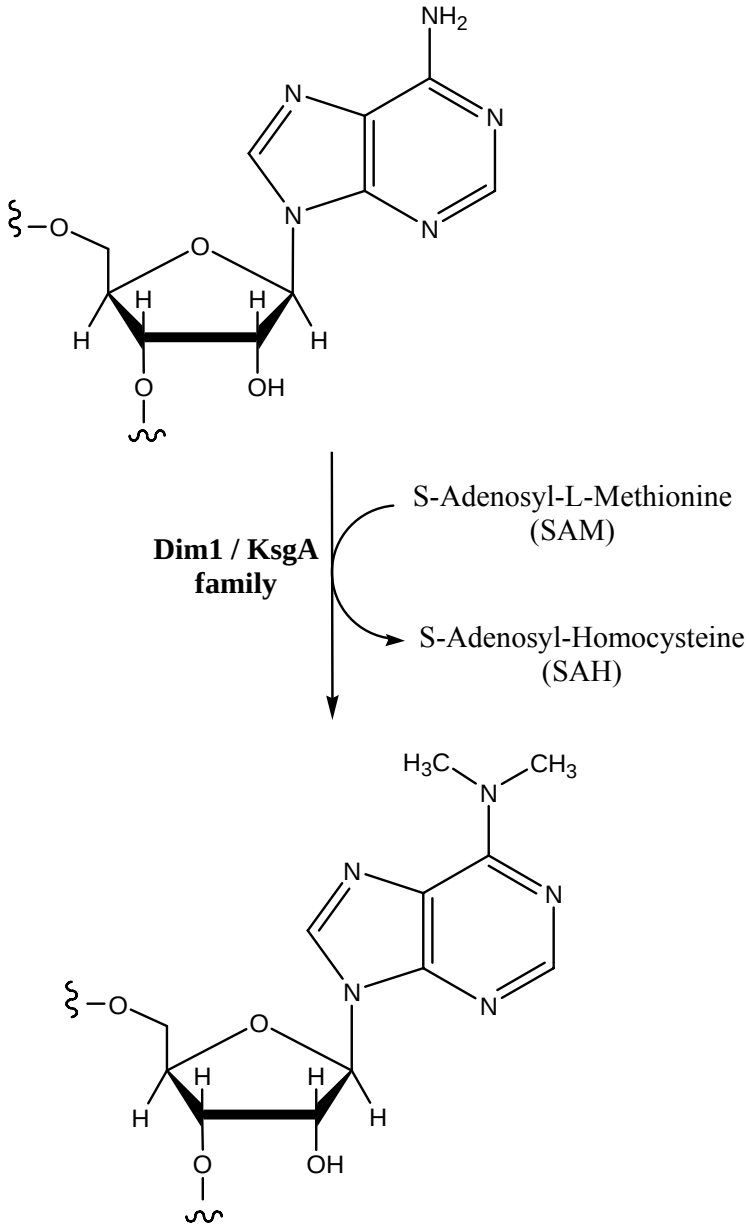

Figure 5: The adenosine dimethylation. During the reaction, two molecules of the co-factor (SAM) are consumed for each adenosine.

carried out in yeast where the encoded protein is referred as 'Dim1p', based on the yeast nomenclature, in contrast to 'Dim1' in other eukaryotes. The *DIM1* gene is present in chromosome XVI between the coordinates 39121-40077, and has a systematic name "YPL266W".

Lafontaine et al. showed that the genetic depletion of Dim1p not only blocked the dimethylation of the pre-rRNA but also strongly inhibited the nucleolar pre-rRNA processing steps at cleavage sites A_1 and A_2[74]. Cleavage at site A_1 gives rise to the mature 5′ end of 18S rRNA and cleavage at site A_2 separates the pre-rRNAs destined for the small and large ribosomal subunits. Inhibition of these cleavages results in the accumulation of 33S pre-rRNA formed after 35S pre-rRNA is cleaved normally at site A_0. The 33S pre-rRNA is then cleaved at site A_3 by RNase MRP[75] which is not affected by the inhibitions at A_1 and A_2. This results in the release of an aberrant 22S pre-rRNA extending from A_0 to A_3 that is neither dimethylated nor can be processed to 18S rRNA inhibiting the formation of 40S subunits (Figure 6). However, cleavage at A_3 also produces the $27SA_3$ precursor that is normally processed to 5.8S and 25S rRNAs and hence the maturation of 60S subunits is unaffected.

It was later demonstrated that the enzymatic function of Dim1p in dimethylation can be separated from its involvement in pre-rRNA processing[50]. Lafontaine et al. have isolated a yeast strain, *dim1-2*, from a library of conditionally lethal alleles of *DIM1*, in which pre-rRNA processing was not affected at the permissive temperature for growth, but dimethylation was blocked, leading to accumulation of nondimethylated 18S rRNA. This proved that the processing defect is a consequence of the absence of Dim1p and not the

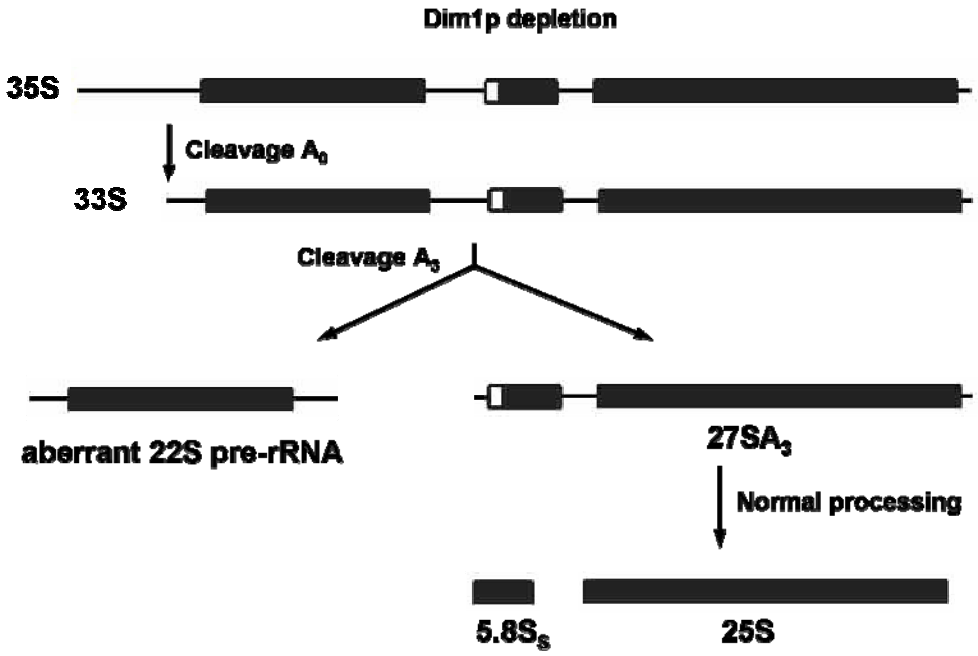

Figure 6: Effects of Dim1p depletion on pre-rRNA processing. 33S pre-rRNA accumulates due to the inhibition of cleavages at sites A_1 and A_2. It is cleaved at site A_3, providing the $27SA_3$ that is normally processed to 5.8S and 25S rRNA. Cleavage at site A_3 also produces the aberrant 22S pre-rRNA extending from site A_0 to A_3, that cannot be processed to 18S rRNA.

dimethylated adenosines. This is also in agreement with the fact that dimethylation is a late event occurring on the cytoplasmic 20S rRNA precursor, whereas the processing events are the early steps occurring in the nucleolus. Although the dimethylation is not essential for survival of yeast, the two adenosines are not dispensable. Replacement of adenosines by guanosines failed to support yeast growth[74].

Interestingly, another factor, Dim2p (also referred as RRP20 and PNO1), was also found to be essential for the A_1, A_2 cleavages and for the dimethylation carried out by Dim1p[76,77]. Dim2p has a conserved KH-domain which is a well characterized RNA binding domain[78] and is also a core constituent of the SSU processome complex. Association of Dim2p with the 35S and methylated 20S pre-rRNAs indicated that the protein joins the preribosomes at an early nucleolar stage and follows the particles to their site of final maturation in the cytoplasm[11,21]. The association between Dim1p and Dim2p was tested by coprecipitation[76], and it is thought that Dim2p associates with Dim1p during the processing and dimethylation events. Information from the recent high-throughput copurification data sets[79-81] revealed that Dim2p also associates with Nob1p, Rio2p, Tsr1p, Utp18p and Utp22p (the last two are U3-snoRNA associated proteins).

Schafer et al. showed that after the A_2 cleavage, most of the SSU processome factors leave the 40S precursor but a few factors which include Dim1p, Dim2p, Enp1p, Hrr25p remain associated with the pre-40S particle[21]. Few other factors such as Nob1p, Rio2p, Tsr1p appear to associate with pre-40S only after the rRNA cleavage at site A_2. Based on the above processing events and composition of pre-ribosomal particles, it can be summarized that Dim1p, Dim2p are among the core constituents of the SSU processome

complex along with U3 snoRNP and other factors that assemble co-transcriptionally on to the pre-rRNA transcript. The 5'-ETS region is highly structured, with the cleavage sites A_0 and A_1 in close proximity at opposite sides and near the base of an extended stem-loop structure[82]. Interestingly, site A_2 in ITS1 is also positioned before a stem-loop structure[83].

It is widely believed that cleavage at sites A_1 and A_2 is coupled as mutations or depletions of many different *trans*-acting factors, including Dim1 and Dim2, apparently resulted in the simultaneous inhibition of both of them[7], but A_0 cleavage is not obligatorily coupled to the other two[84]. This assumption is supported by the fact that U3 snoRNA, which base-pairs to the pre-rRNA in the 5′ ETS region[85,86], is also essential for A_2 along with A_0 and A_1. Although the binding site of Dim1p and Dim2p is not known, they probably associate near the 3′ end of 18S rRNA region and interact with other factors and snoRNPs forming a large complex (SSU processome) in which the cleavage sites are brought closer[6,7] (Figure 7). This may resemble the situation in *E. coli* where the 5′ and 3′ ends of 16S rRNA are brought together by base pairing of sequences present at either end. Processing at sites A_0, A_1, and A_2 are endonucleolytic events, as the spacer fragments released by these steps (A_0-A_1, D-A_2 and A_2-A_3; see Figure 1) could be detected[87,88]. Although the enzyme/s responsible for the cleavages has not yet been identified, it is possible that they are cleaved by the same endonuclease based on the presence of similar recognition signals[6,7].

After the A_1 and A_2 cleavages, most of the factors and snoRNPs leave the pre-40S particle except a few which include Dim1p, Dim2p, Enp1p and Hrr25p, and during the same time few more factors such as Nob1p, Rio2p, Tsr1p and Ltv1p associate with the

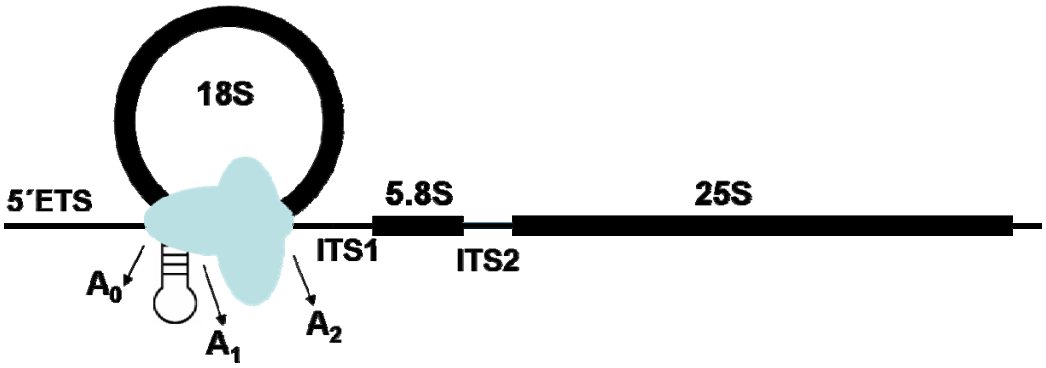

Figure 7: Coupling of cleavage at sites A_1 and A_2. The 5´ and 3´ ends of 18S rRNA are brought together by the snoRNPs and factors of the SSU processome complex (blue ovals). The existence of similar recognition signals near the sites A_1 and A_2 raises the possibility that both sites might be cleaved by the same endonulease.

particle. However, the order of dissociation or association of these factors is not clearly known. Some of the factors such as Ltv1p, Rio2p, Tsr1p and Enp1p are required for the nuclear export of 40S subunits. In the cytoplasm, the pre-40S particle undergoes a few additional maturation steps. Schafer et al. reported that Hrr25p-dependent phosphorylation of an Enp1p/Ltv1p/Rps3p subcomplex, followed by dephosphorylation by an unknown phosphatase, is required for proper incorporation of Rps3p into the 40S subunit and correct formation of a 'beak' structure close to the head of the 40S subunit[89]. This also results in the dissociation of Enp1p, Ltv1p and Hrr25p from the pre-40S particle. The dimethylation of 20S pre-rRNA at residues A_{1779} and A_{1780} is carried out by Dim1p in association with Dim2p. The order of these two events is not clearly known or they might occur simultaneously. However, it is interesting to note that Dim1p methylates the pre-40S particle near the final stages of maturation, although it binds to the pre-rRNA in the nucleolus. It is possible that the target adenosines are oriented in the right position that facilitates the methylation, only after some conformational rearrangements occur in the pre-40S particle involving other factors and ribosomal proteins. Finally, the endonucleolytic processing of 20S pre-rRNA to 18S rRNA at cleavage site D occurs, which is most probably catalyzed by Nob1p[90,91]. Recently, Granneman et al. proposed that a putative NTPase, Fap7, mediates this cleavage by directly interacting with Rps14[92]. Although it is not clearly known which protein is actually implicated in the cleavage, Nob1p appears to be the likely candidate as it contains the characteristic PIN domain. Interestingly, Nob1p has been shown to associate with Dim2p in the maturation of the 20S proteasome[93]. Factors such as Tsr1p, Rio2p are also involved in 3′-end formation of mature

18S rRNA[94,95]. The order in which the processing factors dissociate from the 40S subunit is not clearly known. Similarly, it is also not clearly known if Dim1p and/or Dim2p remain associated to the 40S subunit until the cleavage at site D has occurred or dissociate immediately after the dimethylation event.

Dim1/KsgA family

As mentioned earlier the dimethylated adenosines are conserved across kingdoms including cell organelles. The Dim1/KsgA methyltransferase family has nuclear encoded orthologs that are localized into the chloroplasts[96] and mitochondria[97]. The only known exceptions are in *Saccharomyces cerevisiae* mitochondrial 12S rRNA, which has no methyl groups on the two adenosine bases[98]; *Euglena gracilis* chloroplast rRNA[99] and the 16 S rRNA of the archaebacterium *Sulfolobus solfataricus*[41], both of which have only one dimethylated adenosine base.

The Dim1 ortholog in bacteria, first identified as KsgA[100] carries out the corresponding dimethylation on A_{1518} and A_{1519} and has been named after its phenotype. Interestingly, knockout of KsgA in bacteria, resulting in the loss of methyl groups, confers resistance to the aminoglycoside antibiotic kasugamycin[101,102], with only marginal effects on growth[103-105]. Kasugamycin (Ksg) specifically inhibits translation initiation of canonical, but not of leaderless, messenger RNAs. Ksg binds within the messenger RNA channel of the 30S subunit and forms hydrogen bonds with the universally conserved G926 and A794 nucleotides in the 16S rRNA[106-108]. Lack of dimethylation at A_{1518} and A_{1519}

results in conformational changes which indirectly alter the Ksg binding site and confer resistance to the drug.

Apart from the dimethylation, the members of Dim1/KsgA family have evolved to carryout other functions in the cell, which is clearly evident in eukaryotic Dim1. Recently it has been shown that KsgA is also involved in pre-rRNA processing in *E.coli*. Knockout of KsgA leads to a processing defect resulting in the accumulation of immature small subunit rRNA (Connolly K, Rife JP, Culver GM, unpublished results). However, this processing defect is not detrimental, as functional 30S subunits could still be formed. Pfc1, the Dim1 ortholog in chloroplast has also been found to be important for proper development of chloroplast at low temperatures[96].

The Dim1 ortholog in eukaryotic mitochondria, referred as mtTFB, serves as a mitochondrial transcription factor as well as being the dimethyltransferase for mitochondrial 12S rRNA[97,109]. Similar to Dim1, it has been found that the methylation activity of human-mtTFB can be separated from its transcription activity[110]. h-mtTFB also has an intriguing link with human disease, having been shown to be a phenotypic modifier of deafness associated with a polymorphic A1555G mutation in mitochondrial rRNA[111,112].

The Erm family of methyltransferases is another group of enzymes homologous to Dim1/KsgA family and they mediate resistance to the macrolide-lincosamide-streptogramin B (MLS-B) group of antibiotics in bacteria[113,114]. The Erm enzymes have, probably, descended from one or more bacterial KsgA genes and evolved to recognize a completely different RNA substrate while keeping essentially the same function. The Erms

mono- or dimethylate a single adenosine base of 23S rRNA, near the peptidyl transferase site of the 50S subunit[115].

Objectives

The Dim1/KsgA family of methyltransferases is interesting in two aspects; not only are they universally conserved but also evolved to carryout other cellular functions. Although the sequence homology among members of the same domain is high, the homology is relatively low across the domains. The sequence homology between yeast Dim1p and bacterial KsgA is ~25%, but the homology between yeast and human Dim1 is as high as 80%. This could be attributed to the eukaryotic enzyme's indispensable secondary function in pre-rRNA processing and hence mutations in the enzyme were less tolerated during evolution. Secondly, the homology between KsgA and Dim1 is high only in the SAM binding domain, but very poor in the other regions.

At the onset of this project, the crystal structure of *E. coli* KsgA had been solved in our laboratory[70]. The crystal structures of sc-mtTFB[116] and ErmC′[117] have also been solved earlier by other groups. While these structures can be beneficial to studies of the KsgA family of enzymes in prokaryotes, they are of limited usefulness in answering detailed questions about structure/function relationships in eukaryotes. Strikingly, eukaryotic and archaeal enzymes have a long insert in their C-terminal domain which is absent in prokaryotic enzymes and this could be important for the processing function of Dim1. Almost all of the information regarding Dim1 has been obtained from *in vivo* studies in

yeast[50,73,74] and in order to dissect the structural elements relating to its functions, structural characterization is required.

After several attempts, soluble Dim1p was purified and it was able to methylate bacterial 30S subunits *in vitro* in compliance with the *in vivo* data. During the course of this work the crystal structures of human Dim1 (1ZQ9) and that of *Plasmodium falciparum* (2H1R) became available (Dong et al., Structural Genomics Consortium). Utilizing the information from the crystal structures of KsgA and human-Dim1, further characterization of Dim1p was carried out in yeast.

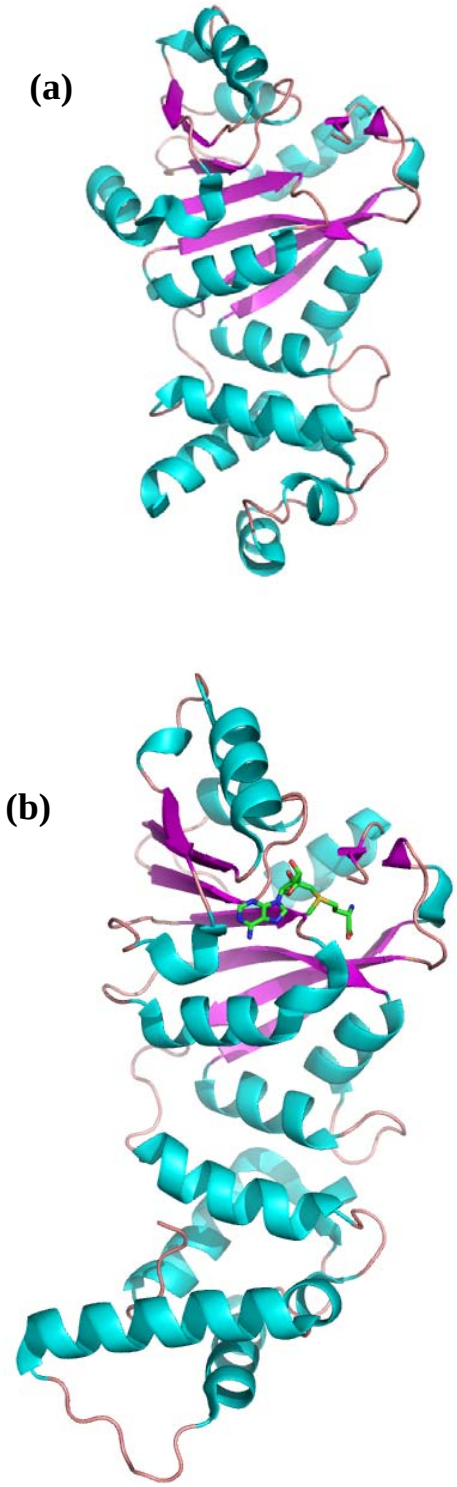

Figure 8: Cyrstal structures of (a) KsgA (PDB Id- 1QYR) and (b) human Dim1 (PDB Id- 1ZQ9).

CHAPTER 2: Expression and purification of soluble Dim1p

Structural and biochemical characterization of any protein requires it to be soluble and stable for a reasonable period of time. In order to study the protein using some of the most powerful and informative methods such as X-ray crystallography and NMR, high protein concentration and long-term stability are required. Preparation of a concentrated and stable protein sample is more often a difficult task, as proteins frequently aggregate or precipitate at higher concentrations, and are sometimes subject to spontaneous proteolytic degradation. The recently published results from high-throughput structural genomics programs[118] identified poor protein solubility as one of the main bottlenecks. The estimates show that on an average only 30% of all the cloned targets could be purified, and the number drops to 20% if only eukaryotes are considered. To improve the yield of soluble proteins, various strategies are in practice, which include expression of proteins in alternative hosts (bacteria, yeast, insect cell, mammalian cell) and optimization of the protocols for expression and purification.

Like many other proteins, expression of soluble yeast 18S rRNA dimethylase, Dim1p, has been a challenging task. Dim1p has a poor solubility profile, although its orthologs in *E. coli* and *M. jannaschii*, KsgA and MjDim1 respectively, were readily soluble and have been purified in our laboratory to high concentrations[49,70]. The sequence

homology between the proteins is ~26% which reflects that there are significant differences resulting in different physical properties.

Following the general practice, initial attempts to produce Dim1p has been carried out in *E. coli* as an expression host, because of its simplicity and the availability of wide variety of tools that can be used to increase the yield of soluble protein[119]. The protein expression strains, BL-21(DE3) and its derivative, BL21-CodonPlus (DE3)-RIL carrying additional tRNAs for eukaryotic codons, were used for expressing Dim1p under general conditions. However, almost all of the protein was insoluble due to the formation of inclusion bodies in *E. coli*. Attempts to express soluble Dim1p in *Pichia pastoris* or as a Nus-Dim1p fusion protein in bacteria were also unsuccessful.

In our next strategy we wanted to express the N and C terminal domains of Dim1p separately. The N-terminal domain contains the conserved SAM binding region and our assumption was that it should be soluble, based on the fact that other methyltransferases with this characteristic domain were soluble and also crystallized. However, when expressed in bacteria, the N-terminal domain was also insoluble. We have not attempted to express the C-terminal domain alone, as another strategy to express the entire protein had been successful. When the entire protein, Dim1p was expressed under mild conditions, considerable amount of protein could be purified in soluble form although some amount of the protein was still insoluble. The concentration of the soluble protein could be enhanced by modifying the buffer conditions.

Expression of Nus-Dim1p fusion protein

NusA protein is highly soluble (> 90%), when expressed in *E. coli*, and has been proven successful in increasing the solubility of many target proteins when attached to it[120]. If the fusion protein was soluble, then NusA protein could be cleaved off and Dim1p could be purified. Therefore, Dim1p was attached at the C-terminal end of Nus and expressed in *E. coli*. The fusion protein (MW ~110 kD) also has His tag. The purification of proteins was carried out by Ni^{2+} affinity chromatography and were analysed by SDS-PAGE. However, the His-tag stain which identifies the His-tagged proteins, clearly shows that a large amount of fusion protein was insoluble (Figure 9). The soluble fractions showed only a small amount of right sized fusion protein but also had a mixture of proteins ranging from 110 kD to 20 kD. This could be due to proteolytic degradation or abrupt ending of translation process.

Expression of Dim1p in *Pichia pastoris*

The next strategy was to express Dim1p in *Pichia pastoris*, a methylotrophic yeast. The *Pichia pastoris* expression system is being used successfully for the production of various recombinant heterologous proteins[121]. This methylotrophic yeast is particularly suited to foreign protein expression for a number of reasons, including ease of genetic manipulation, high-frequency DNA transformation, cloning by functional complementation, high levels of protein expression at the intra- or extracellular level, and the ability to perform higher eukaryotic protein modifications, such as glycosylation, disulfide bond formation and processing. We were very optimistic about the expression Dim1p in another yeast, but to our surprise, the protein could never be expressed.

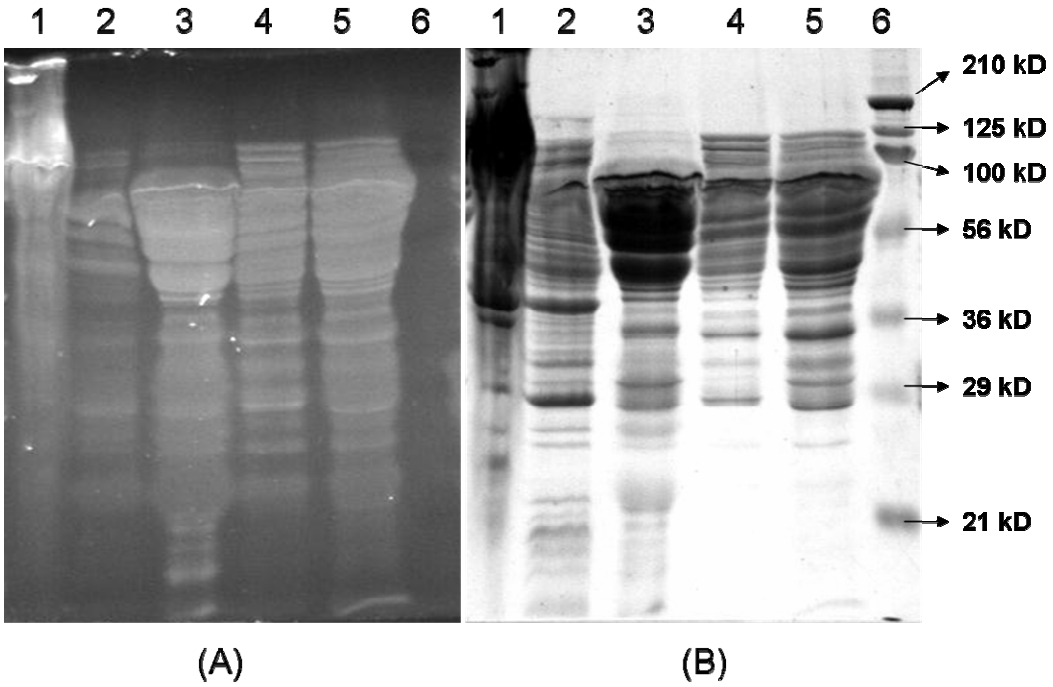

Figure 9: SDS-PAGE analysis of Nus-Dim1p fusion protein. (A) His-tag stain shows the His-tagged proteins as fluorescent bands when exposed to UV light. (B) Coomassie blue staining. Lane 1 has the insoluble portion of the cell lysate; Lane 2 has the soluble portion of cell lysate; Lanes 3-5 have the eluate fractions from the Ni column; Lane 6 has the pre-stained standards.

The plasmid construct encodes Dim1p with N-terminal α-factor secretion signal and C-terminal His-tag. The linearized plasmid was transformed into *P. pastoris* (X-33), which were then grown in a large culture and induced with methanol. The α-factor secretion signal is responsible for secreting the expressed protein into the medium. However, no protein was found after passing the medium over Ni^{2+} column. The cells were also lysed suspecting that the endogenous nuclear localization signal of Dim1p might have prevented it from secretion. However, no his-tagged protein could be detected in the cell lysate.

Expression of Dim1p under mild conditions

Induction of the protein under mild conditions in BL21-CodonPlus (DE3)-RIL cells or Rosetta 2 (DE3) cells with pET15b-*DIM1* plasmid has finally proved to be successful to obtain soluble Dim1p. After growing the culture at 37 ˚C, protein induction was carried out at 25 ˚C using one-fifth of the amount of IPTG normally used. Protein purification was carried out using affinity chromatography and analysed by SDS-PAGE. Incorporation of 15% glycerol and 3 mM β-ME in the purification buffers enhanced the amount of soluble protein considerably. The his-tag and coomassie staining show that the eluted protein is relatively pure and stable during purification procedures (Figure 10). However, the protein precipitated out as aggregates during storage for more than couple of weeks at 4˚C. The aggregation was also enhanced by freeze-thaw cycles and/or reducing the concentration of glycerol and β-ME in the buffer. Attempts to concentrate the protein also led to rapid precipitation.

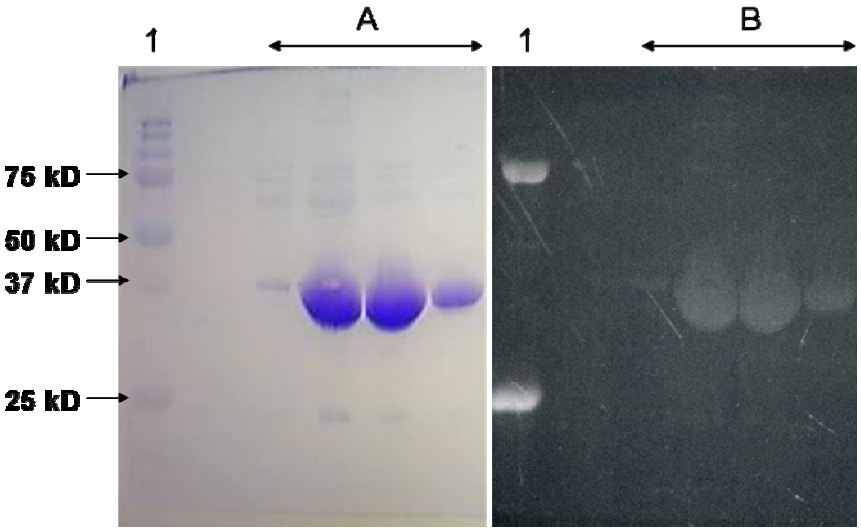

Figure 10: Soluble Dim1p. Protein standards have been loaded in lane 1. Two of standards (75 kD and 25 kD) also show strong fluorescence with His-tag stain. (A) Dim1p eluate fractions stained with coomassie blue; (B) eluate fractions showing fluorescence with His-tag stain.

Discussion

Purification of soluble and stable protein is a tedious process involving several trials. In most cases, strategies are guided by protocols used successfully under similar problems or for similar or related proteins. However, because every protein is different, the strategies and purification protocols must be worked out for every protein based on its intended use. Similarly, the strategies employed for the expression of Dim1p was based on successful trials used for other proteins.

Using large tags, such as the 'Nus' to increase the apparent solubility of a target protein is a well known method. However, in the case of Nus-Dim1p fusion protein, the target protein has dragged considerable amount of soluble carrier into the insoluble portion. Even though some amount of the protein was soluble, it was heterogenous (Figure 9). His-tag stain suggests that the multiple proteins observed in the eluate belong to the fusion protein. Degradation of the fusion protein by a protease could be one of the reason. Another reason might be that the translation process is ending abruptly, as the fusion protein is very large (~860 aa).

Failure of the Dim1p expression in *Pichia pastoris* was also quite surprising. The α-factor signal sequence at the N-terminal end of the protein will direct the translated protein into the secretory pathway and during the process the signal will be cleaved. Dim1p, also has a nuclear localization signal, and the presence of opposing signals on the same protein might cause some problem. Another reason could be the post-translational modifications occurring on the protein expressed in *Pichia*, of which O- and N-linked glycosylation are most common. It is possible that *Pichia* will glycosylate heterologous

proteins, even when those proteins are not normally glycosylated by the native host; and even when the protein is glycosylated in the native host, *Pichia* may glycosylate at another site[122].

The insolubility of the N-terminal domain of Dim1p, when other methyltransferases with the same domain were soluble, was also unexpected. This raises the possibility that the aggregation is due to the presence of hydrophobic patches on the surface of the Dim1p and the problem worsens as the protein concentration increases. So, the expression of soluble Dim1p under mild conditions could be due to the lower concentration of protein in the cell and the presence of glycerol and β-ME in the buffers. It has also been suggested that slower rates of protein production allow newly transcribed recombinant proteins time to fold properly[123].

Materials and Methods

The identification and cloning of *DIM1* gene was described by Lafontaine et al.[73] and the plasmid (pET15b-*DIM1*) was provided to us by Dr. Jean Vandenhaute. It was confirmed by sequencing and the construct results in Dim1p with N-terminal His-tag. Analysis of the *DIM1* gene sequence revealed the use of codons that are rare in *E. coli*; therefore, the protein was expressed in BL21-CodonPlus (DE3)-RIL cells (Stratagene), or Rosetta 2 (DE3) cells (Novagen) which contain extra copies of tRNAs for rare codons.

Expression of Nus-Dim1p fusion protein

DIM1 was amplified from pET15b-*DIM1* as a *Sma*I-*Xho*I fragment and subcloned into pET44a vector (Novagen) to give pET44a-*DIM1* which results in a fusion protein (His

tag-Nus tag-His tag-S tag-Dim1p). Primer information is given in appendix. This clone and all subsequent clones were confirmed by sequencing at Nucleic Acids Research Facilities, Virginia Commonwealth University.

Protein was expressed in BL21-CodonPlus (DE3)-RIL cells (Stratagene). Cell cultures were grown at 37°C to an OD_{600} of 0.6 in the presence of ampicillin and chloramphenicol and induced with 1 mM IPTG. After 4 h at 37°C, cells were harvested by centrifugation. Purification was carried out by affinity chromatography using a HiTrap Chelating column (Amersham) equilibrated with 0.1 M $NiSO_4$, and buffers with 50 mM NaH_2PO_4, 300 mM NaCl, and imidazole (10 mM in lysis buffer, 20 mM in wash buffer 1, 50 mM in wash buffer 2 and 300 mM in elution buffer) at pH 8.0. The cell pellets were resuspended in lysis buffer and broken by passing through an Avestin EmulsiFlex-C3 homogenizer two times at 15,000 psi, and centrifuged to remove cell debris. Cleared lysate was loaded onto the Ni^{2+} column, washed and then eluted.

Expression of N-terminal domain of Dim1p

The N-terminal region of *DIM1* was amplified from pET15b-*DIM1* as a *Nde*I-*Xho*I fragment and subcloned into pET21c vector to give pET21c-*DIM1N*, which encodes the N-terminal domain of Dim1p with C-terminal his-tag. Protein expression and purification protocol is same as described for Nus-Dim1p protein.

Expression of soluble Dim1p under mild conditions

For expression of Dim1p, the plasmid pET15b-*DIM1* is transformed into BL21-CodonPlus (DE3)-RIL cells (Stratagene). Identical results were also obtained with Rosetta 2 (DE3) cells (Novagen). The transformed cells were grown at 37°C to an OD_{600} of 1.2 in

the presence of ampicillin and chloramphenicol. Then the protein expression is induced under mild conditions with 0.2 mM IPTG at 25°C and harvested after 4 h. Purification was carried out by affinity chromatography using a Ni^{2+}-NTA Agarose column (Qiagen) and buffers with 50 mM NaH_2PO_4, 300 mM NaCl, 15% glycerol, 3 mM β-mercaptoethanol and imidazole (10 mM in lysis buffer, 20 mM in wash buffer 1, 50 mM in wash buffer 2 and 300 mM in elution buffer) at pH 8.0. The cell pellets were resuspended in lysis buffer and broken by passing through an Avestin EmulsiFlex-C3 homogenizer two times at 15,000 psi, and centrifuged to remove cell debris. Cleared lysate was loaded onto the Ni^{2+} column, washed and then eluted. To increase the stability of the protein, glycerol and 2-mercaptoethanol were added to the purified protein to final concentrations of 25% and 6 mM, respectively. The eluate fractions with soluble Dim1p were estimated to be >95% pure by SDS-PAGE.

Expression of Dim1p in *Pichia*

DIM1 was amplified from pET15b-*DIM1* as a *Eco*RI-*Xba*I fragment and subcloned into pPICZαA vector to give pPICZαA-*DIM1*, which encodes the Dim1p with N-terminal α-factor secretion signal and C-terminal His-tag. This subcloning procedure was carried out in XL1-blue cells using zeocin as the selection marker. The plasmid was linearized in the *5´AOX1* region using *Sac*I, and then transformed into *Pichia pastoris* (X-33) by electroporation. The construct gets integrated into *AOX1* locus which was confirmed by PCR. The transformed *Pichia* cells were grown at 30˚C to an OD_{600} of 2-6 in baffled flask. The cells were then transferred to a fresh medium containing methanol and the induction is maintained for 4 days by the addition of methanol to a final concentration of 0.5% every

24 hrs. Samples were collected at regular intervals during the four days and centrifuged to separate the medium and cell pellet. Since the protein was intended to be secreted out, the medium was loaded onto a HiTrap Chelating column (Amersham) equilibrated with 0.1 M $NiSO_4$, washed and eluted with buffers described under Nus-Dim1p fusion protein. The cell pellets were resuspended in lysis buffer and broken by passing through an Avestin EmulsiFlex-C3 homogenizer three times at 25,000 psi, and centrifuged to remove cell debris. Cleared lysate was loaded onto the Ni^{2+} column, washed and then eluted. The eluate fractions in both the cases did not have any Dim1p.

All the protein samples were analysed by SDS-PAGE using 'InVision His-tag' stain (Invitrogen) and coomassie blue.

CHAPTER 3: Functional Conservation

All ribosomes share the same general architecture, with small and large subunits made up of roughly similar rRNA species and a variety of ribosomal proteins. However, the fundamental assembly process differs significantly between eukaryotes and eubacteria, not only in distribution and mechanism of modifications but also in organization of assembly steps. Despite these differences, members of the Dim1/ KsgA methyltransferase family and their resultant modification of small-subunit rRNA are found throughout evolution and also present in the last common ancestor. The location of the two adjacent adenosines near the functional core of the ribosome might be one of the reasons, as critical regions of the ribosome have changed very little through out evolution.

Helix 45 (in *E. coli* 30S), containing the two dimethylated adenosines in its loop, is also one of the most highly conserved sequences in small subunit rRNA[47,124]. Although the Dim1/KsgA family members have diverged to carry out secondary functions, both the yeast Dim1p and human mtTFB have been shown to complement for KsgA function in bacteria[74,97]. This indicates that the eukaryotic and organellar enzymes were able to recognize the bacterial substrate, which is supported by the fact that the target adenosines are located in a highly conserved region of small subunit, favoring such cross reaction. Although the actual *in vivo* substrate for the methyltransferase is not known, substantial amount of information is now available from *in vitro* 30S reconstitution experiments. It has

been well established that functional eubacterial ribosomes can be assembled *in vitro* using only the component rRNAs and ribosomal proteins[125], although additional factors are required *in vivo* for optimal assembly[126]. These experiments provided several intermediates that were tested for substrate recognition by KsgA.

16S rRNA alone is not a substrate for KsgA, but a minimal *in vitro* substrate has been found to consist of 16S rRNA plus a subset of ribosomal proteins S4, S6, S8, S11 and S15-S18 which are all located in the body and platform of the 30S subunit[127]. Studies also showed that the ribosomal protein S21 is inhibitory for KsgA activity[102,127], in an indirect way[51]. It is also known that S21 is assembled in the later stages of 30S biogenesis. Therefore, the *in vivo* substrate for KsgA is an intermediate particle in the 30S biogenetic pathway, in which the body and platform have been assembled. KsgA is also able to methylate fully formed 30S subunits, although these subunits must be in a translationally inactive conformation to support methylation[51]. Given this, it is striking that KsgA orthologs from yeast and human mitochondria can recognize their substrate in bacterial ribosomes *in vivo*. Since a soluble Dim1p is now available (chapter 2), we wanted to test if Dim1p can methylate bacterial 30S *in vitro*, confirming the *in vivo* data. We have also included an ortholog (MjDim1) from an archaeal organism, *Methanocaldococcus jannaschii*, as archaeal rRNA modification seems to be more similar to that found in eukaryotic organisms[45]. Although the overall sequence homology is low across the domains, the characteristic motifs responsible for SAM binding (Rossman-like fold) are highly conserved (Figure 11). Accordingly, our results indicate that the bacterial,

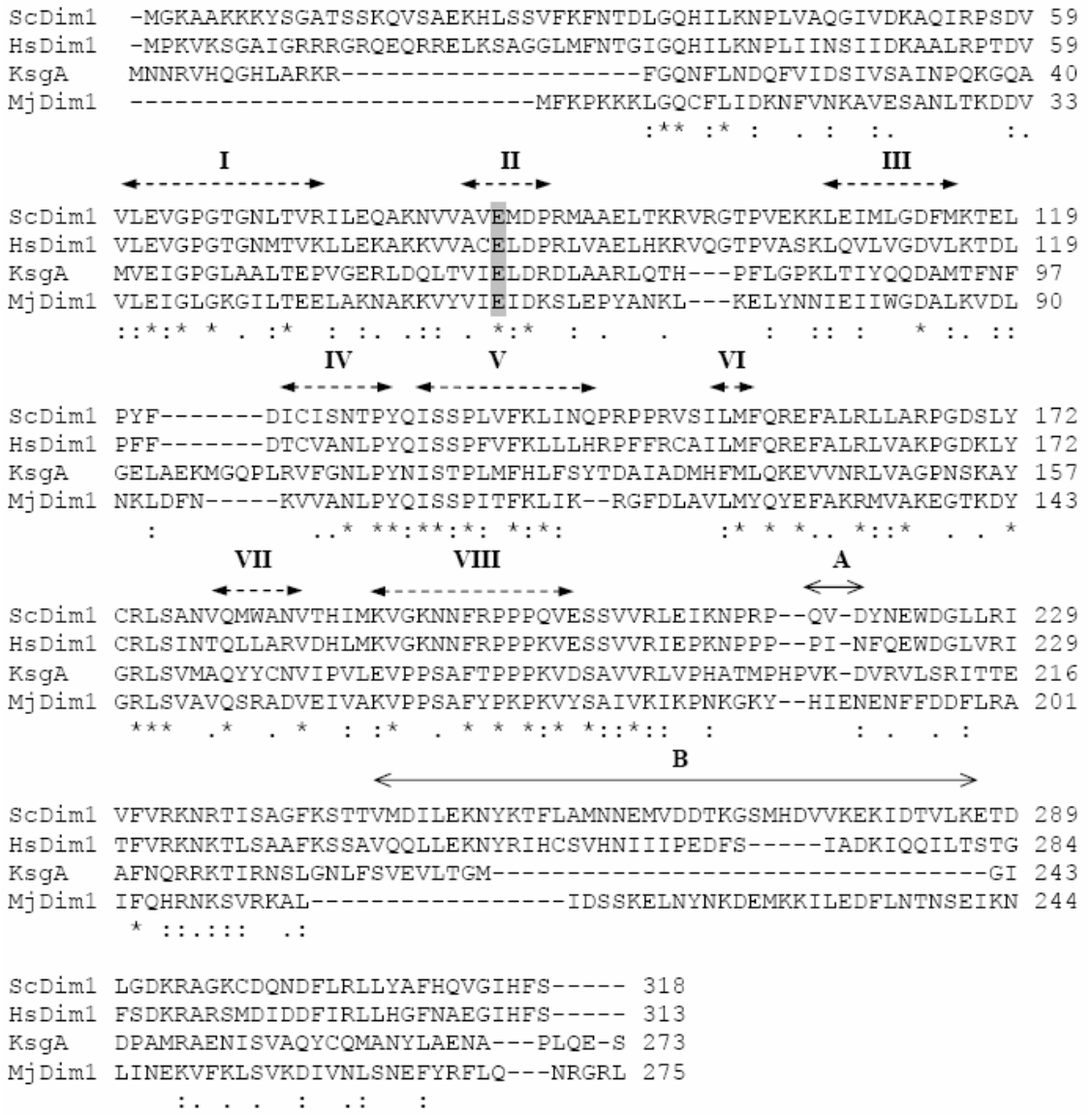

Figure 11. Structure-based sequence alignment of Dim1p from *S. cerevisiae* (ScDim1, P41819), *Homo sapiens* (HsDim1, Q9UNQ2), bacteria (*E. coli*- KsgA, P06992), and archaea (*M. jannaschii*- MjDim1, NP_248023). Structures used for alignment were those of KsgA (PDB ID 1QYR) and HsDim1 (PDB ID 1ZQ9). The alignment was generated using the TCoffee Web server[128]. Identical residues are denoted with an asterisk, strongly conserved residues with a colon, and weakly conserved residues are marked with a period. The glutamate highlighted in grey (85th residue in yeast Dim1p) is mutated to alanine to obtain catalytically inactive enzyme, resulting in non-dimethylated 40S subunits. (A) indicates VD residues in the linker region at which domains were swapped for the construction of chimeras. (B) indicates the insert in C-terminal domain of Dim1 which is absent in KsgA but partially present in MjDim1. Dashed arrows indicate motifs common to SAM-dependent methyltransferases.

eukaryotic, and archaeal enzymes can recognize a common bacterial substrate, despite differences in their respective small subunit maturation processes.

***In vivo* analysis**

Dim1p has been shown to complement for KsgA function in *ksgA* $^{-}$ *E. coli* cells[73], demonstrating functional equivalence of the two proteins. We asked whether MjDim1 could also complement the function of KsgA. *In vivo* activities of both Dim1p and MjDim1 were assessed using a modified minimal inhibitory concentration (MIC) assay, which takes advantage of the fact that loss of KsgA function renders bacteria resistant to the antibiotic kasugamycin (ksg)[100,101]. Plasmids containing the two proteins were transformed separately into a ksg^{R} strain of *E. coli*, which lacks endogenous KsgA activity. This strain was constructed from BL-21 (DE3) cells; this allows leaky expression from the pET15 T7 promoter. Growth on ksg was compared to cells transformed with pET15b-KsgA plasmid (positive control) and cells transformed with empty vector (negative control). Unlike in a traditional MIC, untransformed cells are naturally resistant to the antibiotic and become sensitive when transformed with a functional dimethyltransferase. Therefore, cells transformed with KsgA have a low MIC of 400 μg/mL ksg, while cells transformed with an empty vector have a high MIC, greater than 3000 μg/mL ksg. As shown in Figure 12, MjDim1 is fully functional in this *in vivo* system, with an MIC of 400 μg/mL. Dim1p, on the other hand, shows partial activity on bacterial ribosomes *in vivo*, with an MIC of 1200 μg/mL. While Dim1p does not restore full sensitivity to the antibiotic, it does show increased sensitivity, indicating that the enzyme is able to

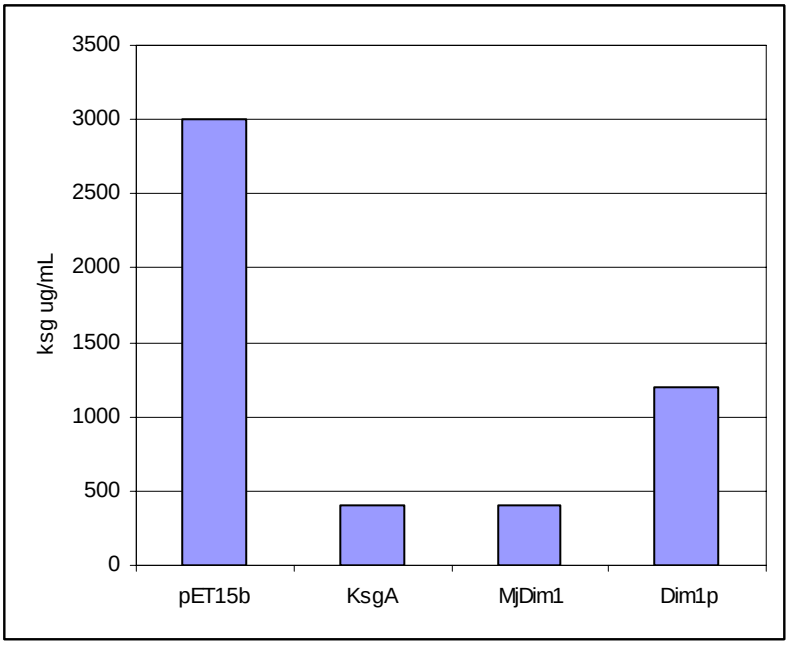

Figure 12: *In vivo* activity of Dim1p orthologs

recognize the small subunit as a substrate. Lack of full complementation may correlate with slower and/or incomplete methylation of 30S as compared to the other two enzymes[73] (see nucleotide analysis).

***In vitro* analysis**

We next tested how efficiently Dim1p and MjDim1 were able to methylate *E. coli* 30S in an *in vitro* assay. Unmethylated 30S subunits were prepared from the ksg^R strain described above. Incorporation of ^{3}H-methyl group from labeled SAM by each enzyme was followed at discrete time points over an interval of two hours. Control experiments were performed with 30S subunits purified from wild-type *E. coli* cells, which are methylated by endogenous KsgA and thus do not serve as substrates. Initial experiments were performed with 10 pmol of 30S substrate and 1 pmol of enzyme. This amount of protein did not allow for completion of the reaction within two hours, so experiments were also performed using 10 pmol each of 30S and enzyme.

Figures 13a, 13b, and 13c show the time course of methylation for Dim1p, KsgA, and MjDim1 respectively. Methylation of *E. coli* 30S by Dim1p and MjDim1 closely followed the KsgA time course, both in rate of incorporation and final level of methylation. In reactions with 1 pmol of enzyme, MjDim1 showed a slightly higher rate of ^{3}H incorporation than KsgA and ScDim1 at later time points. With stoichiometric amounts of protein relative to 30S, the time course of methylation was essentially indistinguishable between the three proteins, thus confirming the ability of the enzymes from eukaryotes and archaea to recognize bacterial 30S subunits as substrates.

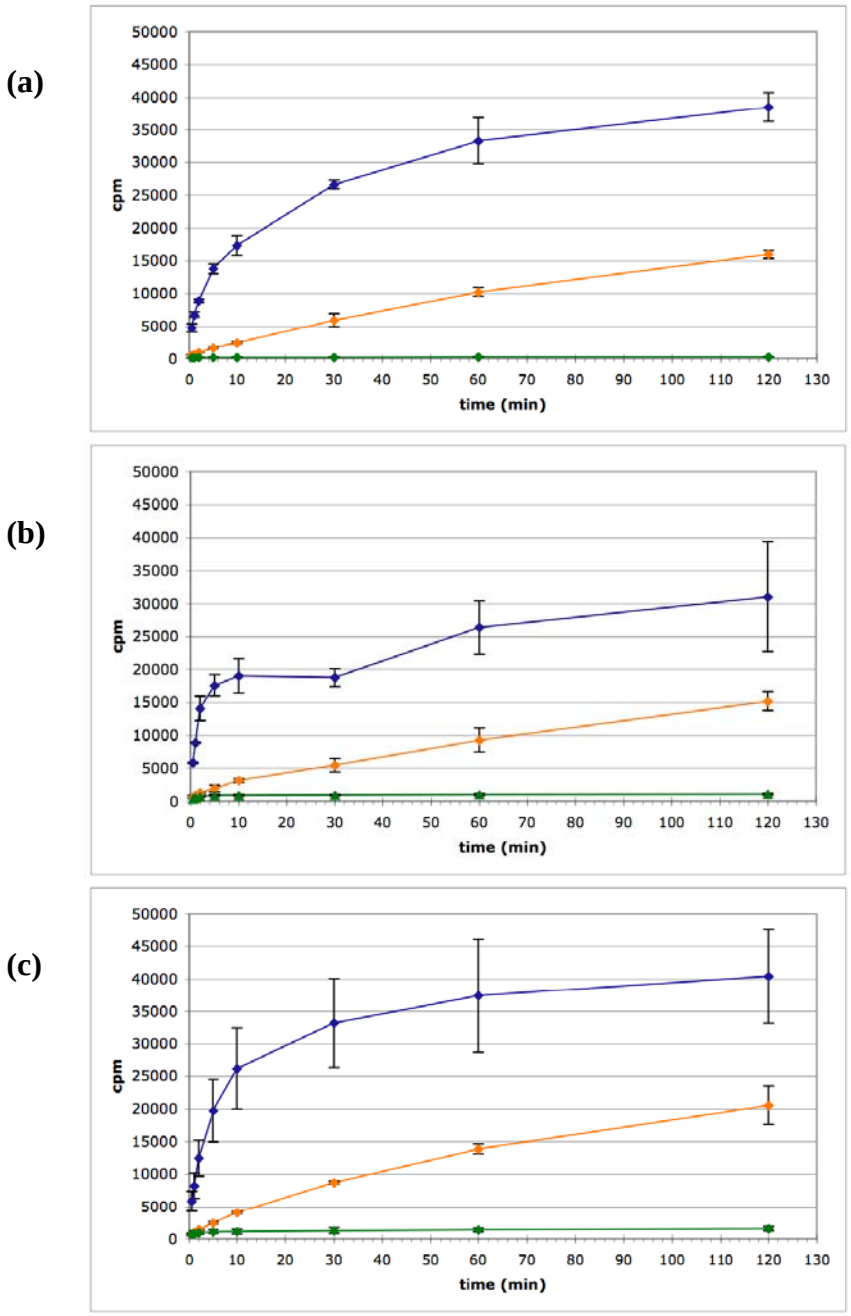

Figure 13: *In vitro* methylation of 30S. Time-course assays for (a) Dim1p, (b) KsgA, and (c) MjDim1. Blue lines indicate assays containing 10 pmol ksg^R 30S, 10 pmol enzyme; orange lines indicate assays containing 10 pmol ksg^R 30S, 1 pmol enzyme; green lines indicate control assays containing 10 pmol wt 30S subunits, 10 pmol enzyme. Assays were performed in triplicate; error bars represent standard deviation.

We then estimated the amount of methyl groups transferred at the two-hour time point by each enzyme, with both 1 pmol and 10 pmol amounts of enzyme, by constructing a standard curve of cpm versus concentration of ^{3}H-methyl-SAM. With 10 pmol of 30S per reaction, and four methylation sites per 30S molecule, we would expect to see transfer of 40 pmol methyl groups if the reactions have gone to completion. As shown in Figure 14, our calculations lead to slight overestimation of methyl group transfer, probably due to error in ^{3}H counting. However, the reactions performed with 10 pmol enzyme appear to be more or less complete after 2 hours. Reactions performed with only 1 pmol enzyme are approximately halfway completed after 2 hours.

Nucleoside analysis

In vitro assays of the three proteins, performed as described above for the time course, were incubated for 2 hours and analyzed to determine relative amounts of m^6A and m_2^6A (Figure 15; Table 1). 16S rRNA isolated from 30S subunits methylated by 10 pmol of either KsgA or MjDim1 contained no detectable labeled m^6A; radioactive incorporation was seen only in the dimethyladenosine peak. This agrees with the *in vitro* data suggesting that these reactions have gone to completion (Figure 14). Dim1p, on the other hand, produced a mixture of m^6A and m_2^6A; approximately 28% of the incorporated radiolabel was found on monomethylated adenosine. This indicates that at most 80% of the potential sites were methylated after two hours.

Partially methylated 30S from reactions using 1 pmol of enzyme showed radioactive peaks at both m^6A and m_2^6A. Surprisingly, although the total level of methylation was similar for all three enzymes (Figure 14), rRNA methylated by the

pmol

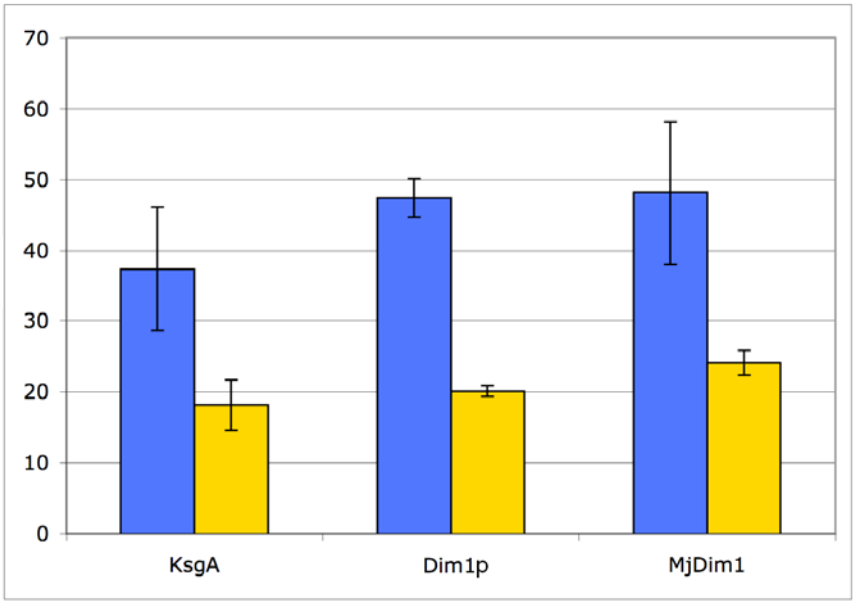

Figure 14: Quantitation of methyl groups transferred after two hours. Blue bars represent assays performed with 10 pmol enzyme; yellow bars represent assays using 1 pmol enzyme. Assays were performed in triplicate; error bars represent standard deviation.

Table 1: Quantitation of methylated adenosine species.

		total CH_3 (pmol)[a]	m^6A : $m_2{}^6A$ ratio	m^6A (pmol)	$m_2{}^6A$ (pmol)[b]
Dim1p	1 pmol	20.1 ± 0.7	1.4 : 1	8.3	5.9
	10 pmol	47.4 ± 2.7	0.8 : 1	13.5	16.9
KsgA	1 pmol	18.1 ± 1.7	0.8 : 1	5.2	6.5
	10 pmol	37.4 ± 10.1	-	ND[c]	37.4
MjDim1	1 pmol	24.1 ± 3.6	0.02 : 1	0.2	11.9
	10 pmol	48.1 ± 8.8	-	ND	48.1

[a]Data from Figure 14.
[b]1 pmol $m_2{}^6A$ corresponds to 2 pmol methyl groups.
[c]ND - none detected.

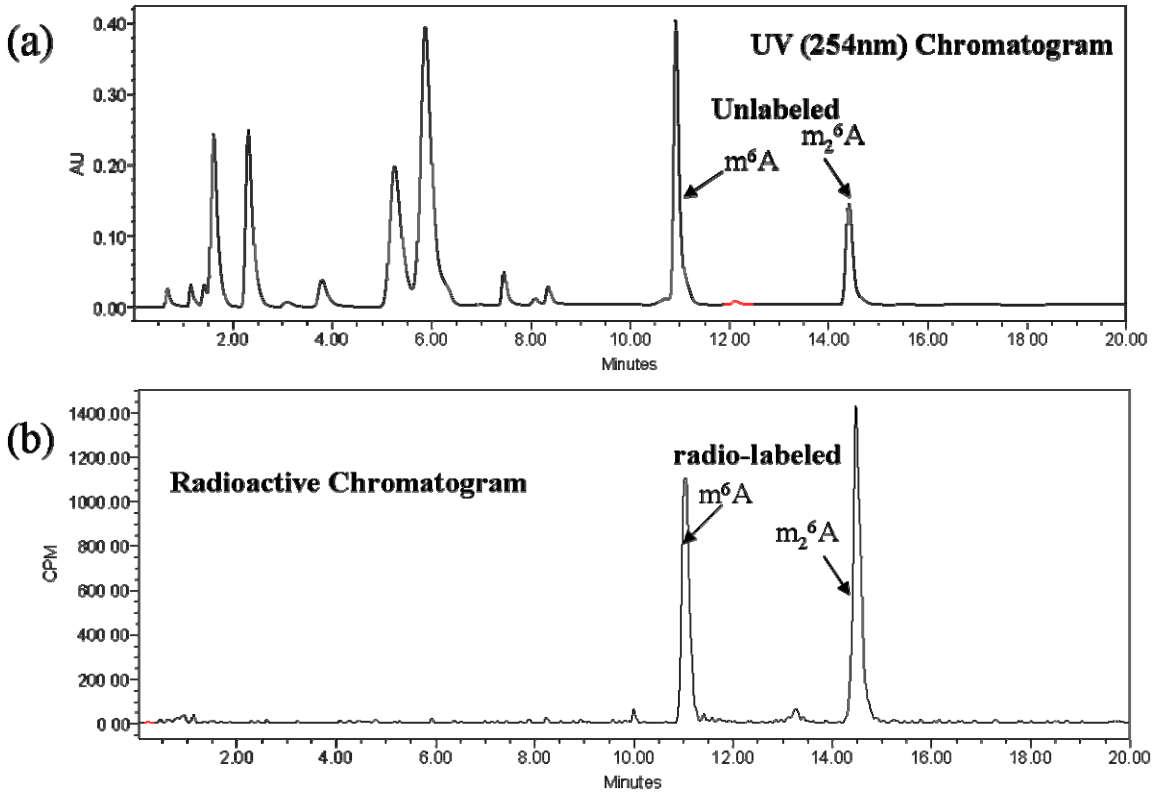

Figure 15: Nucleoside analysis by HPLC. (a) UV chromatogram showing the retention times of 4 major nucleosides present in 16S rRNA along with the exogenously added nonradioactive reference nucleosides, m^6A and $m_2{}^6A$. (b) Chromatogram showing the radio-labeled m^6A and $m_2{}^6A$, obtained after the *in vitro* methylation of 10 pmol ksg^R 30S using 1 pmol Dim1p.

different enzymes showed different ratios of m^6A to m_2^6A. Dim1p produced approximately 1.4 times as much m^6A as m_2^6A. MjDim1, conversely, produced almost no m^6A; only about 1% of the incorporated methyl groups were found on m^6A. KsgA fell somewhere between the other two, producing both m^6A and m_2^6A, with only 0.8 times as much m^6A as m_2^6A. These results could be a result of assaying enzymes from different species on the bacterial substrate, or they could reflect a difference in reaction mechanism.

Discussion

The Dim1/KsgA enzymes transfer a total of four methyl groups from four SAM molecules to two adenosines. The exact mechanism of transfer has not yet been established; questions remain as to order of addition, if any, and the number of binding events required for the four methylations. The above data begin to address the question of the multiple methyl group transfers. Partially methylated 30S were produced in reactions containing 10 pmol 30S subunits and 1 pmol enzyme. Therefore, m^6A produced in excess of 2 pmol (corresponding to two adenosines available for methylation per subunit) will only be seen if the enzyme releases the substrate after monomethylation and rebinds to a new substrate. With 20.1 pmol of methyl groups incorporated by 1 pmol Dim1p, the 1.4:1 m^6A:m_2^6A ratio represents approximately 8.3 pmol labeled m^6A and 5.9 pmol labeled m_2^6A (1 pmol m_2^6A represents 2 pmol incorporated methyl groups). Therefore, under our assay conditions, Dim1p clearly releases the m^6A intermediate, which is subsequently converted to the m_2^6A product after an additional binding event.

In contrast, there is no indication that MjDim1 produces m^6A as anything but a transient intermediate. Of the 24.1 pmol methyl groups transferred, only 0.3 pmol were found on m^6A. These results suggest that the archaeal enzyme preferentially forms dimethyladenosine, without release of the monomethyl intermediate. While release of a monomethyl intermediate and subsequent rebinding and addition of the second methyl cannot be ruled out, such a model requires that MjDim1 prefers the monomethylated substrate to the unmethylated substrate to a large degree.

In terms of m^6A vs. m_2^6A production, KsgA falls somewhere in between Dim1 and MjDim1. Unlike Dim1p, KsgA produces less m^6A than m_2^6A; however, of the 18.1 pmol of methyl groups transferred, 5.2 pmol are found on m^6A, which is still indicative of a released intermediate. Although it is possible that these differences are a result of suboptimal assay conditions, these results also allow the possibility of distinct mechanisms for the three enzymes, thus demonstrating a need for future analysis to dissect the exact scheme of methyl transfer.

Substrate recognition by the Dim1/KsgA methyltransferases is complex. KsgA is able to methylate 30S subunits, but it can also methylate a pre-ribosomal particle containing 16S and a partial complement of ribosomal proteins[127]. Dim1 is essential for early processing of the pre-rRNA, but does not methylate 20S until very late in the 40S maturation process[74]. Despite evolutionary divergence of ribosomal assembly and processing pathways, eukaryotic and archaeal KsgA orthologs are able to methylate *E. coli* 30S both *in vivo* and *in vitro*. This requires the conservation of similar structural cues in small ribosomal subunits across evolution. Also complex is the mechanism of the

modification performed by these enzymes. A total of four methyl groups are transferred, from four SAM molecules, to two separate adenosines. It is clear from the crystal structure of KsgA[70] that only one SAM molecule is bound at a time, and that the adenosines enter the active site separately. It has not been determined in what order, if any, the methyl groups are transferred, or if all four of the transfers take place within a single or multiple binding events. This work demonstrates clear differences in the reaction intermediate profiles produced *in vitro* by Dim1/KsgA enzymes from bacteria, archaea, and yeast, despite the fact that the three enzymes methylate bacterial 30S to a similar extent and at similar rates in the assay used. However, we cannot exclude the possibility that the differences in the respective rates of m^6A and $m_2{}^6A$ production seen here are a result of suboptimal substrate or assay conditions rather than a reflection of true differences in mechanism. For example, the yeast and archaeal enzymes may show different activity if assayed on their respective small ribosomal subunits rather than on bacterial 30S. These results demonstrate the remarkable cross-recognition of a complex substrate by evolutionarily distant members of an enzyme family and emphasize the need to further investigate the multistep reaction mechanism.

Materials and Methods:

KsgA from *E. coli* and *MjDim1* from *M. jannaschii* were previously cloned in our laboratory into pET15b vector[49,129] which results in respective proteins with N-terminal His tag.

Protein expression and purification

pET15b-*KsgA* and pET15b-*MjDim1* plasmids were transformed into BL-21 (DE3) cells for overexpression. Cell cultures were grown to an OD_{600} of 0.6 in the presence of ampicillin and induced with 1 mM IPTG. After 4 h at 37°C, cells were harvested by centrifugation. Purification was carried out by affinity chromatography using a HiTrap Chelating column (Amersham) equilibrated with 0.1 M $NiSO_4$, and buffers with 50 mM NaH_2PO_4, 300 mM NaCl, and imidazole (10 mM in lysis buffer, 20 mM in wash buffer 1, 50 mM in wash buffer 2 and 300 mM in elution buffer) at pH 8.0. The cell pellets were resuspended in lysis buffer and broken by passing through an Avestin EmulsiFlex-C3 homogenizer two times at 15,000 psi, and centrifuged to remove cell debris. Cleared lysate was loaded onto the Ni^{2+} column, washed and then eluted.

Dim1p was expressed and purified as described in Chapter 2. Proteins were estimated to be >95% pure by SDS-PAGE analysis. Protein concentration was measured using the Bio-Rad Protein Assay.

30S purification

An *E. coli* strain lacking functional KsgA was constructed by growing BL-21 (DE3) cells on kasugamycin (ksg) to select for loss of the dimethylations. 30S ribosomes from this ksg^R strain were used in an *in vitro* assay to confirm that the adenosines were able to be methylated, and therefore that the resistance to ksg was due to lack of KsgA activity. 30S subunits from both ksg^R strain and the wild-type strain were prepared as described by Blaha *et al.*[130], except that cells were broken as described above. Purified subunits were dialyzed into reaction buffer (40 mM Tris at pH 7.4; 40 mM NH_4Cl; 4 mM

MgOAc; 6 mM 2-mercaptoethanol) and stored at –80°C in single-use aliquots. 30S concentration was estimated by measuring the absorbance at 260 nm and using a relationship of 67 pmol 30S per 1 unit of optical density.

***In vivo* assay**

ksg^R cells were transformed with the pET15b constructs of *DIM1*, *KsgA*, and *MjDim1* and selected on LB plates containing ampicillin. Transformed colonies were inoculated into liquid media and grown overnight. These cultures were diluted 1:25 in fresh LB containing 50 μg/mL ampicillin and grown to OD_{600} of 0.7-0.8. The cultures were again diluted 1:100 with fresh LB and 3 μL of the dilution was plated onto LB/ ampicillin containing increasing amounts of kasugamycin, from 0 to 3000 μg/mL. Plates were incubated at 37°C overnight and visually inspected for colony formation.

***In vitro* assay**

The *in vitro* assay was adapted from Poldermans *et al*[102]. Time-course reactions were performed in 500 μL volumes containing 40 mM Tris (pH 7.4), 40 mM NH_4Cl, 4 mM MgOAc, 6 mM 2-mercaptoethanol, 1 mM SAM with 0.02 mM ^{3}H-methyl-SAM (780 cpm/pmol; MP Biomedicals), 100 pmol 30S subunits, and 10 or 100 pmol enzyme; volume and components were sufficient for 10 reactions. Buffer and reagents were prewarmed to 37°C and added into prewarmed tubes to minimize any lag in the reaction start. At each of eight designated time points 50 μL was removed and added to a prechilled tube containing 10 μL of 100 mM unlabeled SAM (Sigma-Aldrich) to quench the reaction; the remaining 100 μL was stored at −20°C and used for HPLC analysis (see below). The quenched reactions were deposited onto DE81 filter paper (Whatman), washed twice with ice-cold

5% TCA, and rinsed briefly with ethanol. Filters were air-dried for one hour, placed into scintillation fluid, and counted.

HPLC analysis

Labeled 16S rRNA was extracted from 30S subunits with phenol/ chloroform/ isoamyl alcohol. 16S was digested and dephosphorylated as described by Gehrke and Kuo[131], and subjected to nucleoside analysis by reversed-phase HPLC. Nuclease P1 was obtained from USBiological, shrimp alkaline phosphatase was from MBI Fermentas. HPLC analysis was performed using a Polaris C-18 column (Varian). The HPLC system used consisted of a Waters 600 Controller, a Waters 2487 Dual λ Absorbance Detector, and Waters Empower software. Radioactivity was monitored with a Packard 150TR Flow Scintillation Analyzer. Buffer A was 20 mM NaH_2PO_4 (pH 5.1). Buffer B was 20 mM NaH_2PO_4 (pH 5.1):acetonitrile 70:30. Separation was performed at room temperature using a linear gradient from 100%A-100%B over 20 min, at a flow rate of 1.0 mL/min. Nucleoside standards used were N^6-methyladenosine (Sigma-Aldrich) and N^6 N^6-dimethyladenosine, synthesized as described by Rife *et al.*[132]. Peak integration was calculated by the Empower software and used to determine ratios of m^6A:m_2^6A.

CHAPTER 4: Structural characterization of Dim1p

The members of Dim1/KsgA family, interestingly, have evolved to carryout other functions in the cell, apart from the dimethylation. This is clearly evident in eukaryotic Dim1 which has an indispensable role in pre-rRNA processing and hence survival of the organism. The enzymatic function of Dim1p in dimethylation can be uncoupled from its involvement in pre-rRNA processing indicating that dimethylation is not required for its second function[50]. Recently it has been shown that KsgA is also involved in pre-rRNA processing in *E.coli*. Knockout of KsgA leads to a processing defect resulting in the accumulation of immature small subunit rRNA (Connolly K, Rife JP, Culver GM, unpublished results). Unlike eukaryotes, this processing defect is not detrimental, as functional 30S subunits could still be formed. The Dim1 ortholog in eukaryotic mitochondria, mtTFB, serves as a mitochondrial transcription factor as well as being the dimethyltransferase for mitochondrial 12S rRNA[97,109]. Similar to Dim1, it has been found that the methylation activity of human-mtTFB can be separated from its transcription activity[110]. To perform these secondary functions, the Dim1 orthologs have undergone structural changes which is supported by the fact that the sequence homology (~25%) across the kingdoms is relatively low. In order to comprehend the precise role of Dim1 orthologs in their secondary functions, it is important to explore their structural features in detail.

Despite the low sequence homology, it has been now demonstrated that Dim1p and MjDim1 can methylate bacterial 30S subunits *in vivo* and *in vitro*[49,73] (see Chapter 3). This indicates that the bacterial, eukaryotic and archaeal enzymes can recognize a common bacterial substrate, despite differences in their respective small subunit maturation processes. However, it is not yet known if the bacterial and archaeal enzymes can complement the functions of Dim1p. The recent report that KsgA is also involved in pre-rRNA processing in *E.coli*, appears to support this assumption. Archaeal ribosome biogenesis appears to be more similar to that found in eukaryotes based on the presence of putative homologs to nuclear and nucleolar structural genes from eukaryotes and snoRNA guided nucleotide modifications[133,134]. Considering the above facts, the primary question we wanted to ask is whether KsgA and MjDim1 can recognize a substrate in eukaryotic ribosome biogenesis and complement the multiple functions of Dim1p.

Sequence alignment of eukaryotic Dim1p with bacterial and archaeal orthologs revealed a reasonable similarity in the N-terminal domain which includes the *S*-adenosylmethionine (SAM) binding domain (Figure 11). However, the most outstanding feature in the alignment is the presence of an insert in the C-terminal domain of eukaryotic and in some archaeal Dim1 which is totally absent in the bacterial protein (KsgA). The length of the insert in archaea (MjDim1) is slightly less than that in eukaryotes (Figure 11). Structural alignment using the currently available crystal structures of human Dim1 (HsDim1, PDB Id: 1ZQ9) and KsgA (PDB Id: 1QYR) shows that the insert in the C-terminal domain of Dim1p forms an extra helix along with a section of random coil and another slightly longer helix than that present in KsgA (Figure 16a and 16b). It is possible

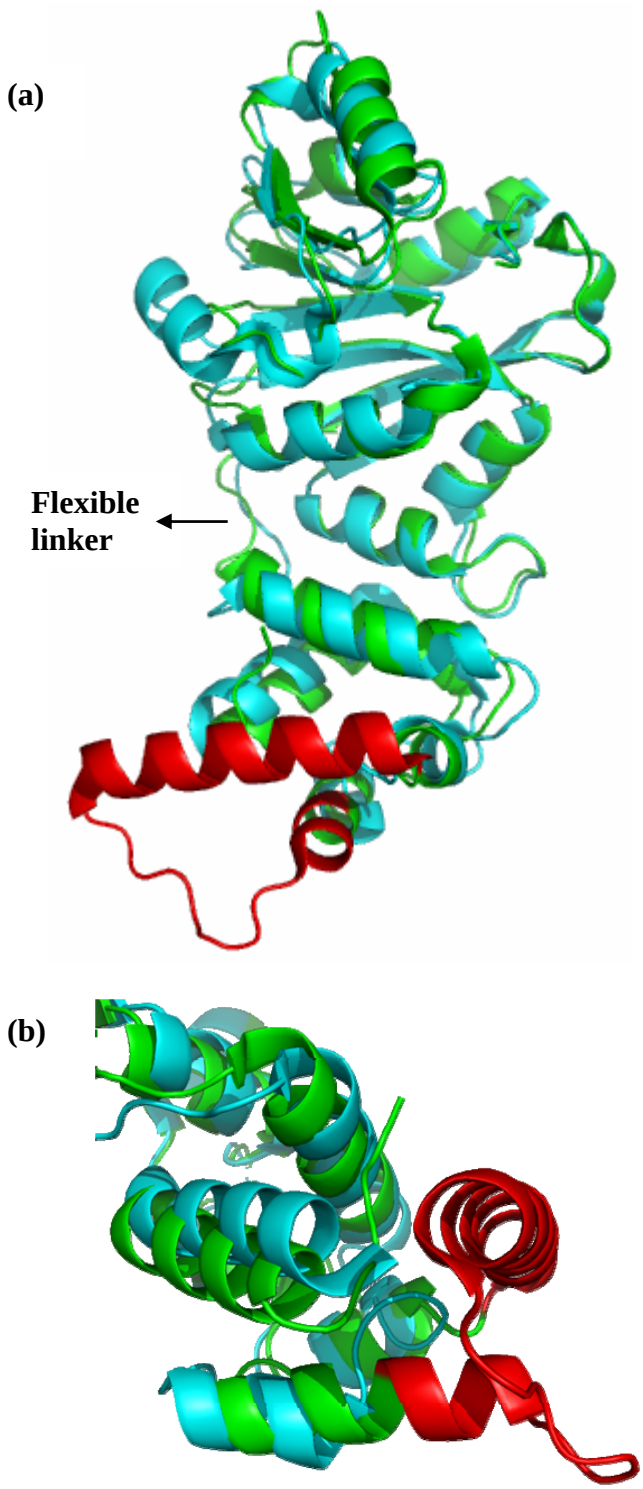

Figure 16: (a) Superposition of KsgA (blue) with HsDim1 (green). The insert in the C-terminal domain of HsDim1 is shown in red. (b) Side view of the C-terminal domain and the insert.

that this extra helix in the C-terminal domain of Dim1p makes an important interaction with RNA or another protein in the 90S pre-ribosomal particle which is essential for cleavage at sites A1 and A2. One possible candidate for such an interaction is Dim2p (also known as RRP20 and PNO1), which also was found to be essential for the A1, A2 cleavages and for the dimethylation carried out by Dim1p[76,77]. It was speculated that Dim2p might associate with Dim1p in the above functions.

Another unresolved question is about the preferred substrate of Dim1p. Binding of Dim1p to 90S pre-ribosomes occurs very early in the biogenetic pathway and Dim1p remains bound to pre-40S particles during nuclear export and cytoplasmic maturation until the dimethylation is complete[21,22]. Dimethylation is thought to be the penultimate step in maturation, occurring just before the final cleavage (Cleavage D) which converts 20S rRNA to 18S. In our earlier work (chapter 3), we have shown that Dim1p can methylate the 30S subunits of *E.coli in vitro*[49], which indicates that Dim1p recognizes the fully assembled 30S subunits, but its activity remains untested against non-dimethylated but otherwise mature 40S subunits. We have generated non-dimethylated 40S subunits and tested Dim1p, MjDim1 and KsgA for their ability to utilize these particles as substrates for methylation.

Complementation Assay

Because the yeast *DIM1* gene is essential, we used the plasmid shuffle technique, a general method for introducing mutations into cloned essential genes[135], to test the ability of *DIM1* orthologs for complementing its function *in vivo* (Figure 17). A haploid yeast

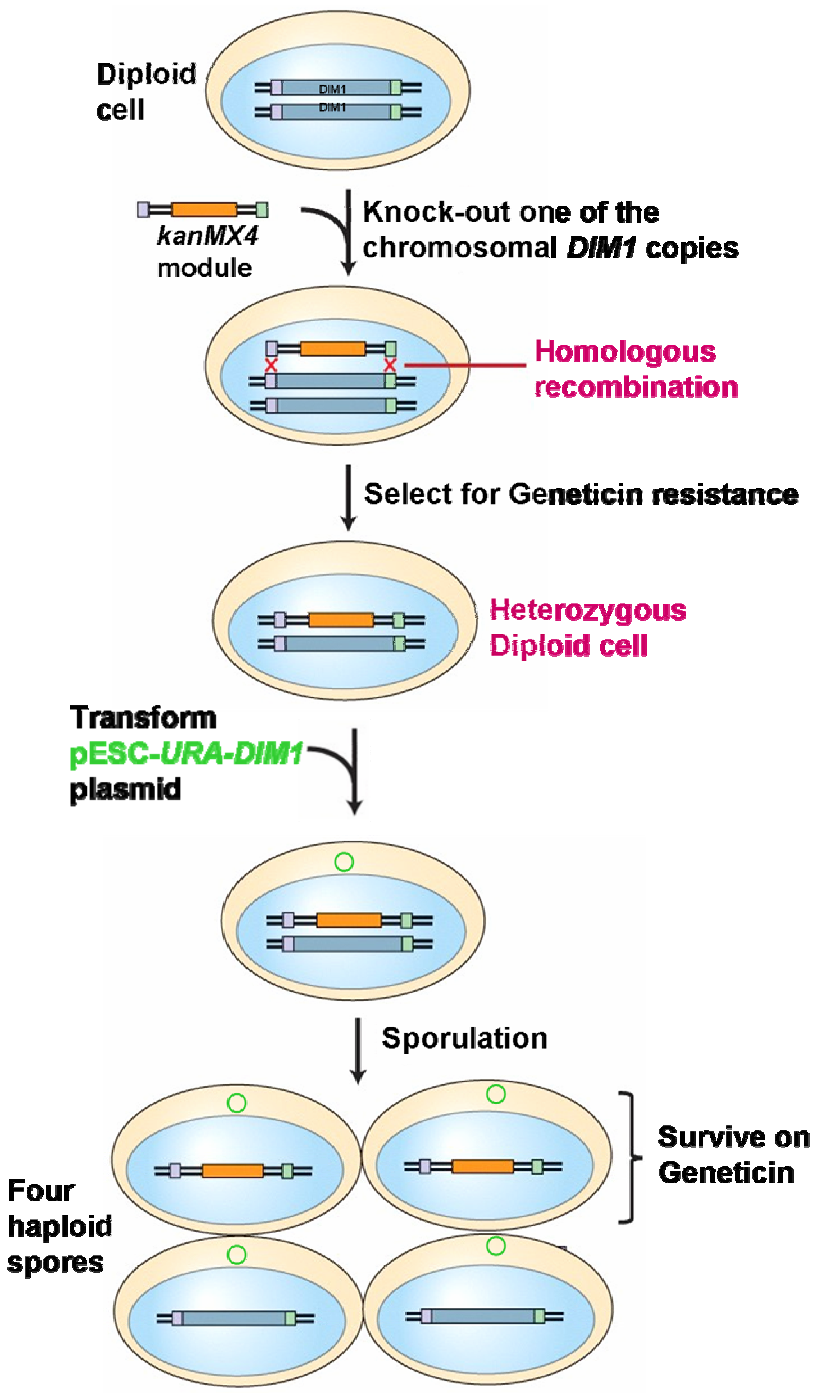

Figure 17: Plasmid shuffling technique. Continued in next page

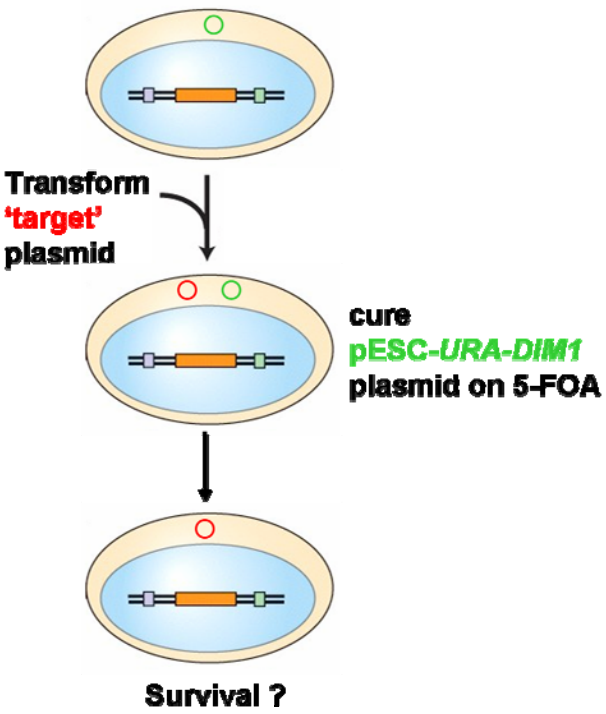

Figure 17: Plasmid shuffling technique. One of the *DIM1* chromosomal copy in the diploid strain was replaced with kanMX4 module by homologous recombination. The heterozygous diploid was then transformed with a plasmid carrying a wild type *DIM1* gene and also a *URA3* marker (pESC-*URA-DIM1*). Sporulation yields a haploid yeast strain with chromosomal *DIM1* knock-out. This strain is used to test a 'target' gene cloned into a second plasmid (pESC-*LEU*) after curing the first plasmid, pESC-*URA-DIM1*, in presence of 5-FOA.

strain was constructed that carried a deletion of the chromosomal copy of *DIM1*. Viability of this strain, Y26hα-URA-DIM1, was maintained with a copy of the wild-type gene on a plasmid that also carries the *URA3* marker (pESC-*URA-DIM1*). To introduce the orthologs of *DIM1*, this strain was transformed separately with pESC-*LEU* vectors containing *KsgA* and *MjDim1*, both with and without an exogenous NLS, to ensure that the expressed proteins would be targeted to the nucleus. As a positive control, the strain was transformed with the pESC-*LEU* vector carrying the wild-type *DIM1* gene (pESC-*LEU-DIM1*) and the strain transformed with the vector alone (pESC-*LEU*) was used as a negative control. To test complementation of the *dim1*-Δ allele by *KsgA* or *MjDim1*, we plated the cells on medium containing 5-fluoroorotic acid (5-FOA). Because 5-FOA is toxic to yeast cells expressing *URA3*, this treatment allows selection of cells that have lost the plasmid carrying *URA3* and at the same time, the wild-type copy of the *DIM1* gene. Plates were incubated for 3 days at 30˚C and except for the positive control (Y2P-DIM1) none of the constructs of KsgA or MjDim1 were able to rescue the lethal phenotype of the *dim1* knockout (Figure 19a). In order to ascertain that the exogenous NLS is not interfering with the activity, another construct in which NLS is fused to the N-terminal end of Dim1p was tested as a control and found that it is innocuous (result not shown).

Role of C-terminal insert in Dim1p function

Next, we wanted to ascertain the role of the extra insert in the C-terminal domain of Dim1p in yeast and other eukaryotes by taking advantage of the two domain architecture of the KsgA/Dim1 family. In KsgA, the N- and C-terminal domains can move independently of each other to some degree[70], allowing construction of chimeric proteins which contain

domains from two proteins. If the insert is critical to Dim1's function as a participant in the A1/A2 cleavage steps, then chimeras that include the C-terminal domain of Dim1 could be suitable Dim1 substitutes.

The linker between the two domains in Dim1p has two residues, valine and aspartate which are also found in the linker region of KsgA but with a lysine in between them. Sequence alignment shows that the corresponding position in MjDim1 has isoleucine and glutamate (indicated in Figure 11). These two residues were selected as a center for domain swapping. To construct chimeric proteins, the N and C terminal domains of *DIM1*, *KsgA* and *MjDim1* were amplified separately and ligated in all six possible combinations. Chimeras were named to indicate the origin of each domain (Table 2 and Figure 18). All of the six chimeric genes were cloned into pET15b and the proteins were overexpressed in *E. coli* and shown to be soluble, although to varying degrees with DK (N-terminal domain of Dim1p and C-terminal domain of KsgA) being poorly soluble (data not shown). The chimeras were also assessed in an *in vivo* assay in bacteria, and shown to complement for KsgA function, again to varying degrees (Table 3). These results show that the chimeric proteins are able to assemble and fold in a productive manner.

The chimeric genes were then subcloned into pESC-*LEU* and transformed into Y26hα-URA-DIM1; the transformants were plated on 5-FOA. Interestingly, only Y2P-DM survived, showing that the only chimera able to complement the function of Dim1p is a construct with the N-terminal domain of Dim1p and C-terminal domain of MjDim1 (Figure 19b).

Table 2: Chimera protein construction

Parent Domains	Chimera protein
N terminal – KsgA C terminal – Dim1	KD
N terminal – Dim1 C terminal – KsgA	DK
N terminal – MjDim1 C terminal – Dim1	MD
N terminal – Dim1 C terminal – MjDim1	DM
N terminal – MjDim1 C terminal – KsgA	MK
N terminal – KsgA C terminal – MjDim1	KM

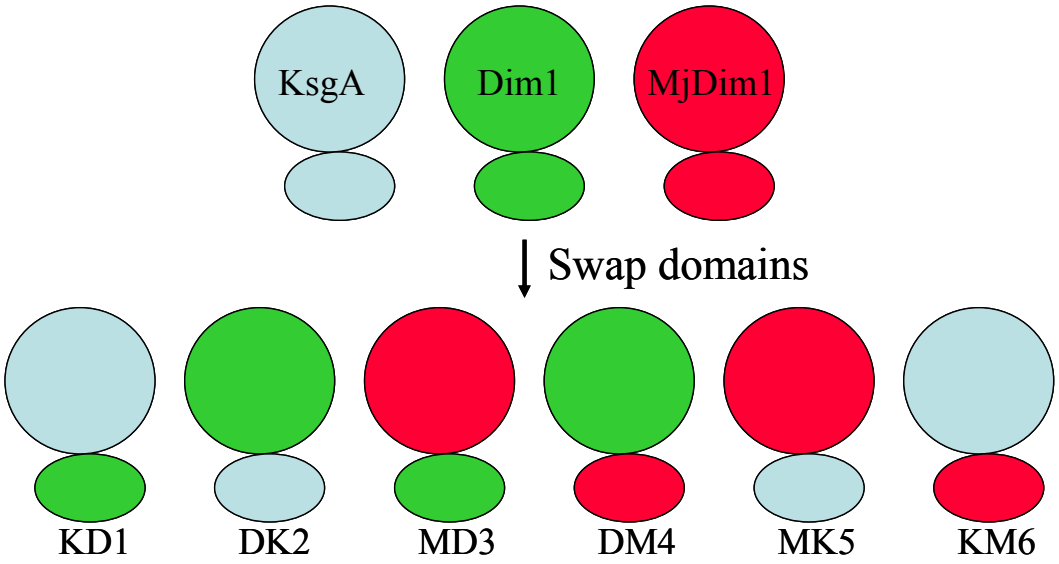

Figure 18: Chimera protein construction. The N and C-terminal domains of KsgA, Dim1p and MjDim1 were swapped to obtain six chimera proteins

Table 3: *In vivo* activity assay in *E.coli*

Plasmid	MIC (µg/mL ksg)†
pET15b	>3000
pET15b-*KsgA*	400
pET15b-*DIM1*	1200
pET15b-*MjDim1*	400
pET15b-*KD*	1200
pET15b-*DK*	2000*
pET15b-*MD*	400
pET15b-*DM*	2000*
pET15b-*MK*	400
pET15b-*KM*	800

† Concentrations of Kasugamycin (Ksg) in µg/mL used in the assay are 0, 200, 400, 600, 800, 1000, 1200, 1500, 2000, 2500, 3000.
* Very small colonies were observed

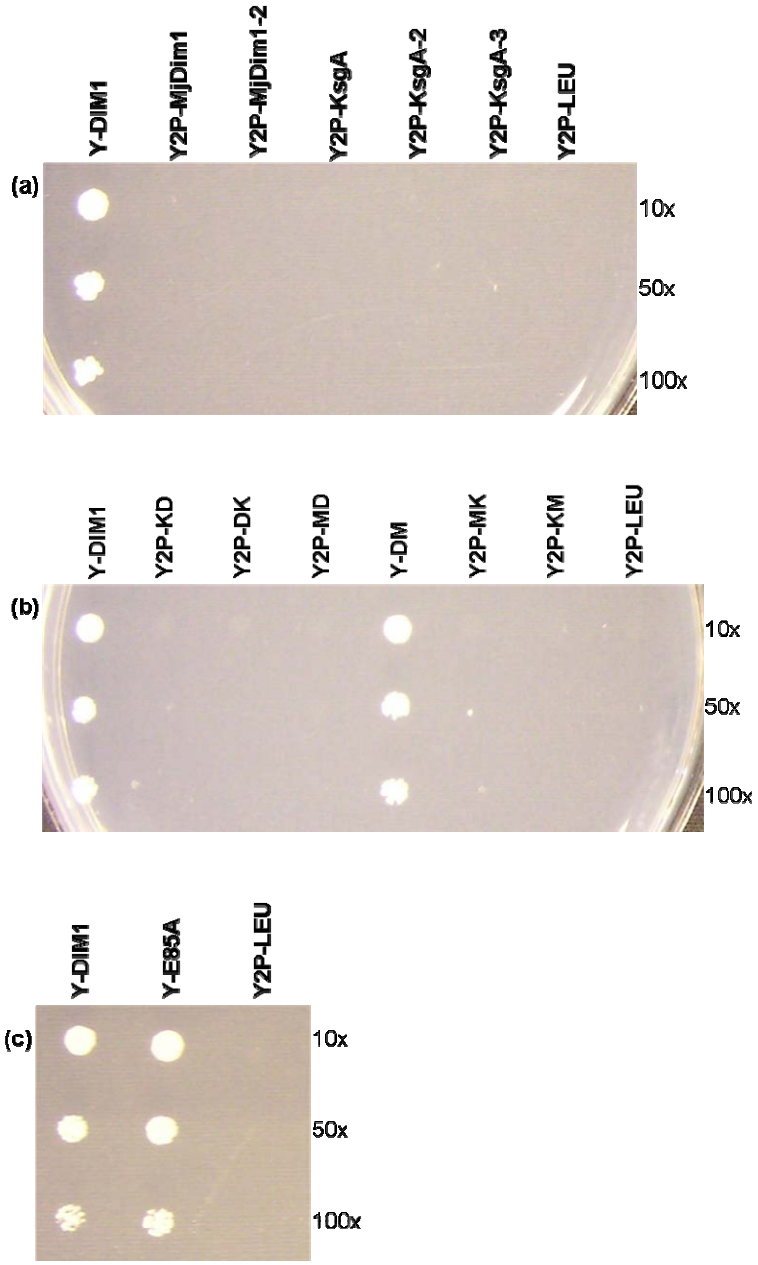

Figure 19: Complementation assay on 5-FOA plates at 30˚C for 3 days (a) of different constructs of KsgA, MjDim1, (b) chimeras and (c) dim1-E85A. Y2P-DIM1 (positive control), Y2P-DM, Y2P-E85A survived on 5-FOA, losing the first plasmid, pESC-*URA*-*DIM1* and hence these clones with only the second plasmid were relabeled Y-DIM1, Y-DM, Y-E85A respectively. Y2P-LEU with no insert in the second plasmid is the negative control.

Table 4: Yeast Strains used in the study

Genotype - *MATα his3Δ1 leu2Δ0 ura3Δ0 dim1Δ0*::*KanMX4*	
Strain	**Plasmid/s**
Y26hα-URA-DIM1	pESC-*URA-DIM1* †
Y2P-DIM1	pESC-*URA-DIM1*, pESC-*LEU-DIM1*
Y2P-DIM1-2	pESC-*URA-DIM1*, pESC-*LEU-DIM1-2**
Y2P-KsgA	pESC-*URA-DIM1*, pESC-*LEU-KsgA**
Y2P-KsgA-2	pESC-*URA-DIM1*, pESC-*LEU-KsgA-2* †
Y2P-KsgA-3	pESC-*URA-DIM1*, pESC-*LEU-KsgA-3*
Y2P-MjDim1	pESC-*URA-DIM1*, pESC-*LEU-MjDim1**
Y2P-MjDim1-2	pESC-*URA-DIM1*, pESC-*LEU-MjDim1-2*
Y2P-LEU	pESC-*URA-DIM1*, pESC-*LEU*
Y2P-KD	pESC-*URA-DIM1*, pESC-*LEU-KD**
Y2P-DK	pESC-*URA-DIM1*, pESC-*LEU-DK*
Y2P-MD	pESC-*URA-DIM1*, pESC-*LEU-MD**
Y2P-DM	pESC-*URA-DIM1*, pESC-*LEU-DM*
Y2P-MK	pESC-*URA-DIM1*, pESC-*LEU-MK**
Y2P-KM	pESC-*URA-DIM1*, pESC-*LEU-KM**
Y2P-E85A	pESC-*URA-DIM1*, pESC-*LEU-dim1-E85A*
5-FOA resistant clones	
Y-DIM1	pESC-*LEU-DIM1*
Y-DIM1-2	pESC-*LEU-DIM1-2**
Y-DM	pESC-*LEU-DM*
Y-E85A	pESC-*LEU-dim1-E85A*

* Protein from pESC-*LEU* plasmid has exogenous NLS at the N-terminal end

† Dim1p from pESC-*URA-DIM1* has N-terminal myc epitope; KsgA from pESC-*LEU-KsgA-2* has N-terminal FLAG epitope. All the remaining protein constructs have a C-terminal FLAG epitope

Immunofluorescence

We next wanted to ascertain that KsgA, MjDim1 and the chimeras were able to enter the nucleus, where A1 and A2 processing occurs. All of the proteins have a FLAG epitope at the C-terminal end, and can thus be tracked by immunofluorescence microscopy (Figures 20-23 and Appendix). Results show that all of the proteins were expressed in good amounts and could be observed everywhere in the cell, including the nucleus. In the case of DM, dim1-E85A, MjDim1 and MD some cells showed a greater nuclear concentration of the protein, while the remaining cells had no distinction between the nuclear and cellular concentration of the protein (Figures 20-23). In the case of KsgA, KD, DK, MK, and KM the protein was mostly ubiquitous in the cells (Appendix-Figures 28-32). However, none of the proteins were excluded from the nucleus, which confirms that the failure of complementation is not because of failure of entry into the nucleus.

***In vitro* activity**

The N-terminal domain of KsgA/Dim1 family shares the Rossman-like fold characteristic of SAM-utilizing methyltransferases, known as the AdoMet dependent MTase fold, and Motif II of this fold has a highly conserved acidic residue (E85 in yeast Dim1p) which forms hydrogen bonds with hydroxyl groups on the ribose moiety of SAM[68] (Figure 24). Mutation of this residue in bacteria leads to a catalytically dead enzyme (data not shown). In order to produce non-dimethylated 40S subunits, the E85A mutation was introduced into *DIM1* and the resultant mutant plasmid, pESC-*LEU-dim1-E85A* was transformed into Y26hα-URA-DIM1 to give Y2P-E85A. As expected, Y2P-E85A

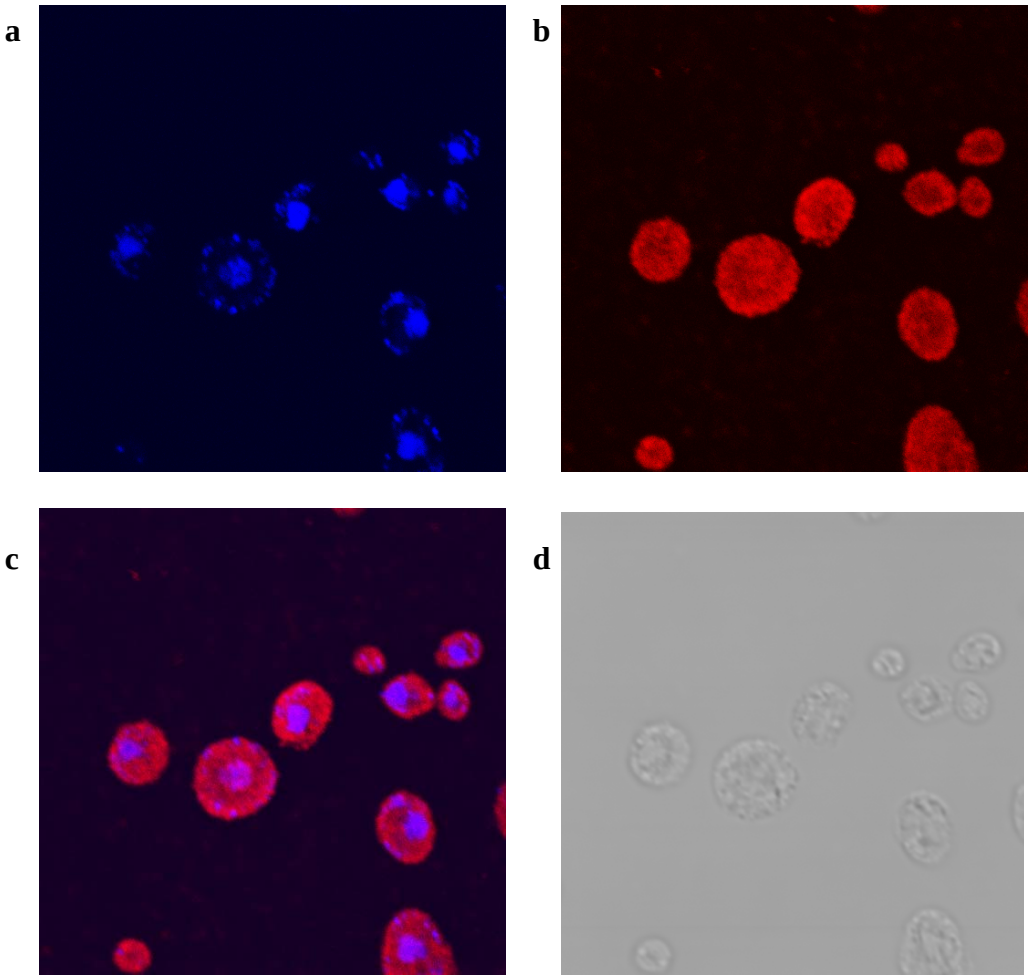

Figure 20: Subcellular localization of MjDim1. (a) the nuclei were stained blue with DAPI; (b) the protein is stained red with anti-FLAG antibody; (c) shows the overlay of the nucleus and protein; (d) shows the DIC image.

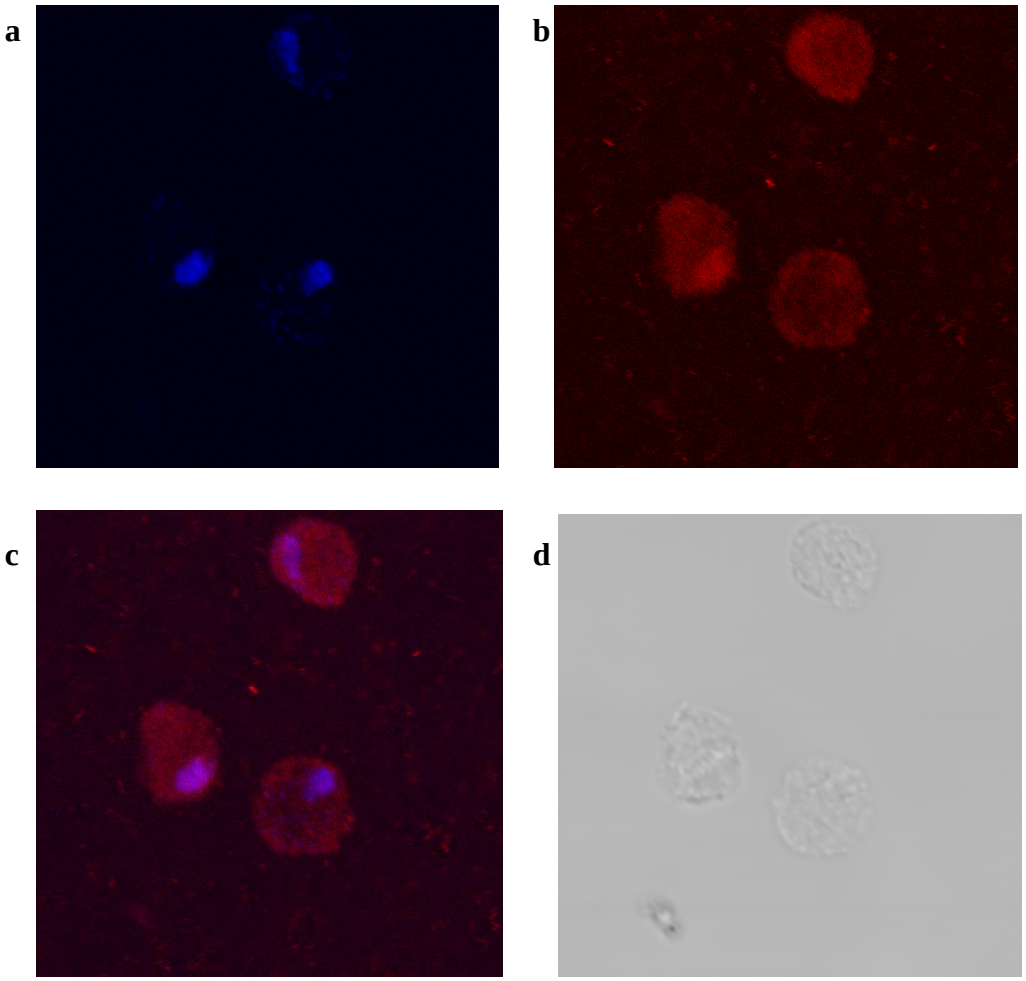

Figure 21: Subcellular localization of the chimera protein, MD. (a) the nuclei were stained blue with DAPI; (b) the protein is stained red with anti-FLAG antibody; (c) shows the overlay of the nucleus and protein; (d) shows the DIC image.

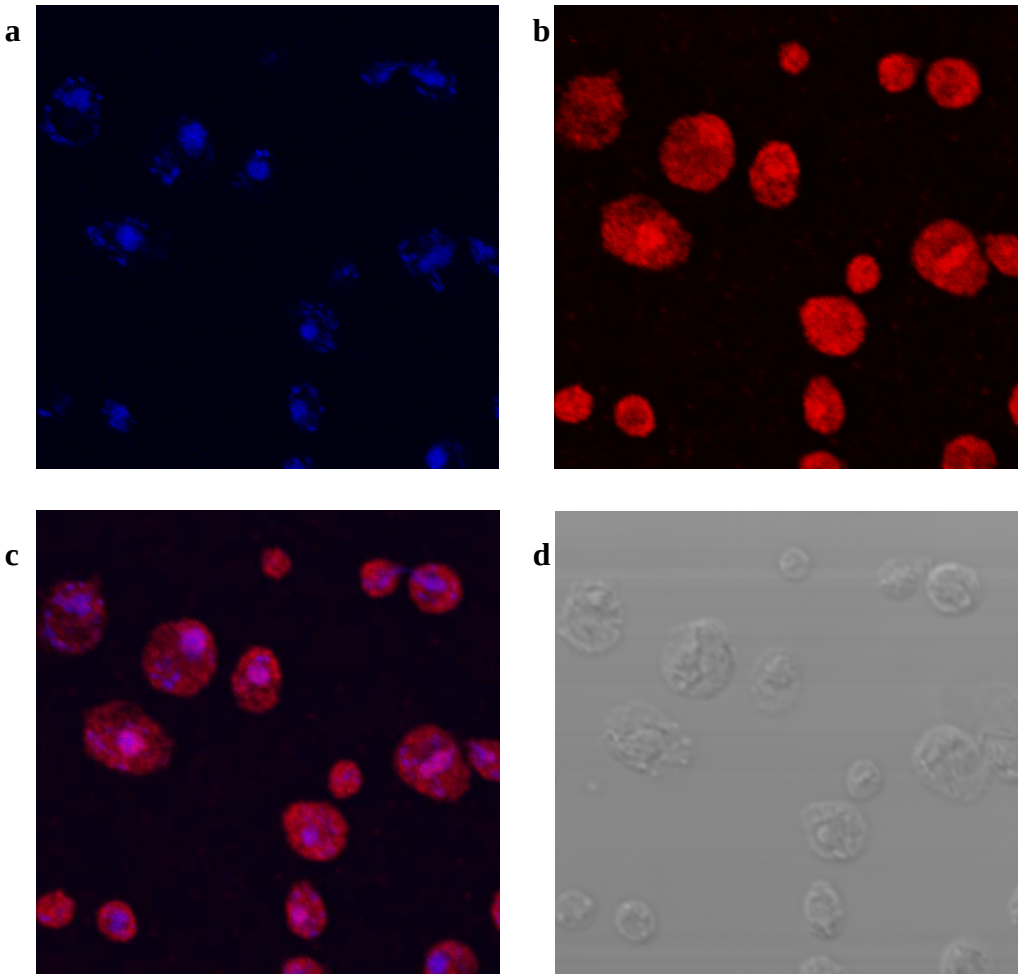

Figure 22: Subcellular localization of the chimera protein, DM. (a) the nuclei were stained blue with DAPI; (b) the protein is stained red with anti-FLAG antibody; (c) shows the overlay of the nucleus and protein; (d) shows the DIC image.

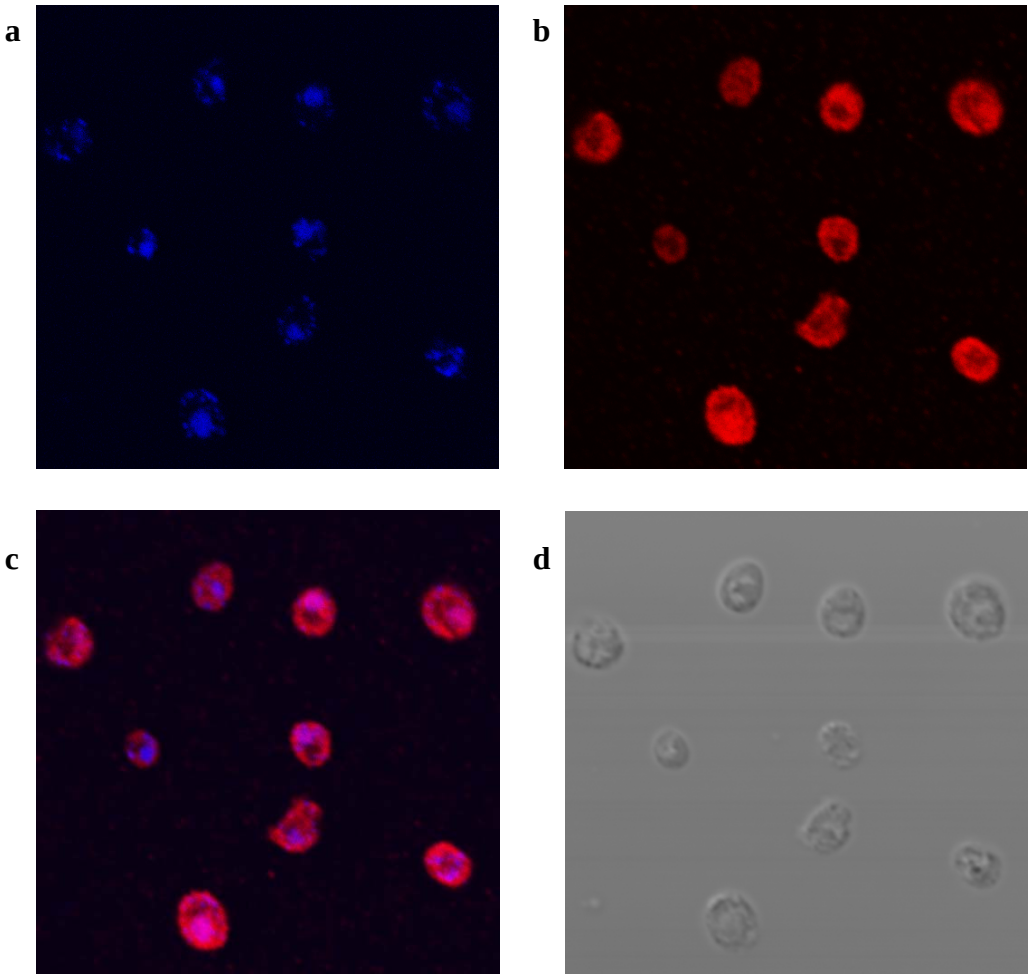

Figure 23: Subcellular localization of the catalytically inactive protein, dim1-E85A. (a) the nuclei were stained blue with DAPI; (b) the protein is stained red with anti-FLAG antibody; (c) shows the overlay of the nucleus and protein; (d) shows the DIC image.
(See Figures 28-32 in appendix for the remaining strains)

survived in the presence of 5-FOA; the resultant clone was relabeled as Y-E85A (Figure 19c).

In order to determine if the absence of dimethyl groups has an effect on the growth phenotype, Y-E85A was spotted on minimal media plates along with Y-DIM1 (with wild type Dim1p) as a control and incubated at 25, 30, 37˚C for 3 days and at 18˚C for 4 days. Both the strains showed identical growth at all the temperatures indicating the loss of methyl groups is not detrimental to cell growth (Figure 25). Non-dimethylated and wild type 40S subunits were then purified from Y-E85A and Y-21026 respectively. The methylation status of the subunits was confirmed by primer extension analysis carried out on 18S rRNA isolated from the subunits with an oligonucleotide complementary to the very 3´ end of the mature 18S rRNA. The primer extension was blocked in wild type 18S rRNA from strain Y-21026 due to the presence of m_2^6A, but not in the non-dimethylated 18S rRNA from strain Y-E85A (Figure 26).

Dim1, KsgA, and MjDim1 were tested *in vitro* for their efficiency to methylate the non-dimethylated 40S using labeled (^{3}H-methyl) SAM. However, none of the proteins was able to do so, but they could all methylate non-dimethylated bacterial 30S, which was used as a control to confirm that the enzymes were active[49]. Dim2p was shown to be required for the dimethylation of 40S by Dim1p *in vivo*[76]. In a separate experiment Dim2p was added to the *in vitro* reaction along with Dim1p. We also carried out the assay in presence of cell lysate, speculating that some other factors might be necessary for the reaction. However, even in the presence of Dim2p or cell lysate the 40S subunits could not be methylated by Dim1p. We confirmed that the catalytically inactive dim1-E85A protein did

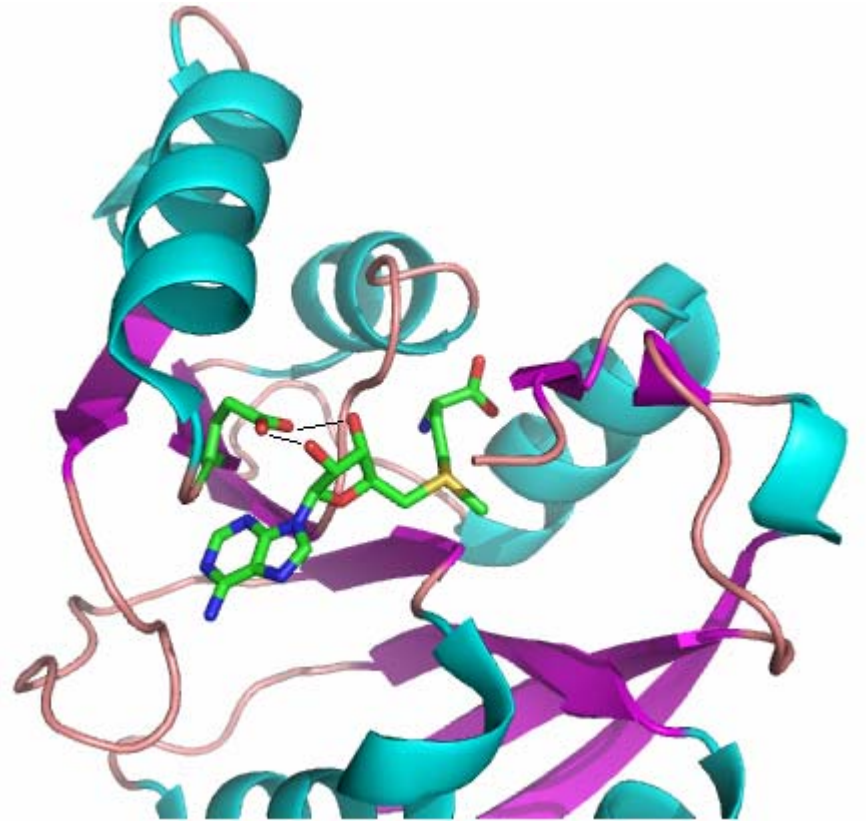

Figure 24: SAM binding to Dim1p. The –COOH groups of the E85 residue (only the side chain is shown) form hydrogen bonds with the hydroxyls of the ribose sugar of SAM. Mutation of E85 to alanine prevents the SAM binding and leads to catalytically dead enzyme.

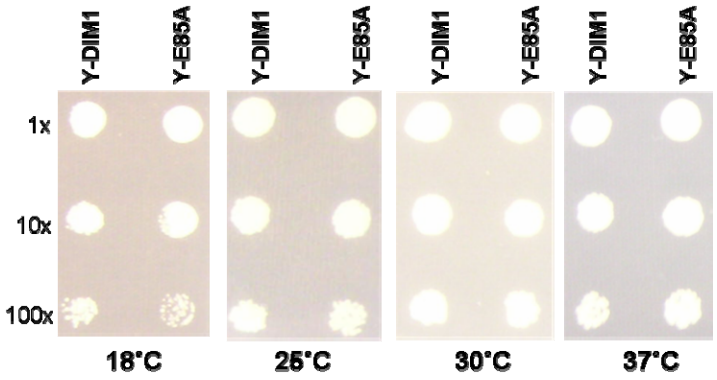

Figure 25: Growth phenotypes of Y-DIM1 (with wild type Dim1p) and Y-E85A (with catalytically inactive dim1-E85A protein). Both the strains showed identical growth rates.

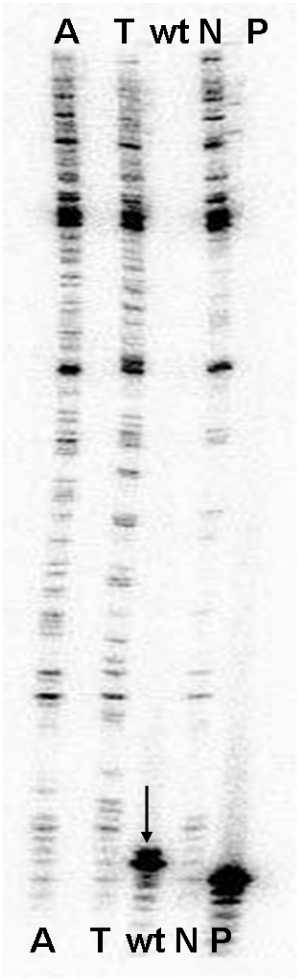

Figure 26: Primer extension analysis on 18S extracted from wild type 40S (wt) and from non-dimethylated 40S (N). Arrow indicates the band representing the primer extension stop resulting from the presence of the dimethylated adenosines in wild type 40S. In case of non-dimethylated 40S, the polymerase reads through the modification site indicating the absence of dimethylation. A partial DNA sequence (A,T) of 18S from the non-dimethylated 40S is also shown. P refers to the N-labeled primer used in the experiment.

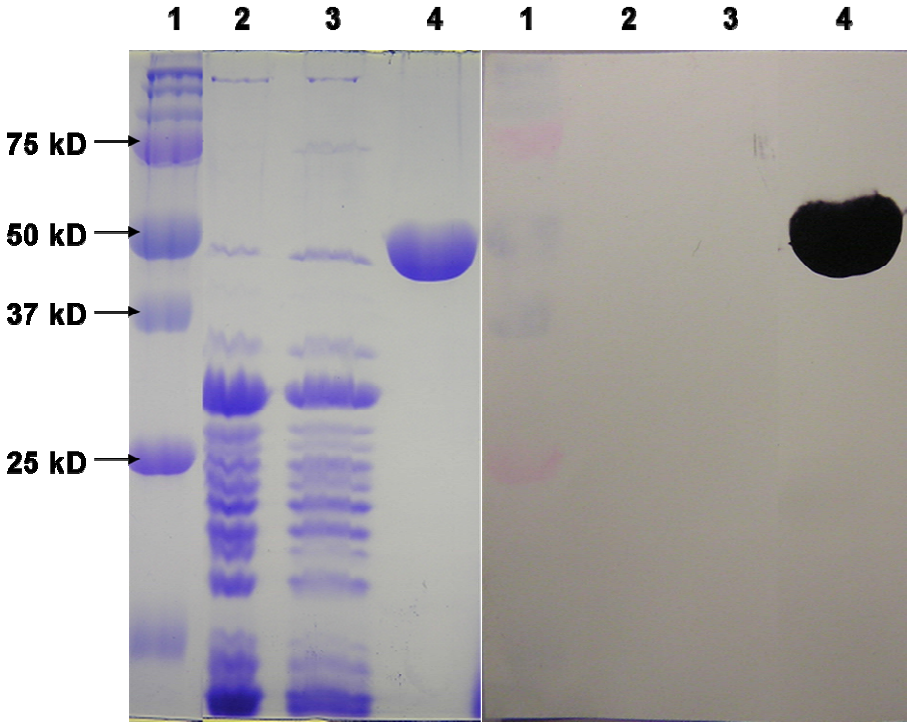

(a) (b)

Figure 27: Western blotting. To confirm the absence of catalytically inactive dim1-E85A protein in the purified non-dimethylated 40S subunits. Lane 1 has the protein standards; lane 2 has wild-type 40S sample; lane 3 has non-dimethylated 40S sample; lane 4 has BAP-Flag (Sigma) fusion protein as a positive control. The dim1-E85A protein with a C-terminal Flag epitope (~38 kD) was not found in the 40S samples as indicated by (a) coomassie stain and (b) western blot using mouse Anti-Flag antibody and goat anti-mouse ab conjugated with HRP.

not co-purify with the 40S subunits (by western blot), which could have potentially blocked the access of catalytically active Dim1p in our *in vitro* assays (Figure 27).

Discussion

Our results show that neither KsgA nor MjDim1 is able to complement the lethal Dim1p knockout in yeast. Since the dimethylation function of these enzymes is dispensable, this indicates that KsgA and MjDim1 failed to carry out the role of Dim1p in the A1 and A2 processing events. Recent studies show that KsgA is also involved in pre-16S rRNA processing, although the processing defects in the KsgA knockout strain are not lethal. Ribosome biogenesis in archaea is speculated to be relatively similar to that of eukaryotes, based on the presence of guide snoRNAs and putative homologs to nuclear and nucleolar structural genes[134]. However, failure of functional complementation by MjDim1 suggests that the eukaryotic enzyme has further evolved to carry out the processing function. We hypothesized that the emergence of this function may be related to the presence of the extra insert in the C-terminal domain of Dim1 throughout the eukaryotes. Chimeric proteins were constructed by swapping the N- and C-terminal domains of Dim1p, KsgA, and MjDim1 and tested for functional complementation. We expected KD and/or MD, both with the C-terminal domain of Dim1p, to complement, however, they were not able to do so. Surprisingly, DM, with the N-terminal domain of Dim1p and the C-terminal domain of MjDim1, could complement for Dim1p's processing function. Sequence alignments show that MjDim1 also has an insert in the C-terminal domain and although it appears shorter than that of eukaryotic proteins, it may nevertheless be

sufficient for functional complementation. Even though there is no sequence similarity in the insert region of Dim1p and MjDim1, it is possible that the insert in MjDim1 forms a helix similar to that in Dim1p which is sufficient for making a vital interaction with another protein or RNA.

Some more information can also be inferred from the above results. There is a relatively good sequence and structural similarity in the N-terminal domain region of KsgA and Dim1p (Figures 11 and 16). Although the structure of MjDim1 is not available, its sequence shows good similarity with Dim1p and KsgA in the N-terminal domain. Despite the similarity, the failure of KD and MD to complement Dim1p function indicates that some feature(s) of the N-terminal domain of Dim1p are essential along with elements in the C-terminal domain. A striking feature is the extended N-terminal end in eukaryotic Dim1p relative to the bacterial and archaeal proteins; unfortunately, the structure of this region is not available in KsgA or human Dim1. The presence of this extension might be essential to Dim1p activity in some way.

In order to purify non-dimethylated 40S subunits and test if Dim1p could methylate them *in vitro*, we have constructed a strain, Y-E85A in which the pre-rRNA processing and dimethylation functions have been uncoupled (Figure 19c). Earlier, Lafontaine et al. have isolated a dim1-2 strain from a library of conditionally lethal alleles of *DIM1* in which the pre-rRNA processing was not affected at the permissive temperature, but the dimethylation was blocked[50]. It has six random mutations scattered throughout the length of the protein and showed a slow growth phenotype at the non-permissive temperature. However, Y-E85A showed identical growth rates at all the temperatures

(Figure 25) resulting in the conclusion that temperature sensitivity of dim1-2 strain is due to the random mutation/s and not because of the loss of dimethyl groups.

Failure of Dim1p as well as KsgA and MjDim1 to methylate the mature 40S subunits *in vitro* was a little surprising to us because all of these proteins were able to methylate mature 30S subunits[49]. This could be due to one or more of the following reasons. The 30S subunits that were methylated by KsgA, Dim1p and MjDim1 were locked in a 'translationally inactive' confirmation which is achieved in low salt and Mg^{2+} concentration[51]. The methylation of 40S subunits was attempted in the same conditions, however, these conditions may not be optimal for 40S methylation because yeast 40S may not have a similar conformational dependence on Mg^{2+} concentration. Another reason could be a requirement for other factors. Dim1p is part of the 90S pre-ribosome and after its separation into a pre-60S and a pre-40S particle, the precursor of the small subunit has a less complex composition, but there are still trans-acting factors present along with the 20S pre-rRNA and small ribosomal subunit proteins[21]. It is possible that Dim1p requires the presence of other factors; a prominent candidate is Dim2p, which was shown to be required for A1, A2 cleavages and also for methylation carried out by Dim1p[76]. However, addition of Dim2p or cell lysate to the *in vitro* assays did not allow methylation by Dim1p. Another problem could be that Dim1p can recognize only a particular 40S precursor as its substrate for methylation. Processing of 20S pre-rRNA to 18S rRNA is considered to be the last event in 40S biogenesis, occurring after the dimethylation event, but the processing can still occur in the absence of dimethylation[50,91]. This processing might induce conformational changes in the 40S subunit which are not favorable for methylation.

Previous work in our lab showed that conservation in the KsgA/Dim1 family, as well as in the small ribosomal subunit, is high enough that KsgA orthologs from all three domains can still recognize bacterial 30S as a substrate[49]. This work, conversely, shows that Dim1p and the ribosome biogenesis process have co-evolved, leading to a well defined function for Dim1p upstream of its methyl transfer reaction that cannot be complemented by the bacterial and archeal proteins. Although it is established that Dim1p and other factors are required for A1 and A2 processing, the details of their interactions with each other and with the rRNA is not known yet. Further studies of the interactions between these factors would help us in better understanding of the intricate steps of ribosome biogenesis.

Materials and methods

Plasmids

DIM1 was amplified from pET15b-*DIM1* as a *Xho*I-*Nhe*I fragment and subcloned into pESC-*URA* vector (Stratagene) to give pESC-*URA*-*DIM1* which results in Dim1p with N-terminal myc epitope. This clone and all subsequent clones were confirmed by sequencing at Nucleic Acids Research Facilities, Virginia Commonwealth University.

KsgA was amplified from pET15b-*KsgA* as a *Not*I-*Spe*I fragment with an exogenous NLS (nuclear localization signal – PPKKKRKV) and subcloned into pESC-*LEU* vector (Stratagene) to give pESC-*LEU*-*KsgA* which results in KsgA with N-terminal NLS and C-terminal FLAG epitope. Similarly *MjDim1* was amplified from pET15b-*MjDim1* as a *Not*I-*Spe*I fragment with the exogenous NLS and subcloned into pESC-*LEU*

vector to give pESC-*LEU-MjDim1* which results in MjDim1 with N-terminal NLS and C-terminal FLAG epitope. *KsgA* was also amplified as a *Bgl*II-*Pac*I fragment (without exogenous NLS) and subcloned into pESC-*LEU* vector to give pESC-*LEU-KsgA-2* which results in KsgA with N-terminal FLAG epitope. *DIM1*, *KsgA, MjDim1* were also amplified as *Not*I-*Spe*I fragment (without exogenous NLS) and subcloned into pESC-*LEU* vector to give pESC-*LEU-DIM1*, pESC-*LEU-KsgA-3*, pESC-*LEU-MjDim1-2* respectively, which results in respective protein with C-terminal FLAG epitope. As a control *DIM1* was amplified from pET15b-*DIM1* as a *Not*I-*Spe*I fragment with the exogenous NLS and subcloned into pESC-*LEU* vector to give pESC-*LEU-DIM1-2* which results in Dim1p with N-terminal NLS and C-terminal FLAG epitope.

Chimera plasmids

The N-terminal and C-terminal domains of *DIM1*, *KsgA, MjDim1* were amplified separately as *Nde*I-*Sal*I and *Sal*I-*Xho*I fragments. The amplicons were then digested with *Sal*I and ligated as following. N-terminal domain of *KsgA* is ligated with C-terminal domain of *DIM1* and *MjDim1* to generate *KD* and *KM* chimeras respectively. N-terminal domain of *DIM1*is ligated with C-terminal domain of *KsgA* and *MjDim1* to generate *DK* and *DM* chimeras respectively. N-terminal domain of *MjDim1* is ligated with C-terminal domain of *DIM1* and *KsgA* to generate *MD* and *MK* chimeras respectively. All the six chimeras were inserted into pET15b as an *Nde*I-*Xho*I fragment. *DK* and *DM* were again amplified as *Not*I-*Spe*I fragments and subcloned into pESC-*LEU* vector to give pESC-*LEU-DK*, pESC-*LEU-DM*, which results in protein with C-terminal FLAG epitope. *KD, KM, MD, MK* were amplified as *Not*I-*Spe*I fragments (with exogenous NLS) and

subcloned into pESC-*LEU* vector to give pESC-*LEU-MD*, pESC-*LEU-MK*, pESC-*LEU-KD*, pESC-*LEU-KM*, which results in respective protein with N-terminal NLS and C-terminal FLAG epitope. (See Appendix (Table 5) for primer information)

***In vivo* assay in bacteria**

The in vivo assay was carried out as described in chapter 3 (see Table 3 for pET15b constructs).

Mutagenesis

The E85A mutation in pESC-*LEU-DIM1* was generated using QuikChange XL Site-Directed Mutagenesis Kit (Stratagene) and primers 5′-C GTA GTG GCA GTA G**C**A ATG GAT CCC AGA ATG G-3′ and 5′-C CAT TCT GGG ATC CAT T**G**C TAC TGC CAC TAC G-3′ to give pESC-*LEU-dim1-E85A*.

Yeast Strains

Standard *S.cerevisiae* growth and handling techniques were employed. Media were standard yeast extract/peptone supplemented with either glucose (YPD) or 2% galactose (YPGal) or minimal medium (0.67% YNB, appropriate aminoacids, 2% galactose) containing 200 mg/L Geneticin (G418). In order to maintain selective pressure for the plasmid/s, either uracil or leucine or both were dropped appropriately, from the minimal media. Transformation was carried out using LiOAc/PEG method[136].

The yeast deletion clone (#21026) generated by the Saccharomyces Genome Deletion Project (http://www-sequence.stanford.edu/group/yeast_deletion_project/deletions3.html) was obtained from Invitrogen (catalog no. 95400). Y-21026 is a diploid strain, derived from BY4743, that is heterozygous for a *DIM1* deletion (one chromosomal *DIM1* copy is

replaced with the *KanMX4* module). BY4743 is auxotrophic for histidine, leucine and uracil and hence the genotype of Y-21026 is *MAT a/α his3Δ1/his3Δ1 leu2Δ0 /leu2Δ0 lys2Δ0/LYS2 MET15/met15Δ0 ura3Δ0 /ura3Δ0 DIM1/dim1Δ0*::*KanMX4*. This strain was transformed with pESC-*URA-DIM1* and induced to sporulate. Tetrads were dissected on synthetic medium lacking uracil to maintain selection for the plasmid. Spore colonies that were Ura^+ and geneticin-resistant were tested for mating type. From these spores, a strain of the genotype, *MATα his3Δ1 leu2Δ0 ura3Δ0 dim1Δ0*::*KanMX4* (pESC-*URA-DIM1*), labeled as Y26hα-URA-DIM1 was selected for further transformations.

Complementation Assay

Y26hα-URA-DIM1 was transformed again with a second plasmid, pESC-*LEU-DIM1*, pESC-*LEU-DIM1-2*, pESC-*LEU-KsgA*, pESC-*LEU-KsgA-2*, pESC-*LEU-KsgA-3*, pESC-*LEU-MjDim1*, pESC-*LEU-MjDim1-2*, pESC-*LEU*(no insert) to give Y2P-DIM1, Y2P-DIM1-2, Y2P-KsgA, Y2P-KsgA-2, Y2P-KsgA-3, Y2P-MjDim1, Y2P-MjDim1-2, Y2P-LEU respectively.

Y26hα-URA-DIM1 was also transformed with chimera plasmids, pESC-*LEU-KD*, pESC-*LEU-DK*, pESC-*LEU-MD*, pESC-*LEU-DM*, pESC-*LEU-MK*, pESC-*LEU-KM* and plasmid with mutant *DIM1*, pESC-*LEU-dim1-E85A* to give Y2P-KD, Y2P-DK, Y2P-MD, Y2P-DM, Y2P-MK, Y2P-KM and Y2P-E85A respectively.

Fluoro-orotate resistant clones were selected on minimal medium (YNB, histidine, uracil, galactose) containing 1 g/L 5-Fluoro-orotic acid (5-FOA)[135]. Plates were incubated for 3 days at 30˚C. Y2P-DIM1, Y2P-DIM1-2, Y2P-DM, Y2P-E85A survived on 5-FOA, losing the first plasmid, pESC-*URA-DIM1* and hence these 5-FOA resistant clones with

only the second plasmid were labeled Y-DIM1, Y-DIM1-2, Y-DM, Y-E85A respectively (Table 4).

The plasmids in the yeast strains were confirmed by PCR followed by sequencing.

Cell growth comparison between Y-DIM1 and Y-E85A

Colonies of Y-DIM1 and Y-E85A were inoculated into 2ml of minimal medium and grown to an OD_{600} of 1.0. Dilutions (1x to 100x) of both strains were spotted on minimal media plates and incubated for 3 days at 25, 30, 37˚C and for 4 days at 18˚C (Figure 25).

Immunofluorescence

The immunofluorescence procedure was adapted from the methods described by Pringle et al.[137]. Cells were inoculated into 2ml of minimal medium and grown to an OD_{600} of 1.0. The cells were fixed by adding 1/10 volume of 37% formaldehyde to the culture and incubating for 1 h at room temperature. The cells were then washed twice with 100 mM phosphate buffer (pH 7.4) and once with SP buffer (1.2 M sorbitol, 20 mM potassium phosphate buffer, pH 7.4). Cell walls were digested with Zymolyase-20T (50µg/ml) in SP buffer containing 1µl/ml β-mercaptoethanol at 30˚C for 30 min. The spheroplasts were washed twice with SP buffer and resuspended in 200 µl of SP buffer. 20 µl of cell suspension was applied to multi-well Teflon-faced slides coated with poly-L-lysine, incubated for 10 min at RT and the excess suspension was aspirated out. Slides were immersed in methanol at -20˚C for 5 min. The wells were washed 10 times with 50 µl of 1% BSA in PBS. The primary antibodies, Anti-FLAG M2 Monoclonal antibody from mouse (Sigma) and/or Anti-c-Myc antibody from rabbit (Sigma) were applied to each well

(15 µl of 200 fold dilution) and incubated at RT for 2 h. Slides were further washed 10 times with 1% BSA in PBS. The secondary antibodies, Alexa Fluor 594 goat anti-mouse IgG (Invitrogen) and/or Alexa Fluor 488 goat anti-rabbit IgG (Invitrogen) were applied (15 µl of 500-fold dilution) and incubated for 1 h at RT. The cells were washed 5 times with PBS and finally 15 µl of DAPI (100 ng/ml) was applied to each well and incubated for 30 min in the dark. The cells were again washed 5 times with PBS, mounting medium was added and cover glasses were sealed with nail polish. Cells were observed under a Leica TCS-SP2 AOBS confocal laser scanning microscope.

Purification of 40S subunits

The 40S purification procedure was adapted from Maag *et al.*[138]. An overnight culture of Y-21026 cells in YPD medium was used to inoculate 1 liter of YPD medium (for wild type 40S) and an overnight culture of Y-E85A cells in minimal medium was used to inoculate 1 liter of YPGal medium (for non-dimethylated 40S). Cells were grown at 30 ˚C to an OD_{600} of 1.0 and harvested by centrifugation. After rinsing the cell pellets with water, they were resuspended in 40 ml of lysis buffer (100 mM potassium acetate, 20 mM Hepes-KOH (pH 7.6), 2.5 mM magnesium acetate, 1 mg/ml of heparin, 2 mM DTT and 1mM PMSF). Cells were lysed by passing 3 times through an Avestin EmulsiFlex-C3 homogenizer at 25,000 psi. The lysate was then clarified by centrifugation at 11,000 rpm for 20 min at 4 ˚C and recentrifugation of the supernatant at 14,500 rpm for 45 min at 4 ˚C. The supernatant was gently layered onto 2.5 ml of sucrose cushion (100 mM potassium acetate, 20 mM Hepes-KOH (pH 7.6), 2.5 mM magnesium acetate, 500 mM KCl, 1 M sucrose, 2 mM DTT) and ribosomes were pelleted by ultracentrifugation in a Beckman

70Ti rotor at 35,000 rpm for 20 h. The pellets (ribosomes) were resuspended in 3 ml of high-salt wash (100 mM potassium acetate, 20 mM Hepes-KOH (pH 7.6), 2.5 mM magnesium acetate, 500 mM KCl, 2 mM DTT) and stirred gently at 4 °C for 1 h. This solution was then layered again upon a sucrose cushion (1.5 ml suspension and 2.5 ml cushion per tube) and ribosomes were pelleted by ultracentrifugation at 35,000 rpm in a Beckman type 70Ti rotor for 20 h. The pelleted 80S ribosomes were resuspended in 3 ml of subunit separation buffer (50 mM Hepes-KOH (pH 7.4), 2 mM $MgCl_2$, 500 mM KCl, 2 mM DTT, 1 mM puromycin) and incubated on ice for 15 min, then at 37 °C for 10 min. A portion (1 ml) of this solution was then layered upon each of 3 sucrose gradients (36 ml; 50 mM Hepes-KOH (pH 7.4), 5 mM $MgCl_2$, 500 mM KCl, 2 mM DTT, 0.1 mM EDTA and 10%-30% (w/v) sucrose). After centrifugation for 17 h at 19,000 rpm and 4 °C in a Beckman SW28 rotor, gradients were fractionated. The 40 S and 60 S peaks were pooled separately, the 40S subunits were dialysed against buffer K (40 mM Tris (pH 7.4), 40 mM NH_4Cl, 4 mM magnesium acetate, 6 mM 2-mercaptoethanol) and stored at −80 °C.

For confirmation, the rRNA was isolated from both wild type and non-dimethylated 40S subunits and primer extension was carried out on both using the primer, 5′-TAA TGA TCC TTC CGC A-3′, which is complementary to the very end of 18S rRNA[50,74]. Primer extension was seen only in the non-dimethylated 18S and not in the wild type 18S (Figure 26).

Western blot

In order to confirm the absence of catalytically inactive dim1-E85A protein in the purified non-dimethylated 40S subunits, western blot was carried out. Approximately 30

pmol of wild-type and non-dimethylated 40S samples were boiled in protein cracking buffer and loaded on a SDS gel. As a positive control FLAG-BAP (Sigma) fusion protein was also loaded. After running the gel, proteins were transferred to a PVDF membrane. After blocking the membrane with 3% non-fat dry milk, it is incubated with mouse anti-FLAG M2 antibody (Sigma) followed by anti-mouse IgG-HRP conjugate (sigma). Color was developed using 4-CN as the substrate. The dim1-E85A protein with a C-terminal Flag epitope (~38 kD) was not found in the 40S samples (Figure 27).

Cloning of *DIM2*

S. cerevisiae genomic DNA was obtained from Invitrogen (#40802). *DIM2* was amplified as a *Nde*I-*Xho*I fragment and then inserted into pET15b vector which results in Dim2p with N-terminal His-tag. (See Appendix (Table 5) for primer information)

Protein expression and purification

Dim1p was purified as described in chapter 2. KsgA and MjDim1 were purified as described in chapter 3. For expression of Dim2p, the plasmid pET15b-*DIM2* was transformed into Rosetta 2 (DE3) cells. The cells were grown at 37°C to an OD_{600} of 1.2 in the presence of ampicillin and chloramphenicol. Protein induction was carried out under mild conditions with 0.2 mM IPTG at 25°C and harvested after 4 h. Purification was carried out by affinity chromatography using a Ni^{2+}-NTA Agarose column (Qiagen) and buffers had 50 mM NaH_2PO_4, 300 mM NaCl, 15% glycerol, 1 mM PMSF and imidazole (10 mM in lysis buffer, 20 mM in wash buffer 1, 50 mM in wash buffer 2 and 300 mM in elution buffer) at pH 8.0. The cell pellets were resuspended in lysis buffer and broken by passing through an Avestin EmulsiFlex-C3 homogenizer two times at 15,000 psi, and

centrifuged to remove cell debris. Cleared lysate was loaded onto the Ni^{2+} column, washed and then eluted. Initial studies showed that Dim2p undergoes degradation within a few days and it is assumed to be caused by a protease. The degradation decreased when the purification procedure was carried out at 4°C and by the addition of protease inhibitors to the buffers.

Proteins were estimated to be >95% pure by SDS-PAGE analysis and their concentrations were measured using the Bradford Protein Assay (Bio-Rad).

***In vitro* assay**

The *in vitro* assay was adapted from Poldermans et al. Non-dimethylated 30S subunits were purified as described in chapter 3. Reactions were performed in 50 µL volumes containing 40 mM Tris (pH 7.4), 40 mM NH_4Cl, 4 mM MgOAc, 6 mM 2-mercaptoethanol, 1 mM SAM with 0.02 mM ^{3}H-methyl-SAM (780 cpm/pmol; MP Biomedicals), 10 pmol 40S/30S subunits, and 10 pmol enzyme/protein. The reactions were incubated at 37˚C. After 2 h the entire reaction volume was deposited onto DE81 filter paper (Whatman), washed twice with ice-cold 5% TCA, and rinsed briefly with ethanol. Filters were air-dried for 1 h, placed into scintillation fluid, and counted.

The *in vitro* assay in presence of cell lysate was carried out using the following procedure. An overnight culture of Y-DIM1 cells in minimal medium was used to inoculate 500 mL of YPGal medium and grown at 30 °C to an OD_{600} of 1.0. After rinsing the cell pellets with water, they were resuspended in 20 ml of lysis buffer (40 mM Tris-HCl (pH 7.4), 40 mM NH_4Cl, 4 mM MgOAc, 3 mM DTT and 1mM PMSF). Cells were lysed by passing 3 times through an Avestin EmulsiFlex-C3 homogenizer at 25,000 psi.

The lysate was then clarified by centrifugation at 15,000 rpm for 45 min at 4˚C followed by ultracentrifugation in a Beckman 70Ti rotor at 35,000 rpm for 20 h to separate the ribosomes. The supernatant was then mixed with 200 pmol 40S subunits (wild type and non-dimethylated), 200 pmol Dim1p, and ^{3}H-SAM to a final volume of 500 µL. The reactions were incubated at 37˚C for 2 h. The entire reaction volume was then layered upon sucrose gradient (36 ml; 50 mM Hepes-KOH (pH 7.4), 5 mM $MgCl_2$, 500 mM KCl, 2 mM DTT, 0.1 mM EDTA and 10%-30% (w/v) sucrose). After centrifugation for 17 h at 19,000 rpm and 4 °C in a Beckman SW28 rotor, gradients were fractionated. 360 µL of the fractions corresponding to the 40S peak was added into 3 mL of scintillation fluid and counted.

CHAPTER 5: Conclusions and future work

The eukaryotic 18S rRNA dimethyltransferase, Dim1 is an essential factor required for the ribosome biogenesis. The importance of this enzyme family is emphasized by its universal conservation. Apart from the dimethylation of small subunit rRNA, the members of Dim1/KsgA family have diverged to carryout secondary functions in the cell, which in most cases are vital. In eukaryotes, Dim1 is essential for the earliest pre-rRNA processing events occurring in the nucleolus. Though bound to the pre-ribosomal particles, the dimethylation of small subunit rRNA is not carried out until the final stages of ribosome biogenesis. We have characterized the yeast dimethylase, Dim1p, and obtained significant information regarding its structural features necessary for the processing function. Eukaryotes have an extra helix in their C-terminal domain which is absent in the bacterial orthologs and partially present in archaeal orthologs. Our data suggests that along with this C-terminal insert, some features of the N-terminal domain are also necessary for the processing function of Dim1p. Similar characterization of N-terminal domain has to be carried out using our plasmid shuffling technique, to identify the essential regions on the domain. A striking feature is the extended N-terminal end in eukaryotic Dim1p relative to the bacterial and archaeal proteins; unfortunately, the structure of this region is not available in KsgA or human Dim1. We speculate that the presence of this extension might be essential to Dim1p activity in some way.

Surprisingly, the entire C-terminal domain of Dim1p could be replaced with that of MjDim1 without any effect on the cell survival or growth. Although appearing to be shorter than that of eukaryotic proteins, it is possible that the C-terminal domain of MjDim1 is nevertheless sufficient for functional complementation. Even though there is no sequence similarity in the insert region of Dim1p and MjDim1, it is possible that the insert in MjDim1 forms a helix similar to that in Dim1p which is sufficient for making a vital interaction with another protein or RNA. With this result, any attempts to characterize the C-terminal insert by point mutations may not be successful.

Another possibility is that Dim1p might be associating with Dim2p with the help of C-terminal insert. One way to test this interaction is by yeast two hybrid screening. But there is a problem with such as experiment. Both Dim1p and Dim2p are part of the SSU processome complex which also has more than 70 factors, most of them shuttling between nucleus and cytoplasm. Both of them also interact[76] with other factors which may interfere with yeast two hybrid screening. Physical methods of studying the association, such as surface plasmon resonance or size exclusion chromatography, can be used. However, the poor solubility profile of Dim1p renders such studies difficult.

During the course of this project, we have also tried to crystallize Dim2p, although without any success yet. But if solved, the information would be very helpful in studying the association with Dim1p.

Another current project in our lab, in collaboration with Dr.Gloria Culver's lab, aims to study the binding site of KsgA on 30S subunit using directed hydroxyl radical probing experiments. It has been recently reported that KsgA interacts with small

ribosomal subunits near functional sites, including initiation factor 3 and 50S subunit binding sites[139]. Such studies could also be extended to Dim1p and 40S subunits. Since Dim1p methylates 20S pre-rRNA *in vivo*, the non-dimethylated pre-40S subunits would be the ideal substrate for such experiments. The same subunits could also be tested for *in vitro* methylation using Dim1p, KsgA, and MjDim1 as they were not able to methylate the non-dimethylated mature 40S subunits containing 18S rRNA (chapter 4). The strain Y-E85A produces non-dimethylated but mature 40S subunits. Therefore, knocking out any one of the factors/ proteins required for cleavage D would result in the inhibition of 20S rRNA processing to 18S rRNA. Processing factors Nob1p, Fap7p and ribosomal protein Rps14p are implicated in 20S processing and depletion of any one of them in Y-E85A, would result in the production of non-dimethylated pre-40S subunits.

The binding site of Dim1p on 40S would, most probably, be similar to that of KsgA on 30S subunit. This information would be helpful in identifying the binding site of other factors, most prominently Dim2p. Recent studies by many groups have identified the composition of many pre-ribosomal particles and the picture of the pre-rRNA processing/ assembly machinery that is emerging is one of great complexity and interactivity. However, very little or almost no information is available at the structural level. Dim1p is one of the core constituents of the SSU processome, and remains bound until the late cytoplasmic stages. Further structural characterization of Dim1p and other processome factors would enable us to understand the functional interactions between them and the dynamics of ribosome biogenesis at a closer level.

List of References

List of References

1. Tschochner, H.; Hurt, E. Pre-ribosomes on the road from the nucleolus to the cytoplasm. *Trends Cell Biol.* **2003**, *13,* 255-263.

2. Fromont-Racine, M.; Senger, B.; Saveanu, C.; Fasiolo, F. Ribosome assembly in eukaryotes. *Gene* **2003**, *313,* 17-42.

3. Granneman, S.; Baserga, S. J. Ribosome biogenesis: of knobs and RNA processing. *Exp. Cell Res.* **2004**, *296,* 43-50.

4. Johnson, A. W.; Lund, E.; Dahlberg, J. Nuclear export of ribosomal subunits. *Trends Biochem. Sci.* **2002**, *27,* 580-585.

5. Kressler, D.; Linder, P.; de La Cruz, J. Protein trans-acting factors involved in ribosome biogenesis in Saccharomyces cerevisiae. *Mol. Cell. Biol.* **1999**, *19,* 7897-7912.

6. Nazar, R. N. Ribosomal RNA processing and ribosome biogenesis in eukaryotes. *IUBMB Life* **2004**, *56,* 457-465.

7. Venema, J.; Tollervey, D. Ribosome synthesis in Saccharomyces cerevisiae. *Annu. Rev. Genet.* **1999**, *33,* 261-311.

8. Warner, J. R. The economics of ribosome biosynthesis in yeast. *Trends Biochem. Sci.* **1999**, *24,* 437-440.

9. Brown, J. D. Ribosome biogenesis: stripping for AAAction? *Curr. Biol.* **2001**, *11,* R710-2.

10. Ferreira-Cerca, S.; Poll, G.; Gleizes, P. E.; Tschochner, H.; Milkereit, P. Roles of eukaryotic ribosomal proteins in maturation and transport of pre-18S rRNA and ribosome function. *Mol. Cell* **2005**, *20,* 263-275.

11. Grandi, P.; Rybin, V.; Bassler, J.; Petfalski, E.; Strauss, D.; Marzioch, M.; Schafer, T.; Kuster, B.; Tschochner, H.; Tollervey, D.; Gavin, A. C.; Hurt, E. 90S pre-ribosomes include the 35S pre-rRNA, the U3 snoRNP, and 40S subunit processing factors but predominantly lack 60S synthesis factors. *Mol. Cell* **2002**, *10,* 105-115.

12. Rigaut, G.; Shevchenko, A.; Rutz, B.; Wilm, M.; Mann, M.; Seraphin, B. A generic protein purification method for protein complex characterization and proteome exploration. *Nat. Biotechnol.* **1999**, *17,* 1030-1032.

13. Miller, O. L.,Jr; Beatty, B. R. Visualization of nucleolar genes. *Science* **1969**, *164,* 955-957.

14. Mougey, E. B.; O'Reilly, M.; Osheim, Y.; Miller, O. L.,Jr; Beyer, A.; Sollner-Webb, B. The terminal balls characteristic of eukaryotic rRNA transcription units in chromatin spreads are rRNA processing complexes. *Genes Dev.* **1993**, *7,* 1609-1619.

15. Udem, S. A.; Warner, J. R. Ribosomal RNA synthesis in Saccharomyces cerevisiae. *J. Mol. Biol.* **1972**, *65,* 227-242.

16. Udem, S. A.; Warner, J. R. The cytoplasmic maturation of a ribosomal precursor ribonucleic acid in yeast. *J. Biol. Chem.* **1973**, *248,* 1412-1416.

17. Trapman, J.; Retel, J.; Planta, R. J. Ribosomal precursor particles from yeast. *Exp. Cell Res.* **1975**, *90,* 95-104.

18. Osheim, Y. N.; French, S. L.; Keck, K. M.; Champion, E. A.; Spasov, K.; Dragon, F.; Baserga, S. J.; Beyer, A. L. Pre-18S ribosomal RNA is structurally compacted into the SSU processome prior to being cleaved from nascent transcripts in Saccharomyces cerevisiae. *Mol. Cell* **2004**, *16,* 943-954.

19. Dragon, F.; Gallagher, J. E.; Compagnone-Post, P. A.; Mitchell, B. M.; Porwancher, K. A.; Wehner, K. A.; Wormsley, S.; Settlage, R. E.; Shabanowitz, J.; Osheim, Y.; Beyer, A. L.; Hunt, D. F.; Baserga, S. J. A large nucleolar U3 ribonucleoprotein required for 18S ribosomal RNA biogenesis. *Nature* **2002**, *417,* 967-970.

20. Granneman, S.; Baserga, S. J. Crosstalk in gene expression: coupling and co-regulation of rDNA transcription, pre-ribosome assembly and pre-rRNA processing. *Curr. Opin. Cell Biol.* **2005**, *17,* 281-286.

21. Schafer, T.; Strauss, D.; Petfalski, E.; Tollervey, D.; Hurt, E. The path from nucleolar 90S to cytoplasmic 40S pre-ribosomes. *EMBO J.* **2003**, *22,* 1370-1380.

22. Zemp, I.; Kutay, U. Nuclear export and cytoplasmic maturation of ribosomal subunits. *FEBS Lett.* **2007**, *581,* 2783-2793.

23. Nissan, T. A.; Bassler, J.; Petfalski, E.; Tollervey, D.; Hurt, E. 60S pre-ribosome formation viewed from assembly in the nucleolus until export to the cytoplasm. *EMBO J.* **2002**, *21,* 5539-5547.

24. Takahashi, N.; Yanagida, M.; Fujiyama, S.; Hayano, T.; Isobe, T. Proteomic snapshot analyses of preribosomal ribonucleoprotein complexes formed at various stages of ribosome biogenesis in yeast and mammalian cells. *Mass Spectrom. Rev.* **2003**, *22,* 287-317.

25. Rouquette, J.; Choesmel, V.; Gleizes, P. E. Nuclear export and cytoplasmic processing of precursors to the 40S ribosomal subunits in mammalian cells. *EMBO J.* **2005**, *24,* 2862-2872.

26. Nierhaus, K. H. The assembly of prokaryotic ribosomes. *Biochimie* **1991**, *73,* 739-755.

27. Traub, P.; Nomura, M. Structure and function of E. coli ribosomes. V. Reconstitution of functionally active 30S ribosomal particles from RNA and proteins. *Proc. Natl. Acad. Sci. U. S. A.* **1968**, *59,* 777-784.

28. Culver, G. M.; Noller, H. F. In vitro reconstitution of 30S ribosomal subunits using complete set of recombinant proteins. *Methods Enzymol.* **2000**, *318,* 446-460.

29. Traub, P.; Nomura, M. Structure and function of Escherichia coli ribosomes. VI. Mechanism of assembly of 30 s ribosomes studied in vitro. *J. Mol. Biol.* **1969**, *40,* 391-413.

30. Held, W. A.; Nomura, M. Rate determining step in the reconstitution of Escherichia coli 30S ribosomal subunits. *Biochemistry* **1973**, *12,* 3273-3281.

31. Guthrie, C.; Nashimoto, H.; Nomura, M. Structure and function of E. coli ribosomes. 8. Cold-sensitive mutants defective in ribosome assembly. *Proc. Natl. Acad. Sci. U. S. A.* **1969**, *63,* 384-391.

32. Nashimoto, H.; Held, W.; Kaltschmidt, E.; Nomura, M. Structure and function of bacterial ribosomes. XII. Accumulation of 21 s particles by some cold-sensitive mutants of Escherichia coli. *J. Mol. Biol.* **1971**, *62,* 121-138.

33. Maki, J. A.; Schnobrich, D. J.; Culver, G. M. The DnaK chaperone system facilitates 30S ribosomal subunit assembly. *Mol. Cell* **2002**, *10,* 129-138.

34. Herold, M.; Nierhaus, K. H. Incorporation of six additional proteins to complete the assembly map of the 50 S subunit from Escherichia coli ribosomes. *J. Biol. Chem.* **1987**, *262,* 8826-8833.

35. Nierhaus, K. H.; Dohme, F. Total reconstitution of functionally active 50S ribosomal subunits from Escherichia coli. *Proc. Natl. Acad. Sci. U. S. A.* **1974**, *71,* 4713-4717.

36. Ofengand, J.; Bakin, A. Mapping to nucleotide resolution of pseudouridine residues in large subunit ribosomal RNAs from representative eukaryotes, prokaryotes, archaebacteria, mitochondria and chloroplasts. *J. Mol. Biol.* **1997**, *266,* 246-268.

37. Maden, B. E.; Hughes, J. M. Eukaryotic ribosomal RNA: the recent excitement in the nucleotide modification problem. *Chromosoma* **1997**, *105,* 391-400.

38. Decatur, W. A.; Fournier, M. J. rRNA modifications and ribosome function. *Trends Biochem. Sci.* **2002**, *27,* 344-351.

39. Piekna-Przybylska, D.; Decatur, W. A.; Fournier, M. J. The 3D rRNA modification maps database: with interactive tools for ribosome analysis. *Nucleic Acids Res.* **2008**, *36,* D178-83.

40. Bakin, A.; Lane, B. G.; Ofengand, J. Clustering of pseudouridine residues around the peptidyltransferase center of yeast cytoplasmic and mitochondrial ribosomes. *Biochemistry* **1994**, *33,* 13475-13483.

41. Noon, K. R.; Bruenger, E.; McCloskey, J. A. Posttranscriptional modifications in 16S and 23S rRNAs of the archaeal hyperthermophile Sulfolobus solfataricus. *J. Bacteriol.* **1998**, *180,* 2883-2888.

42. Gustafsson, C.; Reid, R.; Greene, P. J.; Santi, D. V. Identification of new RNA modifying enzymes by iterative genome search using known modifying enzymes as probes. *Nucleic Acids Res.* **1996**, *24,* 3756-3762.

43. Caldas, T.; Binet, E.; Bouloc, P.; Richarme, G. Translational defects of Escherichia coli mutants deficient in the Um(2552) 23S ribosomal RNA methyltransferase RrmJ/FTSJ. *Biochem. Biophys. Res. Commun.* **2000**, *271,* 714-718.

44. Kiss, T. Small nucleolar RNA-guided post-transcriptional modification of cellular RNAs. *EMBO J.* **2001**, *20,* 3617-3622.

45. Ziesche, S. M.; Omer, A. D.; Dennis, P. P. RNA-guided nucleotide modification of ribosomal and non-ribosomal RNAs in Archaea. *Mol. Microbiol.* **2004**, *54,* 980-993.

46. Watanabe, Y.; Gray, M. W. Evolutionary appearance of genes encoding proteins associated with box H/ACA snoRNAs: cbf5p in Euglena gracilis, an early diverging eukaryote, and candidate Gar1p and Nop10p homologs in archaebacteria. *Nucleic Acids Res.* **2000**, *28,* 2342-2352.

47. Van Knippenberg, P. H.; Van Kimmenade, J. M.; Heus, H. A. Phylogeny of the conserved 3' terminal structure of the RNA of small ribosomal subunits. *Nucleic Acids Res.* **1984**, *12,* 2595-2604.

48. Cannone, J. J.; Subramanian, S.; Schnare, M. N.; Collett, J. R.; D'Souza, L. M.; Du, Y.; Feng, B.; Lin, N.; Madabusi, L. V.; Muller, K. M.; Pande, N.; Shang, Z.; Yu, N.; Gutell, R. R. The comparative RNA web (CRW) site: an online database of comparative sequence and structure information for ribosomal, intron, and other RNAs. *BMC Bioinformatics* **2002**, *3,* 2.

49. O'Farrell, H. C.; Pulicherla, N.; Desai, P. M.; Rife, J. P. Recognition of a complex substrate by the KsgA/Dim1 family of enzymes has been conserved throughout evolution. *RNA* **2006**, *12,* 725-733.

50. Lafontaine, D. L.; Preiss, T.; Tollervey, D. Yeast 18S rRNA dimethylase Dim1p: a quality control mechanism in ribosome synthesis? *Mol. Cell. Biol.* **1998**, *18,* 2360-2370.

51. Desai, P. M.; Rife, J. P. The adenosine dimethyltransferase KsgA recognizes a specific conformational state of the 30S ribosomal subunit. *Arch. Biochem. Biophys.* **2006**, *449,* 57-63.

52. Decatur, W. A.; Fournier, M. J. RNA-guided nucleotide modification of ribosomal and other RNAs. *J. Biol. Chem.* **2003**, *278,* 695-698.

53. Yu, Y. T.; Shu, M. D.; Steitz, J. A. A new method for detecting sites of 2'-O-methylation in RNA molecules. *RNA* **1997**, *3,* 324-331.

54. Arnez, J. G.; Steitz, T. A. Crystal structure of unmodified tRNA(Gln) complexed with glutaminyl-tRNA synthetase and ATP suggests a possible role for pseudo-uridines in stabilization of RNA structure. *Biochemistry* **1994**, *33,* 7560-7567.

55. Charette, M.; Gray, M. W. Pseudouridine in RNA: what, where, how, and why. *IUBMB Life* **2000**, *49,* 341-351.

56. Williams, D. J.; Boots, J. L.; Hall, K. B. Thermodynamics of 2'-ribose substitutions in UUCG tetraloops. *RNA* **2001**, *7,* 44-53.

57. Lovgren, J. M.; Wikstrom, P. M. The rlmB gene is essential for formation of Gm2251 in 23S rRNA but not for ribosome maturation in Escherichia coli. *J. Bacteriol.* **2001**, *183,* 6957-6960.

58. Ni, J.; Tien, A. L.; Fournier, M. J. Small nucleolar RNAs direct site-specific synthesis of pseudouridine in ribosomal RNA. *Cell* **1997**, *89,* 565-573.

59. Green, R.; Noller, H. F. Reconstitution of functional 50S ribosomes from in vitro transcripts of Bacillus stearothermophilus 23S rRNA. *Biochemistry* **1999**, *38,* 1772-1779.

60. Khaitovich, P.; Tenson, T.; Kloss, P.; Mankin, A. S. Reconstitution of functionally active Thermus aquaticus large ribosomal subunits with in vitro-transcribed rRNA. *Biochemistry* **1999**, *38,* 1780-1788.

61. Tollervey, D.; Lehtonen, H.; Jansen, R.; Kern, H.; Hurt, E. C. Temperature-sensitive mutations demonstrate roles for yeast fibrillarin in pre-rRNA processing, pre-rRNA methylation, and ribosome assembly. *Cell* **1993**, *72,* 443-457.

62. Zebarjadian, Y.; King, T.; Fournier, M. J.; Clarke, L.; Carbon, J. Point mutations in yeast CBF5 can abolish in vivo pseudouridylation of rRNA. *Mol. Cell. Biol.* **1999**, *19,* 7461-7472.

63. Cunningham, P. R.; Richard, R. B.; Weitzmann, C. J.; Nurse, K.; Ofengand, J. The absence of modified nucleotides affects both in vitro assembly and in vitro function of the 30S ribosomal subunit of Escherichia coli. *Biochimie* **1991**, *73,* 789-796.

64. Ofengand, J. Ribosomal RNA pseudouridines and pseudouridine synthases. *FEBS Lett.* **2002**, *514,* 17-25.

65. Kowalak, J. A.; Bruenger, E.; McCloskey, J. A. Posttranscriptional modification of the central loop of domain V in Escherichia coli 23 S ribosomal RNA. *J. Biol. Chem.* **1995**, *270,* 17758-17764.

66. Green, R.; Noller, H. F. In vitro complementation analysis localizes 23S rRNA posttranscriptional modifications that are required for Escherichia coli 50S ribosomal subunit assembly and function. *RNA* **1996**, *2,* 1011-1021.

67. Nissen, P.; Hansen, J.; Ban, N.; Moore, P. B.; Steitz, T. A. The structural basis of ribosome activity in peptide bond synthesis. *Science* **2000**, *289,* 920-930.

68. Fauman, E. B.; Blumenthal, R. M.; Cheng, X. Structure and Evolution of AdoMet-Dependent Methyltransferases. In *S-Adenosylmethionine-Dependent Methyltransferases: Structures and Functions;* **1998**, pp 1-38.

69. Malone, T.; Blumenthal, R. M.; Cheng, X. Structure-guided analysis reveals nine sequence motifs conserved among DNA amino-methyltransferases, and suggests a catalytic mechanism for these enzymes. *J. Mol. Biol.* **1995**, *253,* 618-632.

70. O'Farrell, H. C.; Scarsdale, J. N.; Rife, J. P. Crystal structure of KsgA, a universally conserved rRNA adenine dimethyltransferase in Escherichia coli. *J. Mol. Biol.* **2004**, *339,* 337-353.

71. Jeltsch, A. Molecular enzymology of mammalian DNA methyltransferases. *Curr. Top. Microbiol. Immunol.* **2006**, *301,* 203-225.

72. Luo, J.; Bruice, T. C. Low-frequency normal mode in DNA HhaI methyltransferase and motions of residues involved in the base flipping. *Proc. Natl. Acad. Sci. U. S. A.* **2005**, *102,* 16194-16198.

73. Lafontaine, D.; Delcour, J.; Glasser, A. L.; Desgres, J.; Vandenhaute, J. The DIM1 gene responsible for the conserved m6(2)Am6(2)A dimethylation in the 3'-terminal loop of 18 S rRNA is essential in yeast. *J. Mol. Biol.* **1994**, *241,* 492-497.

74. Lafontaine, D.; Vandenhaute, J.; Tollervey, D. The 18S rRNA dimethylase Dim1p is required for pre-ribosomal RNA processing in yeast. *Genes Dev.* **1995**, *9,* 2470-2481.

75. Schmitt, M. E.; Clayton, D. A. Nuclear RNase MRP is required for correct processing of pre-5.8S rRNA in Saccharomyces cerevisiae. *Mol. Cell. Biol.* **1993**, *13,* 7935-7941.

76. Vanrobays, E.; Gelugne, J. P.; Caizergues-Ferrer, M.; Lafontaine, D. L. Dim2p, a KH-domain protein required for small ribosomal subunit synthesis. *RNA* **2004**, *10,* 645-656.

77. Senapin, S.; Clark-Walker, G. D.; Chen, X. J.; Seraphin, B.; Daugeron, M. C. RRP20, a component of the 90S preribosome, is required for pre-18S rRNA processing in Saccharomyces cerevisiae. *Nucleic Acids Res.* **2003**, *31,* 2524-2533.

78. Adinolfi, S.; Bagni, C.; Castiglione Morelli, M. A.; Fraternali, F.; Musco, G.; Pastore, A. Novel RNA-binding motif: the KH module. *Biopolymers* **1999**, *51,* 153-164.

79. Gavin, A. C.; Bosche, M.; Krause, R.; Grandi, P.; Marzioch, M.; Bauer, A.; Schultz, J.; Rick, J. M.; Michon, A. M.; Cruciat, C. M.; Remor, M.; Hofert, C.; Schelder, M.; Brajenovic, M.; Ruffner, H.; Merino, A.; Klein, K.; Hudak, M.; Dickson, D.; Rudi, T.; Gnau, V.; Bauch, A.; Bastuck, S.; Huhse, B.; Leutwein, C.; Heurtier, M. A.; Copley, R. R.; Edelmann, A.; Querfurth, E.; Rybin, V.; Drewes, G.; Raida, M.; Bouwmeester, T.; Bork, P.; Seraphin, B.; Kuster, B.; Neubauer, G.; Superti-Furga, G. Functional organization of the yeast proteome by systematic analysis of protein complexes. *Nature* **2002**, *415,* 141-147.

80. Ho, Y.; Gruhler, A.; Heilbut, A.; Bader, G. D.; Moore, L.; Adams, S. L.; Millar, A.; Taylor, P.; Bennett, K.; Boutilier, K.; Yang, L.; Wolting, C.; Donaldson, I.; Schandorff, S.; Shewnarane, J.; Vo, M.; Taggart, J.; Goudreault, M.; Muskat, B.; Alfarano, C.; Dewar, D.; Lin, Z.; Michalickova, K.; Willems, A. R.; Sassi, H.; Nielsen, P. A.; Rasmussen, K. J.; Andersen, J. R.; Johansen, L. E.; Hansen, L. H.; Jespersen, H.; Podtelejnikov, A.; Nielsen, E.; Crawford, J.; Poulsen, V.; Sorensen, B. D.; Matthiesen, J.; Hendrickson, R. C.; Gleeson, F.; Pawson, T.; Moran, M. F.;

Durocher, D.; Mann, M.; Hogue, C. W.; Figeys, D.; Tyers, M. Systematic identification of protein complexes in Saccharomyces cerevisiae by mass spectrometry. *Nature* **2002**, *415,* 180-183.

81. Vazquez, A.; Flammini, A.; Maritan, A.; Vespignani, A. Global protein function prediction from protein-protein interaction networks. *Nat. Biotechnol.* **2003**, *21,* 697-700.

82. Intine, R. V.; Good, L.; Nazar, R. N. Essential structural features in the Schizosaccharomyces pombe pre-rRNA 5' external transcribed spacer. *J. Mol. Biol.* **1999**, *286,* 695-708.

83. Allmang, C.; Henry, Y.; Wood, H.; Morrissey, J. P.; Petfalski, E.; Tollervey, D. Recognition of cleavage site A(2) in the yeast pre-rRNA. *RNA* **1996**, *2,* 51-62.

84. Lee, S. J.; Baserga, S. J. Functional separation of pre-rRNA processing steps revealed by truncation of the U3 small nucleolar ribonucleoprotein component, Mpp10. *Proc. Natl. Acad. Sci. U. S. A.* **1997**, *94,* 13536-13541.

85. Beltrame, M.; Tollervey, D. Base pairing between U3 and the pre-ribosomal RNA is required for 18S rRNA synthesis. *EMBO J.* **1995**, *14,* 4350-4356.

86. Beltrame, M.; Henry, Y.; Tollervey, D. Mutational analysis of an essential binding site for the U3 snoRNA in the 5' external transcribed spacer of yeast pre-rRNA. *Nucleic Acids Res.* **1994**, *22,* 5139-5147.

87. Dichtl, B.; Stevens, A.; Tollervey, D. Lithium toxicity in yeast is due to the inhibition of RNA processing enzymes. *EMBO J.* **1997**, *16,* 7184-7195.

88. Petfalski, E.; Dandekar, T.; Henry, Y.; Tollervey, D. Processing of the precursors to small nucleolar RNAs and rRNAs requires common components. *Mol. Cell. Biol.* **1998**, *18,* 1181-1189.

89. Schafer, T.; Maco, B.; Petfalski, E.; Tollervey, D.; Bottcher, B.; Aebi, U.; Hurt, E. Hrr25-dependent phosphorylation state regulates organization of the pre-40S subunit. *Nature* **2006**, *441,* 651-655.

90. Fatica, A.; Tollervey, D.; Dlakic, M. PIN domain of Nob1p is required for D-site cleavage in 20S pre-rRNA. *RNA* **2004**, *10,* 1698-1701.

91. Fatica, A.; Oeffinger, M.; Dlakic, M.; Tollervey, D. Nob1p is required for cleavage of the 3' end of 18S rRNA. *Mol. Cell. Biol.* **2003**, *23,* 1798-1807.

92. Granneman, S.; Nandineni, M. R.; Baserga, S. J. The putative NTPase Fap7 mediates cytoplasmic 20S pre-rRNA processing through a direct interaction with Rps14. *Mol. Cell. Biol.* **2005**, *25,* 10352-10364.

93. Tone, Y.; Toh-E, A. Nob1p is required for biogenesis of the 26S proteasome and degraded upon its maturation in Saccharomyces cerevisiae. *Genes Dev.* **2002**, *16,* 3142-3157.

94. Peng, W. T.; Robinson, M. D.; Mnaimneh, S.; Krogan, N. J.; Cagney, G.; Morris, Q.; Davierwala, A. P.; Grigull, J.; Yang, X.; Zhang, W.; Mitsakakis, N.; Ryan, O. W.; Datta, N.; Jojic, V.; Pal, C.; Canadien, V.; Richards, D.; Beattie, B.; Wu, L. F.; Altschuler, S. J.; Roweis, S.; Frey, B. J.; Emili, A.; Greenblatt, J. F.; Hughes, T. R. A panoramic view of yeast noncoding RNA processing. *Cell* **2003**, *113,* 919-933.

95. Gelperin, D.; Horton, L.; Beckman, J.; Hensold, J.; Lemmon, S. K. Bms1p, a novel GTP-binding protein, and the related Tsr1p are required for distinct steps of 40S ribosome biogenesis in yeast. *RNA* **2001**, *7,* 1268-1283.

96. Tokuhisa, J. G.; Vijayan, P.; Feldmann, K. A.; Browse, J. A. Chloroplast development at low temperatures requires a homolog of DIM1, a yeast gene encoding the 18S rRNA dimethylase. *Plant Cell* **1998**, *10,* 699-711.

97. Seidel-Rogol, B. L.; McCulloch, V.; Shadel, G. S. Human mitochondrial transcription factor B1 methylates ribosomal RNA at a conserved stem-loop. *Nat. Genet.* **2003**, *33,* 23-24.

98. Klootwijk, J.; Klein, I.; Grivell, L. A. Minimal post-transcriptional modification of yeast mitochondrial ribosomal RNA. *J. Mol. Biol.* **1975**, *97,* 337-350.

99. Van Buul, C. P.; Hamersma, M.; Visser, W.; Van Knippenberg, P. H. Partial methylation of two adjacent adenosines in ribosomes from Euglena gracilis chloroplasts suggests evolutionary loss of an intermediate stage in the methyl-transfer reaction. *Nucleic Acids Res.* **1984**, *12,* 9205-9208.

100. Van Buul, C. P.; Damm, J. B.; Van Knippenberg, P. H. Kasugamycin resistant mutants of Bacillus stearothermophilus lacking the enzyme for the methylation of two adjacent adenosines in 16S ribosomal RNA. *Mol. Gen. Genet.* **1983**, *189,* 475-478.

101. Helser, T. L.; Davies, J. E.; Dahlberg, J. E. Mechanism of kasugamycin resistance in Escherichia coli. *Nat. New Biol.* **1972**, *235,* 6-9.

102. Poldermans, B.; Roza, L.; Van Knippenberg, P. H. Studies on the function of two adjacent N6,N6-dimethyladenosines near the 3' end of 16 S ribosomal RNA of

Escherichia coli. III. Purification and properties of the methylating enzyme and methylase-30 S interactions. *J. Biol. Chem.* **1979**, *254,* 9094-9100.

103. Igarashi, K.; Kishida, K.; Kashiwagi, K.; Tatokoro, I.; Kakegawa, T.; Hirose, S. Relationship between methylation of adenine near the 3' end of 16-S ribosomal RNA and the activity of 30-S ribosomal subunits. *Eur. J. Biochem.* **1981**, *113,* 587-593.

104. Sorensen, M. A.; Fricke, J.; Pedersen, S. Ribosomal protein S1 is required for translation of most, if not all, natural mRNAs in Escherichia coli in vivo. *J. Mol. Biol.* **1998**, *280,* 561-569.

105. Cunningham, P. R.; Weitzmann, C. J.; Nurse, K.; Masurel, R.; Van Knippenberg, P. H.; Ofengand, J. Site-specific mutation of the conserved m6(2)A m6(2)A residues of E. coli 16S ribosomal RNA. Effects on ribosome function and activity of the ksgA methyltransferase. *Biochim. Biophys. Acta* **1990**, *1050,* 18-26.

106. Schluenzen, F.; Takemoto, C.; Wilson, D. N.; Kaminishi, T.; Harms, J. M.; Hanawa-Suetsugu, K.; Szaflarski, W.; Kawazoe, M.; Shirouzu, M.; Nierhaus, K. H.; Yokoyama, S.; Fucini, P. The antibiotic kasugamycin mimics mRNA nucleotides to destabilize tRNA binding and inhibit canonical translation initiation. *Nat. Struct. Mol. Biol.* **2006**, *13,* 871-878.

107. Schuwirth, B. S.; Day, J. M.; Hau, C. W.; Janssen, G. R.; Dahlberg, A. E.; Cate, J. H.; Vila-Sanjurjo, A. Structural analysis of kasugamycin inhibition of translation. *Nat. Struct. Mol. Biol.* **2006**, *13,* 879-886.

108. Mankin, A. Antibiotic blocks mRNA path on the ribosome. *Nat. Struct. Mol. Biol.* **2006**, *13,* 858-860.

109. McCulloch, V.; Seidel-Rogol, B. L.; Shadel, G. S. A human mitochondrial transcription factor is related to RNA adenine methyltransferases and binds S-adenosylmethionine. *Mol. Cell. Biol.* **2002**, *22,* 1116-1125.

110. McCulloch, V.; Shadel, G. S. Human mitochondrial transcription factor B1 interacts with the C-terminal activation region of h-mtTFA and stimulates transcription independently of its RNA methyltransferase activity. *Mol. Cell. Biol.* **2003**, *23,* 5816-5824.

111. Bykhovskaya, Y.; Mengesha, E.; Wang, D.; Yang, H.; Estivill, X.; Shohat, M.; Fischel-Ghodsian, N. Human mitochondrial transcription factor B1 as a modifier gene for hearing loss associated with the mitochondrial A1555G mutation. *Mol. Genet. Metab.* **2004**, *82,* 27-32.

112. Shadel, G. S. Coupling the mitochondrial transcription machinery to human disease. *Trends Genet.* **2004**, *20,* 513-519.

113. Skinner, R.; Cundliffe, E.; Schmidt, F. J. Site of action of a ribosomal RNA methylase responsible for resistance to erythromycin and other antibiotics. *J. Biol. Chem.* **1983**, *258,* 12702-12706.

114. van Buul, C. P.; van Knippenberg, P. H. Nucleotide sequence of the ksgA gene of Escherichia coli: comparison of methyltransferases effecting dimethylation of adenosine in ribosomal RNA. *Gene* **1985**, *38,* 65-72.

115. Weisblum, B. Erythromycin resistance by ribosome modification. *Antimicrob. Agents Chemother.* **1995**, *39,* 577-585.

116. Schubot, F. D.; Chen, C. J.; Rose, J. P.; Dailey, T. A.; Dailey, H. A.; Wang, B. C. Crystal structure of the transcription factor sc-mtTFB offers insights into mitochondrial transcription. *Protein Sci.* **2001**, *10,* 1980-1988.

117. Bussiere, D. E.; Muchmore, S. W.; Dealwis, C. G.; Schluckebier, G.; Nienaber, V. L.; Edalji, R. P.; Walter, K. A.; Ladror, U. S.; Holzman, T. F.; Abad-Zapatero, C. Crystal structure of ErmC', an rRNA methyltransferase which mediates antibiotic resistance in bacteria. *Biochemistry* **1998**, *37,* 7103-7112.

118. Structural Genomics Consortium; China Structural Genomics Consortium; Northeast Structural Genomics Consortium; Graslund, S.; Nordlund, P.; Weigelt, J.; Hallberg, B. M.; Bray, J.; Gileadi, O.; Knapp, S.; Oppermann, U.; Arrowsmith, C.; Hui, R.; Ming, J.; dhe-Paganon, S.; Park, H. W.; Savchenko, A.; Yee, A.; Edwards, A.; Vincentelli, R.; Cambillau, C.; Kim, R.; Kim, S. H.; Rao, Z.; Shi, Y.; Terwilliger, T. C.; Kim, C. Y.; Hung, L. W.; Waldo, G. S.; Peleg, Y.; Albeck, S.; Unger, T.; Dym, O.; Prilusky, J.; Sussman, J. L.; Stevens, R. C.; Lesley, S. A.; Wilson, I. A.; Joachimiak, A.; Collart, F.; Dementieva, I.; Donnelly, M. I.; Eschenfeldt, W. H.; Kim, Y.; Stols, L.; Wu, R.; Zhou, M.; Burley, S. K.; Emtage, J. S.; Sauder, J. M.; Thompson, D.; Bain, K.; Luz, J.; Gheyi, T.; Zhang, F.; Atwell, S.; Almo, S. C.; Bonanno, J. B.; Fiser, A.; Swaminathan, S.; Studier, F. W.; Chance, M. R.; Sali, A.; Acton, T. B.; Xiao, R.; Zhao, L.; Ma, L. C.; Hunt, J. F.; Tong, L.; Cunningham, K.; Inouye, M.; Anderson, S.; Janjua, H.; Shastry, R.; Ho, C. K.; Wang, D.; Wang, H.; Jiang, M.; Montelione, G. T.; Stuart, D. I.; Owens, R. J.; Daenke, S.; Schutz, A.; Heinemann, U.; Yokoyama, S.; Bussow, K.; Gunsalus, K. C. Protein production and purification. *Nat. Methods* **2008**, *5,* 135-146.

119. Peti, W.; Page, R. Strategies to maximize heterologous protein expression in Escherichia coli with minimal cost. *Protein Expr. Purif.* **2007**, *51,* 1-10.

120. Davis, G. D.; Elisee, C.; Newham, D. M.; Harrison, R. G. New fusion protein systems designed to give soluble expression in Escherichia coli. *Biotechnol. Bioeng.* **1999**, *65,* 382-388.

121. Macauley-Patrick, S.; Fazenda, M. L.; McNeil, B.; Harvey, L. M. Heterologous protein production using the Pichia pastoris expression system. *Yeast* **2005**, *22,* 249-270.

122. Cereghino, J. L.; Cregg, J. M. Heterologous protein expression in the methylotrophic yeast Pichia pastoris. *FEMS Microbiol. Rev.* **2000**, *24,* 45-66.

123. Vera, A.; Gonzalez-Montalban, N.; Aris, A.; Villaverde, A. The conformational quality of insoluble recombinant proteins is enhanced at low growth temperatures. *Biotechnol. Bioeng.* **2007**, *96,* 1101-1106.

124. Mears, J. A.; Cannone, J. J.; Stagg, S. M.; Gutell, R. R.; Agrawal, R. K.; Harvey, S. C. Modeling a minimal ribosome based on comparative sequence analysis. *J. Mol. Biol.* **2002**, *321,* 215-234.

125. Held, W. A.; Mizushima, S.; Nomura, M. Reconstitution of Escherichia coli 30 S ribosomal subunits from purified molecular components. *J. Biol. Chem.* **1973**, *248,* 5720-5730.

126. Culver, G. M. Assembly of the 30S ribosomal subunit. *Biopolymers* **2003**, *68,* 234-249.

127. Thammana, P.; Held, W. A. Methylation of 16S RNA during ribosome assembly in vitro. *Nature* **1974**, *251,* 682-686.

128. Armougom, F.; Moretti, S.; Poirot, O.; Audic, S.; Dumas, P.; Schaeli, B.; Keduas, V.; Notredame, C. Expresso: automatic incorporation of structural information in multiple sequence alignments using 3D-Coffee. *Nucleic Acids Res.* **2006**, *34,* W604-8.

129. O'Farrell, H. C.; Musayev, F. N.; Scarsdale, J. N.; Wright, H. T.; Rife, J. P. Crystallization and preliminary X-ray diffraction analysis of KsgA, a universally conserved RNA adenine dimethyltransferase in Escherichia coli. *Acta Crystallogr. D Biol. Crystallogr.* **2003**, *59,* 1490-1492.

130. Blaha, G.; Stelzl, U.; Spahn, C. M.; Agrawal, R. K.; Frank, J.; Nierhaus, K. H. Preparation of functional ribosomal complexes and effect of buffer conditions on tRNA positions observed by cryoelectron microscopy. *Methods Enzymol.* **2000**, *317,* 292-309.

131. Gehrke, C. W.; Kuo, K. C. Ribonucleoside analysis by reversed-phase high-performance liquid chromatography. *J. Chromatogr.* **1989**, *471,* 3-36.

132. Rife, J. P.; Cheng, C. S.; Moore, P. B.; Strobel, S. A. The Synthesis of RNA Containing the Modified Nucleotides N 2-Methylguanosine and N 6, N 6-Dimethyladenosine. *Nucleosides, Nucleotides and Nucleic Acids* **1998**, *17,* 2281-2288.

133. Omer, A. D.; Ziesche, S.; Decatur, W. A.; Fournier, M. J.; Dennis, P. P. RNA-modifying machines in archaea. *Mol. Microbiol.* **2003**, *48,* 617-629.

134. Pace, N. R. A molecular view of microbial diversity and the biosphere. *Science* **1997**, *276,* 734-740.

135. Boeke, J. D.; Trueheart, J.; Natsoulis, G.; Fink, G. R. 5-Fluoroorotic acid as a selective agent in yeast molecular genetics. *Methods Enzymol.* **1987**, *154,* 164-175.

136. Ito, H.; Fukuda, Y.; Murata, K.; Kimura, A. Transformation of intact yeast cells treated with alkali cations. *J. Bacteriol.* **1983**, *153,* 163-168.

137. Pringle, J. R.; Adams, A. E.; Drubin, D. G.; Haarer, B. K. Immunofluorescence methods for yeast. *Methods Enzymol.* **1991**, *194,* 565-602.

138. Maag, D.; Algire, M. A.; Lorsch, J. R. Communication between eukaryotic translation initiation factors 5 and 1A within the ribosomal pre-initiation complex plays a role in start site selection. *J. Mol. Biol.* **2006**, *356,* 724-737.

139. Xu, Z.; O'Farrell, H. C.; Rife, J. P.; Culver, G. M. A conserved rRNA methyltransferase regulates ribosome biogenesis. *Nat. Struct. Mol. Biol.* **2008**.

APPENDIX A

Table 5: Primers used for cloning and chimera construction

	Primers
1.	*DIM1* - *Xho*I-*Nhe*I fragment for subcloning into pESC-*URA* vector
For	5′- CGT CTG CTC GAG ATG GGA AAG GCT GCG - 3′
Rev	5′- CTG GGC GCT AGC TCA TGA AAA ATG GAT ACC AAC CTG G - 3′
2.	*DIM1* - *Not*I-*Spe*I fragment for subcloning into pESC-*LEU* vector
For	5′- GCC ACT GCG GCC GCA TGG GAA AGG CTG CG - 3′
Rev	5′- CTG GAC ACT AGT GCT GAA AAA TGG ATA CCA ACC TGG - 3′
3.	*DIM1* - *Not*I-*Spe*I fragment with the exogenous NLS for subcloning into pESC-*LEU* vector
For	5′- CTG ACT GCG GCC GCA TGC CAC CAA AGA AGA AGA GAA AGG TTA TGG GAA AGG CTG CGA AAA AGA AG - 3′
Rev	5′- CTG GAC ACT AGT GCT GAA AAA TGG ATA CCA ACC TGG - 3′
4.	*KsgA* - *Not*I-*Spe*I fragment with the exogenous NLS for subcloning into pESC-*LEU* vector
For	5′- CTG GAC GCG GCC GCA TGC CAC CAA AGA AGA AGA GAA AGG TTA TGA ATA ATC GAG TCC ACC - 3′
Rev	5′- GCA CTG ACT AGT GCA CTC TCC TGC AAA GGC GCG - 3′
5.	*KsgA* - *Bgl*II-*Pac*I fragment for subcloning into pESC-*LEU* vector
For	5′- CCA GCC AGA TCT ATA TGA ATA ATC GAG TCC ACC AGG GCC - 3′
Rev	5′- GCC TCG TTA ATT AAT TAA CTC TCC TGC AAA GGC GCG - 3′

6.	*KsgA* - *Not*I-*Spe*I fragment for subcloning into pESC-*LEU* vector
For	5′- AGT CAG GCG GCC GCA TGA ATA ATC GAG TCC ACC AGG - 3′
Rev	5′- GCA CTG ACT AGT GCA CTC TCC TGC AAA GGC GCG - 3′
7.	*MjDim1* - *Not*I-*Spe*I fragment with the exogenous NLS for subcloning into pESC-*LEU* vector
For	5′- CTG GAC GCG GCC GCA TGC CAC CAA AGA AGA AGA GAA AGG TTA TGT TCA AAC CAA AGA AAA AAT TAG GGC - 3′
Rev	5′- GCA CTG ACT AGT GCT AAC CTA CCC CTA TTT TGC AG - 3′
8.	*MjDim1* - *Not*I-*Spe*I fragment for subcloning into pESC-*LEU* vector
For	5′- AGT CAG GCG GCC GCA TGT TCA AAC CAA AGA AAA AAT TAG GGC - 3′
Rev	5′- GCA CTG ACT AGT GCT AAC CTA CCC CTA TTT TGC AG - 3′
9.	N-terminal domain of *DIM1* - as *Nde*I-*Sal*I fragment for chimera construction
For	5′- CCG ACG CAT ATG GGA AAG GCT GCG - 3′
Rev	5′- AGT CAG GTC GAC TTG CGG TCT TGG ATT TTT AAT CTC - 3′
10.	C-terminal domain of *DIM1* - as *Sal*I-*Xho*I fragment for chimera construction
For	5′- CAG AGT GTC GAC TAC AAC GAA TGG GAT GGT TTG - 3′
Rev	5′- CCG GAT CCT CGA GTC ATG AAA AAT GGA TAC C - 3′
11.	N-terminal domain of *KsgA* - as *Nde*I-*Sal*I fragment for chimera construction
For	5′- AGT GAC CAT ATG AAT AAT CGA GTC CAC CAG G - 3′
Rev	5′- AGT CAG GTC GAC CGG GTG AGG CAT CGT TGC - 3′
12.	C-terminal domain of *KsgA* - as *Sal*I-*Xho*I fragment for chimera construction
For	5′- CAG AGT GTC GAC GTT CGT GTG TTG AGC CGC - 3′

Rev	5′- CAG AGT CTC GAG TTA ACT CTC CTG CAA AGG CGC G - 3′
13.	N-terminal domain of *MjDim1* - as *Nde*I-*Sal*I fragment for chimera construction
For	5′- GCC GCA CCA TAT GTT CAA ACC AAA GAA AAA ATT AGG - 3′
Rev	5′- AGT CAG GTC GAC GTG GTA TTT GCC TTT GTT AGG TT - 3′
14.	C-terminal domain of *MjDim1* - as *Sal*I-*Xho*I fragment for chimera construction
For	5′- CAG AGT GTC GAC AAT GAA AAT TTC TTT GAT GAT TTT TTG AGA GC - 3′
Rev	5′- GCT ACT CGA GCT ATA ACC TAC CCC TAT TTT GCA G - 3′
15.	*KD* - *Nde*I-*Xho*I fragment for cloning into pET15b vector
For	5′- AGT GAC CAT ATG AAT AAT CGA GTC CAC CAG G - 3′
Rev	5′- CCG GAT CCT CGA GTC ATG AAA AAT GGA TAC C - 3′
16.	*DK* - *Nde*I-*Xho*I fragment for cloning into pET15b vector
For	5′- CCG ACG CAT ATG GGA AAG GCT GCG - 3′
Rev	5′- CAG AGT CTC GAG TTA ACT CTC CTG CAA AGG CGC G - 3′
17.	*MD* - *Nde*I-*Xho*I fragment for cloning into pET15b vector
For	5′- GCC GCA CCA TAT GTT CAA ACC AAA GAA AAA ATT AGG - 3′
Rev	5′- CCG GAT CCT CGA GTC ATG AAA AAT GGA TAC C - 3′
18.	*DM* - *Nde*I-*Xho*I fragment for cloning into pET15b vector
For	5′- CCG ACG CAT ATG GGA AAG GCT GCG - 3′
Rev	5′- GCT ACT CGA GCT ATA ACC TAC CCC TAT TTT GCA G - 3′
19.	*MK* - *Nde*I-*Xho*I fragment for cloning into pET15b vector
For	5′- GCC GCA CCA TAT GTT CAA ACC AAA GAA AAA ATT AGG - 3′

Rev	5′- CAG AGT CTC GAG TTA ACT CTC CTG CAA AGG CGC G - 3′
20.	*KM* - *Nde*I-*Xho*I fragment for cloning into pET15b vector
For	5′- AGT GAC CAT ATG AAT AAT CGA GTC CAC CAG G - 3′
Rev	5′- GCT ACT CGA GCT ATA ACC TAC CCC TAT TTT GCA G - 3′
21.	*KD* - *Not*I-*Spe*I fragment with the exogenous NLS for subcloning into pESC-*LEU* vector
For	5′- CTG GAC GCG GCC GCA TGC CAC CAA AGA AGA AGA GAA AGG TTA TGA ATA ATC GAG TCC ACC - 3′
Rev	5′- CTG GAC ACT AGT GCT GAA AAA TGG ATA CCA ACC TGG - 3′
22.	*DK* - *Not*I-*Spe*I fragment for subcloning into pESC-*LEU* vector
For	5′- GCC ACT GCG GCC GCA TGG GAA AGG CTG CG - 3′
Rev	5′- GCA CTG ACT AGT GCA CTC TCC TGC AAA GGC GCG - 3′
23.	*MD* - *Not*I-*Spe*I fragment with the exogenous NLS for subcloning into pESC-*LEU* vector
For	5′- CTG GAC GCG GCC GCA TGC CAC CAA AGA AGA AGA GAA AGG TTA TGT TCA AAC CAA AGA AAA AAT TAG GGC - 3′
Rev	5′- CTG GAC ACT AGT GCT GAA AAA TGG ATA CCA ACC TGG - 3′
24.	*DM* - *Not*I-*Spe*I fragment for subcloning into pESC-*LEU* vector
For	5′- GCC ACT GCG GCC GCA TGG GAA AGG CTG CG - 3′
Rev	5′- GCA CTG ACT AGT GCT AAC CTA CCC CTA TTT TGC AG - 3′
25.	*MK* - *Not*I-*Spe*I fragment with the exogenous NLS for subcloning into pESC-*LEU* vector
For	5′- CTG GAC GCG GCC GCA TGC CAC CAA AGA AGA AGA GAA AGG TTA TGT TCA AAC CAA AGA AAA AAT TAG GGC - 3′
Rev	5′- GCA CTG ACT AGT GCA CTC TCC TGC AAA GGC GCG - 3′

26.	*KM* - *Not*I-*Spe*I fragment with the exogenous NLS for subcloning into pESC-*LEU* vector
For	5′- CTG GAC GCG GCC GCA TGC CAC CAA AGA AGA AGA GAA AGG TTA TGA ATA ATC GAG TCC ACC - 3′
Rev	5′- GCA CTG ACT AGT GCT AAC CTA CCC CTA TTT TGC AG - 3′
27.	*DIM1* - E85A mutation in pESC-*LEU*-*DIM1*
For	5′-C GTA GTG GCA GTA G**C**A ATG GAT CCC AGA ATG G-3′
Rev	5′-C CAT TCT GGG ATC CAT T**G**C TAC TGC CAC TAC G-3′
28.	*DIM2* - *Nde*I-*Xho*I fragment for cloning into pET15b vector
For	5′- CCG ACG CAT ATG GTT GCG CCT ACT GCT TTG AAA AAG GCT ACT G - 3′
Rev	5′- GCA GCG CTC GAG TTA GTA GCG TTC TTT TAA TCT AGA TGC AAC GGT ACG - 3′
29.	*DIM1* - *Sma*I-*Xho*I fragment for cloning into pET44a vector
For	5′- GCG GTA GCA TGG GAA AGG CTG CG - 3′
Rev	5′- CCG GAT CCT CGA GTC ATG AAA AAT GGA TAC C - 3′
30.	*DIM1* - *Eco*RI-*Xba*I fragment for cloning into pPICZαA vector
For	5′- ACC GAA TTC ATG GGA AAG GCT GCG - 3′
Rev	5′- GCG TCT AGA GCT GAA AAA TGG ATA CCA ACC - 3′
31.	N-terminal domain of *DIM1* (*DIM1N*) - as *Nde*I-*Xho*I fragment for cloning into pET21c vector
For	5′- CCG ACG CAT ATG GGA AAG GCT GCG - 3′
Rev	5′- GG CTC GAG TTG CGG TCT TGG A - 3′

APPENDIX B

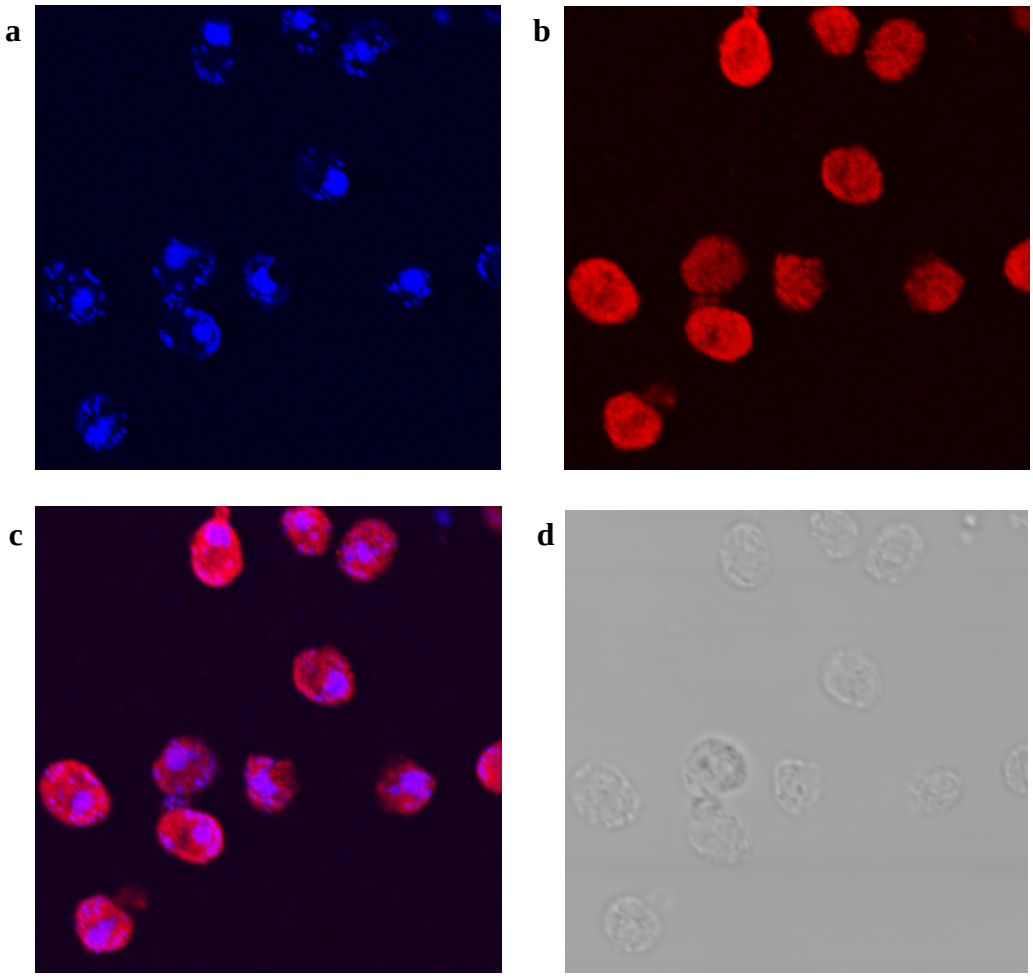

Figure 28: Subcellular localization of KsgA. (a) the nuclei were stained blue with DAPI; (b) the protein is stained red with anti-FLAG antibody; (c) shows the overlay of the nucleus and protein; (d) shows the DIC image.

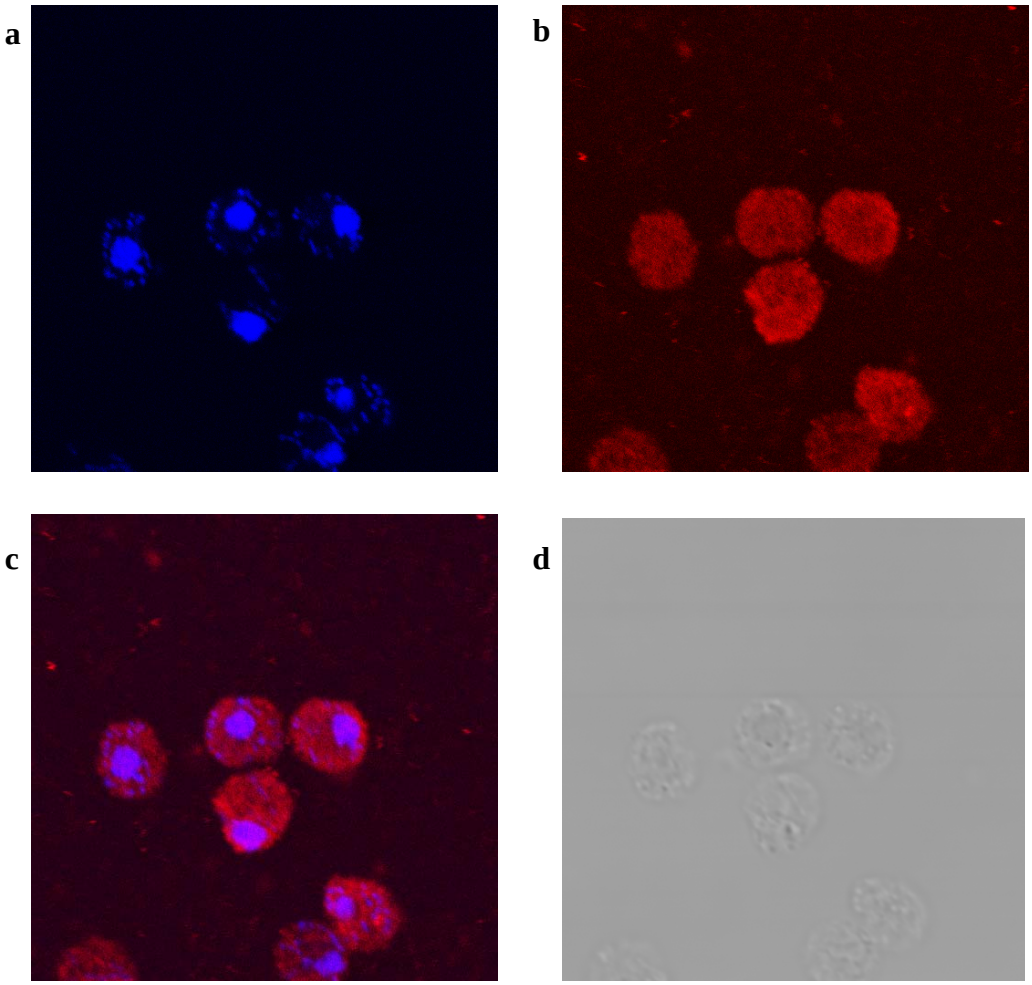

Figure 29: Subcellular localization of the chimera protein, KD. (a) the nuclei were stained blue with DAPI; (b) the protein is stained red with anti-FLAG antibody; (c) shows the overlay of the nucleus and protein; (d) shows the DIC image.

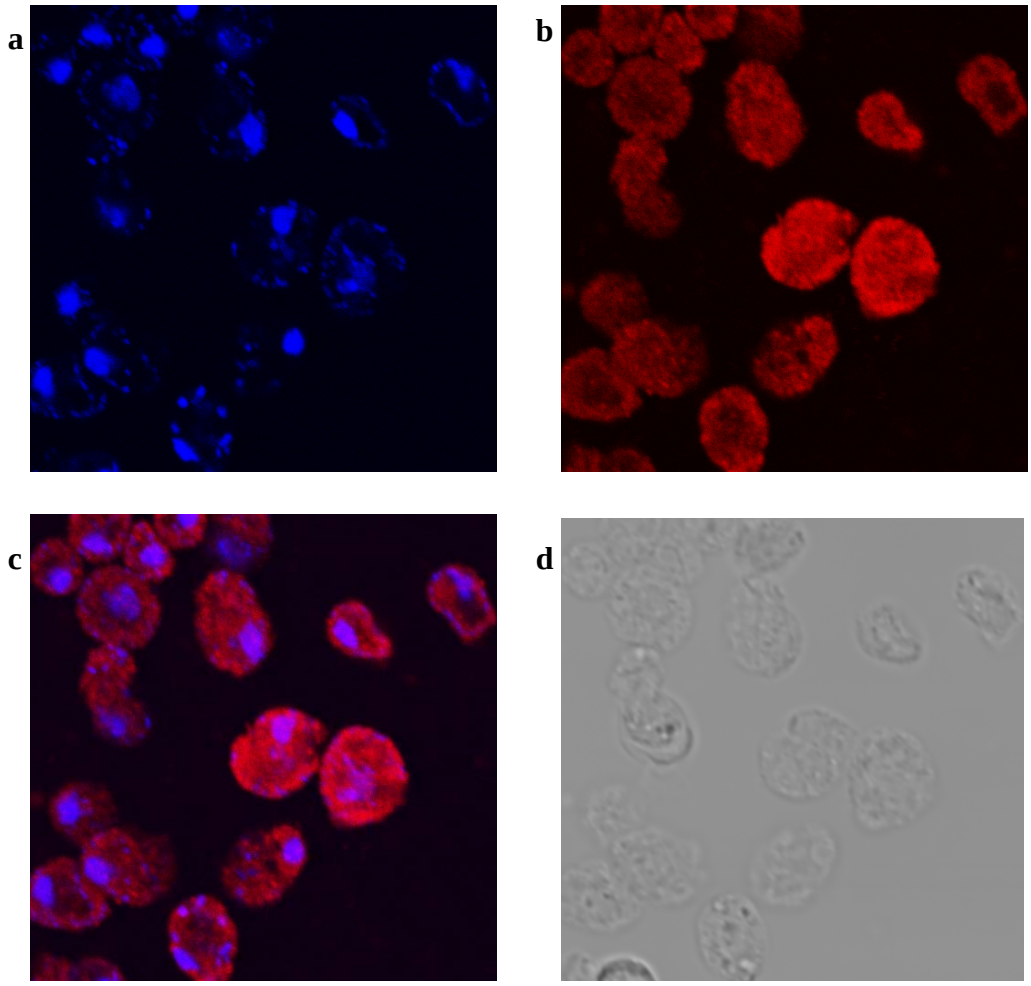

Figure 30: Subcellular localization of the chimera protein, DK. (a) the nuclei were stained blue with DAPI; (b) the protein is stained red with anti-FLAG antibody; (c) shows the overlay of the nucleus and protein; (d) shows the DIC image.

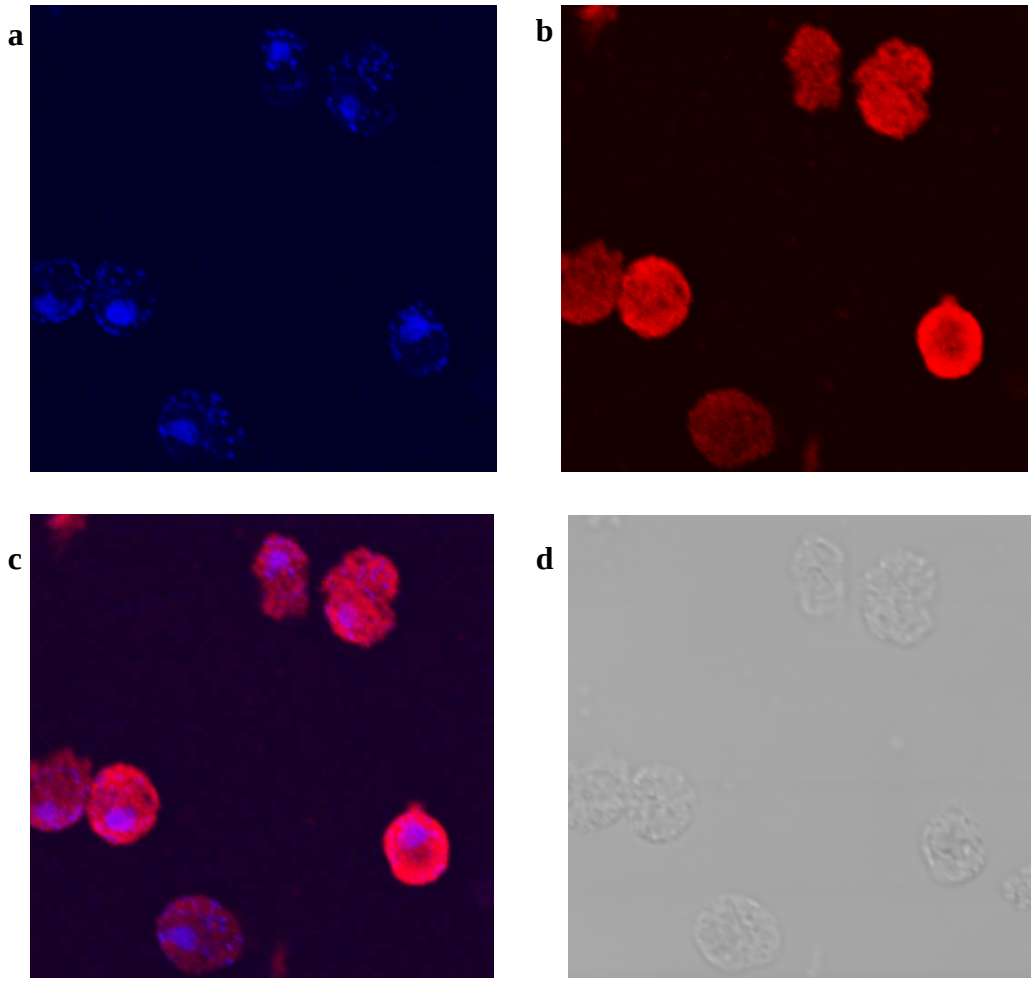

Figure 31: Subcellular localization of the chimera protein, MK. (a) the nuclei were stained blue with DAPI; (b) the protein is stained red with anti-FLAG antibody; (c) shows the overlay of the nucleus and protein; (d) shows the DIC image.

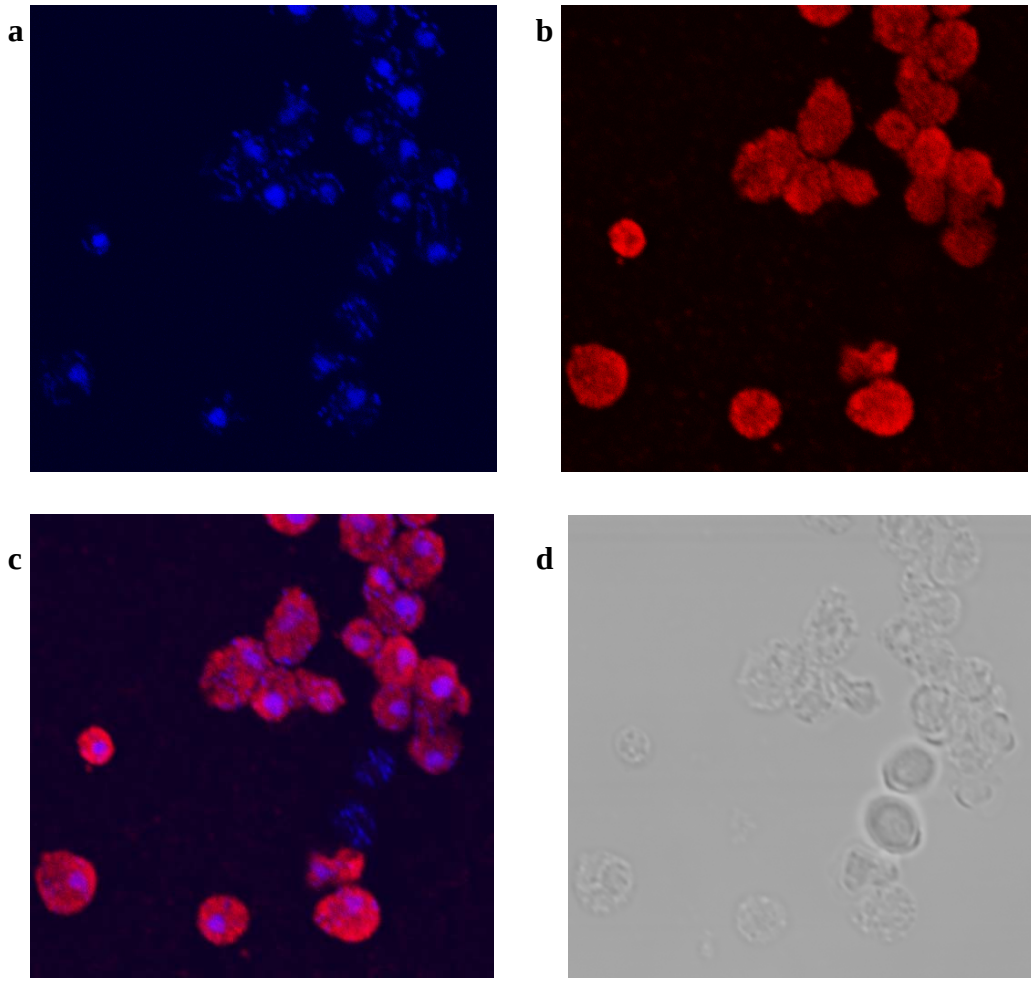

Figure 32: Subcellular localization of the chimera protein, KM. (a) the nuclei were stained blue with DAPI; (b) the protein is stained red with anti-FLAG antibody; (c) shows the overlay of the nucleus and protein; (d) shows the DIC image.

VITA

NAGESH PULICHERLA
Born: April 29, 1978; Guntur, Andhra Pradesh, India
Citizenship: INDIA

EDUCATION

Ph.D. candidate - Pharmaceutical Sciences, Aug 2003 - May 2008
Dept. of Medicinal Chemistry, Virginia Commonwealth University.

Bachelor of Pharmacy, May 2002
Rajiv Gandhi University of Health Sciences, Bangalore, India.
Registered Pharmacist in Andhra Pradesh, India

ABSTRACTS AND PRESENTATIONS

Nagesh Pulicherla, Heather C. O′Farrell, Pooja M. Desai, Jason P. Rife. Yeast 18S rRNA dimethylase, Dim1, complements the function of its orthologs. Presented at the 7th International conference on Ribosome Synthesis, August 16-20, 2006, Warrenton, Virginia.

PUBLICATIONS

Pulicherla, N.; Pogorzola, L. A.; Xu, Z.; O'Farrell, H. C.; Sia, E. A.; Culver, G. M.; Rife, J. P. Complementation among members of the Dim1/KsgA rRNA methyltransferase family is not universal. **2008** (in preparation).

O′Farrell, H. C.; Pulicherla, N.; Desai, P. M.; Rife, J. P. Recognition of a complex substrate by the KsgA/Dim1 family of enzymes has been conserved throughout evolution. *RNA*, **2006**, *12(5),* 725-733.

FELLOWSHIPS/ AWARDS

J. D. Smith Award from the Dept. of Medicinal Chemistry, School of Pharmacy, 2007.

Travel Grant from the Dept. of Medicinal Chemistry for presenting the work at 7th International conference on Ribosome Synthesis, August 16-20, 2006, Warrenton, Virginia.

Certificate of Merit for securing First rank in University during 3rd year B.Pharm (2001), Bangalore, India.